



# FCT

Fundação para a Ciência e a Tecnologia  
MINISTÉRIO DA EDUCAÇÃO E CIÊNCIA

# U. PORTO



FACULDADE DE FARMÁCIA  
UNIVERSIDADE DO PORTO



# CATÓLICA

UNIVERSIDADE CATÓLICA PORTUGUESA | PORTO



# INEB

Instituto de Engenharia Biomédica

# iBiLi

Institute  
for Biomedical Imaging  
and Life Sciences

Faculty of Medicine  
University of Coimbra



# CESPU

INSTITUTO SUPERIOR  
DE CIÊNCIAS DA SAÚDE  
NORTE

**U. PORTO**



**FACULDADE DE FARMÁCIA  
UNIVERSIDADE DO PORTO**

## **Chitosan-based nanomedicine for rosmarinic acid ocular delivery**

---

Thesis presented to obtain the PhD degree in Pharmaceutical Sciences,  
Pharmaceutical Technology Specialty,  
Faculty of Pharmacy of University of Porto

by

Sara Isabel Macedo Baptista da Silva

Under supervision of Prof. Dr. Bruno Sarmiento and co-supervision of Prof. Dr. Domingos  
Ferreira and Prof. Dr. Manuela Pintado

October, 2014

## **Declaration**

The partial reproduction of this thesis is authorized only for research purposes by written declaration of the person concerned.

---

(Sara Baptista da Silva)

## Inspiration

*“Success is a journey, not a destination!”*

Ben Sweetland

## Dedication

*“There are only two ways to live life.  
One is as though nothing is a miracle.  
The other is as though everything is a miracle.”*

Albert Einstein

I dedicate this thesis to the most important persons in my life,  
my family, Oscar and our daughter,  
Catarina Isabel.

## Acknowledgements

*“Lord I can’t say it in words...can you please just listen through my heart”*

Unknown

I would like to formally express my deep gratitude to the following people and institutions – who (and which) have meant a lot to me during my PhD program, and made it possible:

Fundação para a Ciência e a Tecnologia, for financial support via a PhD fellowship (ref.: SFRH/BD/61423/2009), under the supervision of Professor Bruno Sarmento; said grant permitted timely development of my research program, as well as participation in several international scientific meetings to complement my training and sharing my results.

Laboratory of Pharmaceutical Technology, Faculty of Pharmacy, University of Porto for accepting me as a PhD student, for the hospitality and work conditions available, during my doctoral program.

My most sincerely acknowledges to Escola Superior de Biotecnologia of Universidade Católica Portuguesa (ESB-UCP), for the crucial collaboration in my PhD course, the indubitable hospitality and for providing facilities and logistical to best support my studies.

INEB – Instituto de Engenharia Biomédica, ISCS–N – Instituto Superior de Ciências da Saúde – Norte and IBILI-Institute for Biomedical Imaging and Life Sciences – University of Coimbra, for the acceptance, kindness and constant availability cooperation during this project.

Professor Bruno Sarmento my supervisor, who I am sincerely grateful for having accepted me as a PhD student, for the wide support and comprehensive scientific guidance he continuously gave me. His consistent and integrated contribution for my growth, both as a person and as a researcher, has been by all means outstanding. I would like, in particular, to thank him for every effort made in guarantee the best research conditions, going wherever necessary to find the most appropriate support; and for his everlasting encouragement, patience and motivation, as well as his availability to discuss specific and general topics of my dissertation. I am indeed deeply grateful, for having always believed in my abilities, for all the concerns, problems, opportunities and achievements shared along this journey, for the friendship and affection, my heartfelt thanks.

Professor Manuela Pintado my co-supervisor, I would like to thank for always accepting me as a student, having accompanied during these 12 years of academic training, for always believing in my abilities, skills and competences, for her unconditional understanding, patience, friendship and complicity. For her believed and dedication to my work, for all the conversations established and knowledge shared throughout these years and during this doctoral course, as well as for her encouragement, affection and help; and also for providing a healthy, happy and extremely professional working environment, my deepest thanks.

Professor Domingos Ferreira my co-supervisor, I would like to thank for his sympathy, kindness, constant availability and willingness to help during my doctoral program. For every effort to ensure the best institutional reception conditions and every logistical that could ensure the success of my work, my sincere grateful.

Professor Francisco Ambrósio, my deepest gratitude for agreeing to collaborate in this PhD project. For all the help, cooperation, understanding, by all the efforts made the investment of time and resources in better monitoring and performance of this work. For having given me the opportunity to work with his research team and by the unmatched amiability.

My most sincere thanks to Professor Horacina Cavalcante and to the entire Stamford family: Professor Newton, Professor Tania, Thayza and Thathiana, for have accompanied me during my doctoral plan in every possible way, for all the help, dedication, and enormous friendship.

My colleagues and friends within the different research groups – José das Neves, Fernanda Andrade, Filipa Antunes, Pedro Fonte, Francisca Araújo, Rute Nunes, Carla Pereira, Manuela Amorim, Ana Oliveira, Raquel Madureira, Débora Campos, Raquel Boia, Filipe Elvas, Tiago Martins, Pedro Tralhão, Maria Madeira, Joana Martins, and so many others. By somehow helping me in developing my studies and shared by so many difficulties and achievements, which certainly has helped me grow as a person and as a professional.

My closest friends which are the family that I chose for me every day:

Helena Monteiro, thank you for your friendship which already makes “silver wedding”, for our perpetual oath on time, for always find yourself without seeking, for even far in distance seems like I have been with you yesterday, and always.



Sandra Borges, words will be for sure fall short in expressing my eternal friendship. Thank you for bringing a rain-bow to my life, for the craziness shared. For every concern, worry, and happiness moments joint, for listening, advising, for the constant patience and complicity; For being always there.

Manuela Amorim, I will not be able to thank you everything that you art for me and everything what you already has done for me during this project, much less in a nutshell. Above all thank you for the unconditional friendship, complicity, and confidence, for every laugh and tear shared, for being my true friend.

Inês Cravo Roxo, Joana Barbosa, Franklin Costa (and the little Matilde), Ricardo Freixo, Luciana Silva and Renato Resende thank you for always accompanied my life at its best and worst for every moment spent, I appreciate and reciprocate with eternal friendship.

I also have to leave my deepest gratitude to my sweet Francisca Maria, who accompanied my life forever, and thank her for the immense dedication to my family, for their undying affection and unconditional support in every moment of our life, from best to worst; My most sincere and profound thanks.

I would like to thank to my brother Jorge Filipe and my sister Sofia Manuel, being my best friends, for existing and making my life so full field, so complete; For being with me in every dream, fight, step and for never live me alone. I would also have to thank to my nephews (Carlos Eduardo, Filipa Alexandra and Barbara Sofia), for being the best continuity of my brothers, for their love and for being always with me in a health madness.

My Grandmother, Isabel Maria, will always be my sunshine, my companion of all hours, the example of strength and light, and her way of being and living will always inspire my life.

Words will be reductive and insufficient to thank my parents for the unconditional love, for making me what I am today, for everything they have given me throughout my life, by making the development of my academic training possible and for always believed in me. Thank you for the unconditional love, strength, support and courage injected in me, today and every day. Thank you for everything, now and forever.

And last, but far from least – Oscar, is my *Alter Ego*, my companion of dreams and struggles. Oscar is the better half of me, the more aware, responsible and realistic. I grew up with him personal and intellectually. He has accompanied every moment of my life,

from the best to the worst. He has attended my academic formation closely and helped in everything he can so that I can move forward successfully. I would like to thank him for the unreserved love, for the amazing person he is, for all time he invested on me, and for the support, encouragement, patience and motivation that he constantly showed. For being my true love, and for have given me the best of my life, our daughter Catarina Isabel. Catarina born during my PhD workplan, she is the miracle of my life, my endless love, my heart, the reason why I want to get over myself and be better every day, to be her best reference.

## Abstract

Chitosan based nanoparticles prepared by ionic gelation with sodium tripolyphosphate (TPP) were developed and optimized. Chitosan and TPP were tested in different concentrations for the study of the chitosan:TPP best mass ratio until the final proportion of (7:1). The pH of nanoparticles formation medium was adjusted to 5.8, which was the pH value that best favors the interaction of rosmarinic acid and chitosan, thus reaching a maximum leading of rosmarinic acid entrapment. The encapsulation of rosmarinic acid, *Salvia officinalis* (sage) and *Satureja montana* (savory) was also tested in different theoretical loadings fairly to the initial concentration of chitosan. Nanoparticles were prepared and characterized freshly and lyophilized, and the theoretical loading was further fixed in 40% for rosmarinic acid and 50% for sage and savory nanoparticles. The particle size was observed to be dependent on both chitosan and TPP concentrations and minimum sizes were obtained for the lowest chitosan and TPP concentrations. The mean particle size was  $244.0 \pm 18.0$ ,  $278.4 \pm 42.2$  and  $229.3 \pm 29.6$  for rosmarinic acid, sage and savory nanoparticles, respectively. No significant differences ( $P > 0.05$ ) were observed between the different nanoformulations, which was expectable considering that the nanoparticulate system was optimized to encapsulate rosmarinic acid and since it is the major component of natural extracts. The obtained nanoparticles showed values of low dispersity index ( $< 0.25$ ), corresponding to a narrow particle size distribution such as:  $0.193 \pm 0.062$ ,  $0.268 \pm 0.092$  and  $0.149 \pm 0.121$  for rosmarinic acid, sage and savory nanoparticles, respectively. Nanoparticles surface charge ranged from  $29.5 \pm 1.6$ ,  $24.9 \pm 0.1$  and  $26.5 \pm 3.5$  mV for rosmarinic acid, sage and savory nanoparticles, respectively. This indicates that the colloidal systems were stable in storage time. Scanning electron microscopy (SEM) and transmission electron microscopy (TEM) confirmed the particle size distribution, and individual, smooth, spherical and small sizing nanoparticles (ranged from 200-300 nm) containing the rosmarinic acid and extracts were observed. The loading capacity was  $5.3 \pm 0.4$ ,  $8.1 \pm 0.6$ , and  $7.8 \pm 0.2\%$  for rosmarinic acid, sage and savory nanoparticles, respectively. The higher values for extract nanoparticles were intimate correlated to the lower initial amount of rosmarinic acid in the nanocomplexes. In a similar way, the association efficiencies were higher for extracts than rosmarinic acid, with values of  $51.2 \pm 3.0$ ,  $96.1 \pm 0.2$  and  $98.2 \pm 0.1\%$  for rosmarinic acid, sage and savory nanoparticles respectively, quantified by a previously validated high-performance liquid chromatography (HPLC) method. The higher extracts values may be also associated to

lower amount of rosmarinic acid in chitosan nanoparticles, since impairment of association efficiency and the initial concentration is documented as a reverse. The rosmarinic acid *in vitro* release profile was evaluated in phosphate buffer saline (PBS), pH 7.4, for the different nanoparticles and a fast release was observed in all the formulations, reaching almost 100% up to 60 min, with no significant differences ( $P > 0.05$ ). Therefore these nanoparticulate systems may provide a rational strategy for the development of ocular rapid release systems for rosmarinic acid delivery. Differential scanning calorimetry (DSC) and Fourier-transform infrared (FTIR) analysis set that no chemical interactions were found between antioxidants and chitosan, after encapsulation. Antioxidant activity was evaluated by 2,2-azino-bis-(3-ethylbenzothiazoline-6-sulphonic acid) (ABTS) and oxygen radical absorbance capacity (ORAC) methods before and after lyophilization to assure that antioxidant activity was not compromised after the dried process. The best antioxidant activity results were obtained by ORAC method and after nanoparticles lyophilized, the values for rosmarinic acid, sage and savory nanoparticles were  $3.6520 \pm 0.1770$ ,  $0.4251 \pm 0.0069$  and  $0.4526 \pm 0.0087$   $\mu\text{mol}/\text{eq}$  Trolox, respectively. Nonetheless, lower antioxidant activity was observed in the nanoparticles comparing to the free compounds due to the partial entrapment effect of the compounds. Considering the mucin particle method, nanoparticles indicate mucoadhesive properties, by the increase on nanosize and the consequent surface charge decrease, after mucin incubation, suggesting an increase retention time over the ocular mucosa after instillation. All nanoparticles demonstrate to be safe without relevant cytotoxicity (below 10%, for all the formulations and concentrations), by methylthiazolyldiphenyl-tetrazolium bromide conversion (MTT) and lactate dehydrogenase enzyme release (LDH) assays against retina pigment epithelium (ARPE-19) and human cornea (HCE-T) cell lines. Nonetheless, the results in both cell lines were concentration dependent. Chorioallantoic membrane test (HET-CAM) also confirmed the absence of nanoparticles irritancy in the eye. The permeability study in HCE monolayer cell line showed apparent permeability coefficient ( $P_{app}$ ) of  $3.41 \pm 0.99 \times 10^{-5}$  and  $3.24 \pm 0.79 \times 10^{-5}$  cm/s for rosmarinic acid loaded chitosan nanoparticles and free in solution, respectively. In ARPE-19 monolayer cell line the  $P_{app}$  was  $3.39 \pm 0.18 \times 10^{-5}$  and  $3.60 \pm 0.05 \times 10^{-5}$  cm/s for rosmarinic acid loaded chitosan nanoparticles and free in solution, respectively. No significant differences ( $P > 0.05$ ) were achieved neither between both cell lines nor between loaded and unloaded chitosan nanoparticles, probably due to the rapid release profile of nanoparticles described above. Preliminary ocular *in vivo* studies were implemented to evaluate the antioxidant effect of rosmarinic acid through intravitreally injection in Wistar rats using an Ischemia-reperfusion (I-R) model. Electroretinograms

(ERG) and immunohistochemistry showed that at 50  $\mu$ M rosmarinic acid did not present a significant retina protective effect, suggesting acute pro-inflammatory damages in I-R model, difficult to revert with a single injection. Nonetheless and considering the good results achieved during this project, the rosmarinic acid nanoparticles were safe, mucoadhesive, with high ocular permeability, with good antioxidant activity performance and its therapeutical potential may be important to ocular diseases prophylaxis. It can be also concluded that these natural nanocarriers were promising ocular drug delivery systems and the study highlights the need to explore new drug delivery systems to be applied on ocular surface in order to overlap the limitations on topical drug effectiveness.

**Keywords:** Chitosan, rosmarinic acid, extracts, ocular diseases



## Resumo

As nanopartículas de quitosano foram desenvolvidas e otimizadas por gelificação iónica com tripolifosfato de sódio (TPP). O quitosano e TPP foram testados em diferentes concentrações para o estudo da melhor relação quitosano:TPP até à proporção final de (7:1). O pH da solução das nanopartículas foi ajustado para 5,8, para favorecer a interação máxima entre o quitosano e o ácido rosmarínico. A encapsulação de ácido rosmarínico, e dos extractos naturais de *Salvia officinalis* (salva) e *Satureja montana* (segurelha) também foram testados, considerando diferentes cargas teóricas relativamente à concentração inicial de quitosano. As nanopartículas foram preparadas e caracterizadas diretamente após a sua formulação e após liofilização, e foram posteriormente fixados os valores de carga teórica de 40% para o ácido rosmarínico e 50% para a salva e segurelha. O tamanho das partículas demonstrou ser dependente de ambas as concentrações de quitosano e TPP e os tamanhos mínimos foram obtidos para a menor concentração de quitosano e TPP. O tamanho médio das partículas foi  $244,0 \pm 18,0$ ,  $278,4 \pm 42,2$  e  $229,3 \pm 29,6$  nm para as nanopartículas de ácido rosmarínico, salva e segurelha, respetivamente. Não houve diferenças significativas ( $P > 0,05$ ) observadas entre as diferentes nanoformulações o que seria expectável, considerando que o sistema de nanopartículas foi otimizado para encapsular o ácido rosmarínico, e este é o principal componente dos extratos naturais. As nanopartículas obtidas apresentaram valores de baixo índice de polidispersão ( $< 0,25$ ), o que corresponde a uma reduzida distribuição do tamanho das partículas, sendo os valores:  $0,193 \pm 0,062$ ,  $0,268 \pm 0,092$  and  $0,149 \pm 0,121$  para as nanopartículas de ácido rosmarínico, salva e de segurelha, respetivamente. A carga da superfície das nanopartículas foi:  $29,5 \pm 1,6$ ,  $24,9 \pm 0,1$  and  $26,5 \pm 3,5$  mV para as nanopartículas de ácido rosmarínico, salva e de segurelha, respetivamente. Isto sugere que os sistemas coloidais são estáveis ao longo do tempo. A microscopia eletrónica de varrimento (SEM) e a microscopia eletrónica de transmissão (TEM) confirmaram os resultados anteriores e demonstraram nanopartículas individualizadas, lisas, esféricas e pequenas (variando entre 200-300 nm). A capacidade de carga das partículas foi de  $5,3 \pm 0,4$ ,  $8,1 \pm 0,6$  e  $7,8 \pm 0,2\%$  para as nanopartículas de ácido rosmarínico, salva e de segurelha, respetivamente. Os valores mais elevados para as nanopartículas com extrato foram intimamente correlacionados com a menor quantidade inicial de ácido rosmarínico nos nanosistemas. De um modo semelhante, as percentagens de eficiência de associação dos extratos nas nanopartículas foram mais elevadas, em comparação com as do ácido rosmarínico. Os valores foram:  $51,2 \pm 3,0$ ,

96,1 ± 0,2 e 98,2 ± 0,1% para as nanopartículas de ácido rosmarínico, salva e segurelha, respetivamente. Estes valores mais elevados associados à nanoencapsulação dos extratos também podem ser associados à menor quantidade de ácido rosmarínico nas nanopartículas de quitosano, uma vez que a concentração inicial é documentada como inversamente proporcional à própria eficiência de associação. O perfil de libertação *in vitro* do ácido rosmarínico foi avaliado em tampão fosfato (PBS), a pH 7,4 nas diferentes formulações, por um período de 60 min, e não se observaram diferenças significativas ( $P > 0,05$ ). A rápida libertação do ácido rosmarínico dá indicações que estes sistemas de nanopartículas podem fornecer uma estratégia racional para o desenvolvimento de formulações de libertação imediata para administração ocular do ácido rosmarínico. A eficiência de associação e de libertação *in vitro* foram realizadas utilizando um método de cromatografia líquida de alta eficiência (HPLC), especialmente desenvolvido e otimizado para garantir a obtenção de resultados precisos e exatos. As análises de calorimetria diferencial de varrimento (DSC) e a espectrofotometria de infravermelho por transformada de Fourier (FTIR) permitiram concluir que não foram encontradas interações químicas entre os antioxidantes e o quitosano, depois do processo de encapsulação. A atividade antioxidante dos nanosistemas foi avaliada pelos métodos de 2,2-azinobis-(3-etil-benzotiazolin-6-ácido sulfónico) (ABTS) e de capacidade de absorção radical (ORAC), antes e depois do processo de liofilização, para garantir que a atividade antioxidante não é comprometida durante o processo de secagem das partículas. Os melhores resultados de atividade antioxidante foram obtidos pelo método de ORAC após liofilização das partículas, os resultados para as nanopartículas de ácido rosmarínico, salva e segurelha foram: 3,6520 ± 0,1770, 0,4251 ± 0,0069 e 0,4526 ± 0,0087 μmol/eq Trolox, respetivamente. Todavia foi observada uma atividade antioxidante mais baixa nas nanopartículas do que nos compostos livres, devido ao efeito da nanoencapsulação. As partículas demonstraram propriedades mucoadesivas após incubação com mucina, pelo aumento em tamanho e conseqüente diminuição da carga de superfície. Os resultados indicam que pode ser expectável um aumento do tempo de retenção sobre a mucosa ocular após a instilação. Todas as formulações demonstraram ser seguras para o teste de citotoxicidade 3-(4,5-dimetiltiazol-2yl)-2,5-difenil brometo de tetrazolina (MTT) e para o teste da libertação da enzima lactato desidrogenase (LDH), sem citotoxicidade relevante (abaixo de 10%, para todas as formulações e concentrações), em linhas oculares da retina (epitélio pigmentar da retina - ARPE-19) e da córnea (linha de células da córnea humana - HCE-T). O teste da membrana corioalantóide (HET-CAM Teste) foi utilizado como alternativa aos testes biológicos em coelhos (teste de Draize) e também sugere a



ausência de irritação das partículas no olho. Os estudos de permeabilidade em monocamada de células da córnea (HCE) revelou um coeficiente de permeabilidade aparente ( $P_{app}$ ) de  $3,41 \pm 0,99 \times 10^{-5}$  e  $3,24 \pm 0,79 \times 10^{-5}$  cm / s para as nanopartículas de ácido rosmarínico e para o ácido rosmarínico livre, respectivamente. O estudo de permeabilidade em monocamada de células da retina (ARPE-19) revelou valores de  $P_{app}$  de  $3,39 \pm 0,18 \times 10^{-5}$  e  $3,60 \pm 0,05 \times 10^{-5}$  cm/s para as nanopartículas de ácido rosmarínico e para o ácido rosmarínico livre, respectivamente. Não houve diferença significativas ( $P > 0,05$ ) entre os valores de permeabilidade das nanopartículas, composto livre e entre ambas as linhas celulares, provavelmente devido ao perfil de liberação rápido das nanopartículas acima descrito. Foram feitos testes preliminares *in vivo*, em que o ácido rosmarínico foi injetado na cavidade intravítrea de ratos Wistar, num modelo animal isquemia-reperfusão (I-R). Eletroretinogramas (ERG) e ensaios imunohistoquímicos revelaram que o ácido rosmarínico (a uma concentração de: 50  $\mu$ M), por injeção intravítrea, não teve um efeito protector na retina. O que poderá ser devido danos pró-inflamatórias severos no modelo I-R, difíceis de reverter com o estudo de uma única injeção. No entanto, e considerando os bons resultados obtidos neste trabalho, as partículas de quitosano contendo ácido rosmarínico demonstraram ser seguras, mucoadesivas, com elevado potencial de permeabilidade ocular e com um bom perfil de atividade antioxidante, o que permite concluir que estes nanosistemas podem ser importantes para a prevenção de doenças degenerativas oculares. Os resultados desta tese, permitem também concluir que estes nanosistemas naturais são promissores na administração tópica de antioxidantes no olho e ressalta a necessidade de se explorar novos sistemas para ultrapassar as limitações na eficiência da administração tópica de fármacos no olho.

**Palavras-chave:** Quitosano, ácido rosmarínico, extratos, doenças oculares

This work was submitted as a PhD Thesis in partial fulfilment of the requirements for Philosophiæ Doctor (PhD) degree in Pharmaceutical Sciences at the Faculty of Pharmacy, University of Porto.

It was conducted under the guidance of Prof. Dr. Bruno Filipe Carmelino Cardoso Sarmiento, PhD, Affiliated Researcher at INEB - Instituto de Engenharia Biomédica and Assistant Professor at Instituto Superior de Ciências da Saúde-Norte (ISCS-N), and under the co-supervision of Prof. Dr. Maria Manuela Estevez Pintado, Assistant Professor at Biotechnology School of Portuguese Catholic University and Prof. Dr. Domingos Carvalho Ferreira, Full Professor of Faculty of Pharmacy, University of Porto.

The research experimental work was conducted at the Laboratory of Pharmaceutical Technology, Faculty of Pharmacy, University of Porto, in collaboration with CBQF - Biotechnology School of Portuguese Catholic University, INEB - Instituto de Engenharia Biomédica, ISCS-N - Instituto Superior de Ciências da Saúde – Norte and IBILI - Institute for Biomedical Imaging and Life Sciences – University of Coimbra.

## Scope and outline

This thesis was organized in 9 chapters, thus closely reflecting the development of my research work. All chapters were related to each other and the aims and methodology chosen in each chapter were indeed dependent on the conclusions brought about in previous one(s).

Overall, the work described in this thesis encompasses development and characterization of chitosan nanoparticles for the rosmarinic acid, sage and savory encapsulation - to prevent and control degenerative eye diseases.

**Part I** include **Chapter 1**, and entail a bibliographic review regarding chitosan biological proprieties, biomedical potential as well as chitosan-based delivery systems. A particular emphasis was put on the key factor of antioxidants in the degenerative eye diseases prophylaxis, as well as in the nanocarriers as a way to improve antioxidant activity performace and efficacy. In **Part II - Chapter 2**, the project aims and goals were detailed to be a guideline of the work major core. In **Part III - Chapter 3** a high-performance liquid chromatography (HPLC) method was developed and optimized to be used throughout the experimental work of this thesis and to allow the best precise quantification of antioxidant content in the natural extracts, the nanoparticles association efficiency and either release and permeability profiles, developed in the following chapters. In **Part IV - Chapter 4** a comprehensive development, optimization and physical-chemical characterization of antioxidant-chitosan nanoparticles was presented. The effect of rosmarinic acid content, mass correlation and pH of nanoparticle preparation were evaluated for the ionic gelation optimization process. Complementary methodologies were employed to provide a more rational understanding of the interactions between components and the success of the encapsulation, such as the particle size and zeta potential. In **Chapter 5** the nanocarriers were evaluated and characterized regarding the *in vitro* antioxidant activity potential. In **Part V - Chapter 6** the nanocarriers were then tested to guarantee their safety performance, mucoadhesion proprieties and *in vitro* ocular cell permeability. In **Chapter 7**, it was performed the first attempting efforts to prove rosmarinic acid therapeutical potential in an ischemia-reperfusion (I-R) animal model. Finally, in **Part VI**, the overall conclusions were presented in **Chapter 8** - and future prospects, based on critical questions arising from this dissertation, were put forward in **Chapter 9**.

Most information presented in the 9 chapters that constitute this dissertation has been already submitted to international peer review, via publication in scientific journals – according to the following list:

## Part I:

### Chapter 1 – State of the art

Baptista da Silva S., Costa J., Pintado M., Ferreira D., Sarmiento B. (2010). Antioxidants in the prevention and treatment of diabetic retinopathy – A Review. *Jornal of Diabetes and Metabolism* 1:111. doi:10.4172/2155-6156.1000111.

Baptista da Silva S., Fernandes J., Tavira F., Pintado M., Sarmiento B. (2011). The potential of chitosan in drug delivery systems. In *Focus on Chitosan Research*, Edited by Arthur N. Ferguson and Amy G. O'Neill, Nova Publishers, ISBN: 978-1-61324-454-8.

Tavaria, F., Fernandes, J., Santos-Silva, A., Baptista da Silva, S., Sarmiento, B. and Pintado, M. (2011). Biological activities of chitin, chitosan and respective oligomers. In *Focus on Chitosan Research*, Edited by Arthur N. Ferguson and Amy G. O'Neill, Nova Publishers, ISBN: 978-1-61324-454-8.

Andrade F., Antunes F., Nascimento V., Batista da Silva S., Neves J., Ferreira D., Sarmiento B. (2011). Chitosan formulations as carriers for therapeutic proteins. *Current Drug Discovery Technologies*. 8(3):157-172. doi: 10.2174/157016311796799035.

Sarmiento B., Andrade F., Baptista da Silva S., Rodrigues F., Neves J., Ferreira D. (2012). Cell-based *in vitro* models for predicting drug permeability. *Expert Opinion on Drug Metabolism and Toxicology*. 8(5):607-621. doi: 10.1517/17425255.2012.673586.

Silva N., Baptista da Silva S., Sarmiento B., Pintado M. (2013). Chitosan nanoparticles for daptomycin delivery in ocular treatment of bacterial endophthalmitis. *Drug Delivery*, doi: 10.3109/10717544.2013.858195.

Baptista da Silva S., Borges S., Ramos O., Pintado M., Ferreira D., Sarmiento B. (2014). Treating retinopathies: Nanotechnology as a tool in protecting antioxidants agents in

Systems Biology of Free Radicals and Antioxidants. Springer-Verlag (Germany), ISBN: 978-3-642-30017-2.

Baptista da Silva S., Borges S., Pintado M., Sarmiento B. (2014). Formulation of essential oils in pharmaceutical dosage forms - biopharmaceutics and therapeutic potentials, *Pharmaceutical Biology*. (Accepted for publication).

Vasconcelos T., Baptista da Silva S., Ferreira D., Pintado M., Marques S. (2015). Cell-based *in vitro* models for ocular permeability studies. In *Concepts and Models for Drug Permeability Studies: Cell and Tissue-based in vitro Culture Models*. Edited by Bruno Sarmiento, Elsevier. (Accepted for publication).

### **Part III:**

#### **Chapter 3 - High-performance liquid chromatographic method validation;**

Baptista da Silva S., Oliveira A., Ferreira D., Sarmiento B., Pintado M. (2013). Development and validation method for simultaneous quantification of phenolic compounds in natural extracts and nanosystems. *Phytochemical Analysis*. 24(6): 638-644. doi: 10.1002/pca.2446.

### **Part IV:**

#### **Chapter 4 - Development, optimization and physical-chemical characterization of chitosan-based nanoparticles;**

#### **Chapter 5 - *In vitro* assessment of antioxidant activity of chitosan-based nanoparticles;**

Baptista da Silva S., Amorim M., Fonte P., Madureira R., Ferreira D., Pintado M., Sarmiento B. (2015). Natural extracts into chitosan nanocarriers for rosmarinic acid drug delivery. *Pharmaceutical Biology*. doi:10.3109/13880209.2014.935949.

**Part V:**

**Chapter 6 - *In vitro* evaluation of cytotoxicity, mucoadhesion and ocular permeability of rosmarinic acid into chitosan-based nanoparticles;**

**Chapter 7 - Therapeutical potential evaluation in ischemia-reperfusion animal model of chitosan based-nanoparticles;**

Baptista da Silva S., Ferreira D., Pintado M., Sarmiento B. Evaluation of chitosan-based nanoparticles for ocular delivery of rosmarinic acid through *in vitro* mucoadhesion and permeability studies, submitted for publication.

## List of contents

<b>DECLARATION</b> .....	<b>IV</b>
<b>INSPIRATION</b> .....	<b>V</b>
<b>DEDICATION</b> .....	<b>VI</b>
<b>ACKNOWLEDGEMENTS</b> .....	<b>VII</b>
<b>ABSTRACT</b> .....	<b>XI</b>
<b>RESUMO</b> .....	<b>XV</b>
<b>SCOPE AND OUTLINE</b> .....	<b>XIX</b>
<b>LIST OF FIGURES</b> .....	<b>XXVIII</b>
<b>LIST OF TABLES</b> .....	<b>XXXI</b>
<b>LIST OF ABBREVIATIONS</b> .....	<b>XXXII</b>
<b>PART I - INTRODUCTION</b> .....	<b>1</b>
CHAPTER 1 - STATE OF ART .....	<b>3</b>
<b>1. INTRODUCTION</b> .....	<b>5</b>
<b>2. CHITOSAN PROPRIETIES AND BIOMEDICAL APPLICATION</b> .....	<b>8</b>
<b>2.1. CHITOSAN-BASED DRUG DELIVERY SYSTEMS</b> .....	<b>10</b>
2.1.1. CHITOSAN SOLUTIONS .....	<b>11</b>
2.1.2. FILMS .....	<b>12</b>
2.1.3. TABLETS.....	<b>14</b>
2.1.4. HYDROGELS.....	<b>16</b>
2.1.5. MICROPARTICLES .....	<b>19</b>
2.1.6. NANOPARTICLES .....	<b>21</b>
<b>2.2. CLINICAL TRIAL - SAFETY AND TOLERABILITY OF CHITOSA-N-ACETYLCYSTEINE EYE DROPS IN HEALTHY YOUNG VOLUNTEERS</b> .....	<b>23</b>
<b>3. OXIDATIVE PRODUCTS AND THE CLINICAL IMPORTANCE OF ANTIOXIDANTS</b>	<b>24</b>
3.1.1. TYPES OF ANTIOXIDANTS AGENTS.....	<b>25</b>
3.1.2. PHYSIOLOGY AND PATHOBIOLOGY OF REACTIVE OXYGEN SPECIES IN RETINOPATHIES .....	<b>27</b>

3.1.3.    OXIDATIVE STRESS IMBALANCE AND RETINAL AFFECTED DISEASES .....	29
<b>4.    NANOTECHNOLOGY APPLIED TO ANTIOXIDANTS PROTECTION.....</b>	<b>30</b>
4.1.    NANOANTIOXIDANTS PHARMACOTHERAPY .....	35
4.2.    SAFETY ISSUES OF ANTIOXIDANT NANOPARTICLES .....	36
<b>5.    SUMMARY .....</b>	<b>38</b>
<b>PART II - AIMS AND GOALS .....</b>	<b>39</b>
CHAPTER 2 - AIMS AND ORGANIZATION OF THE THESIS.....	41
<b>PART III.....</b>	<b>45</b>
<b>ABSTRACT .....</b>	<b>47</b>
CHAPTER 3 - HIGH-PERFORMANCE LIQUID CHROMATOGRAPHY METHOD VALIDATION .....	49
<b>3.    INTRODUCTION.....</b>	<b>51</b>
<b>3.1.    EXPERIMENTAL.....</b>	<b>52</b>
3.1.1.    MATERIALS .....	52
3.1.2.    EQUIPMENT AND CHROMATOGRAPHIC CONDITIONS .....	52
3.1.3.    PREPARATION OF STANDARD AND SAMPLE SOLUTIONS.....	53
3.1.4.    METHOD VALIDATION .....	53
3.1.5.    METHOD APPLICABILITY .....	54
<b>3.2.    RESULTS AND DISCUSSION .....</b>	<b>54</b>
3.2.1.    APPLICATION OF THE CHROMATOGRAPHIC METHOD .....	54
3.2.2.    LINEARITY.....	55
3.2.3.    PRECISION.....	56
3.2.4.    ACCURACY .....	58
3.2.5.    SPECIFICITY .....	58
3.2.6.    RANGE .....	59
3.2.7.    ROBUSTNESS.....	59
3.2.8.    DETECTION LIMIT AND QUANTITATION LIMIT .....	59
3.2.9.    METHOD APPLICABILITY .....	60
<b>3.3.    CONCLUSION .....</b>	<b>61</b>
<b>PART IV.....</b>	<b>63</b>
<b>ABSTRACT .....</b>	<b>65</b>



CHAPTER 4 - DEVELOPMENT, OPTIMIZATION AND PHYSICAL-CHEMICAL CHARACTERIZATION OF CHITOSAN-BASED NANOPARTICLES .....	67
<b>4. INTRODUCTION.....</b>	<b>69</b>
<b>4.1. EXPERIMENTAL.....</b>	<b>70</b>
4.1.1. MATERIALS .....	70
4.1.2. PREPARATION OF CHITOSAN-BASED NANOPARTICLES .....	70
4.1.3. ENCAPSULATION OF SAGE, SAVORY AND ROSMARINIC ACID INTO CHITOSAN-BASED NANOPARTICLES.....	71
4.1.4. SIZE AND SURFACE CHARGE.....	71
4.1.5. MORPHOLOGY.....	72
4.1.6. ASSOCIATION EFFICIENCY .....	72
4.1.7. <i>IN VITRO</i> RELEASE OF ROSMARINIC ACID FROM CHITOSAN NANOPARTICLES .....	73
4.1.8. HIGH PERFORMANCE LIQUID CHROMATOGRAPHY ANALYSIS AND ROSMARINIC ACID QUANTIFICATION.....	73
4.1.9. DIFFERENTIAL SCANNING CALORIMETRY ANALYSIS.....	74
4.1.10. FOURIER-TRANSFORM INFRARED ANALYSIS.....	74
4.1.11. STATISTICAL ANALYSIS .....	75
<b>4.2. RESULTS AND DISCUSSION .....</b>	<b>75</b>
4.2.1. PARTICLE SIZE, POLYDISPERSITY AND ZETA POTENTIAL.....	75
4.2.2. MORPHOLOGY.....	77
4.2.3. ASSOCIATION EFFICIENCY AND DRUG LOADING .....	79
4.2.4. <i>IN VITRO</i> ROSMARINIC ACID RELEASE FROM CHITOSAN NANOPARTICLES .....	80
4.2.5. THERMAL BEHAVIOR BY DIFFERENTIAL SCANNING CALORIMETRY ANALYSIS.....	82
4.2.6. SPECTROSCOPY BY FOURIER-TRANSFORM INFRARED ANALYSIS.....	85
<b>4.3. CONCLUSION .....</b>	<b>88</b>
CHAPTER 5 – <i>IN VITRO</i> ASSESSMENT OF ANTIOXIDANT ACTIVITY OF CHITOSAN-BASED NANOPARTICLES.....	89
<b>5. INTRODUCTION.....</b>	<b>91</b>
<b>5.1. EXPERIMENTAL.....</b>	<b>91</b>
5.1.1. MATERIALS .....	91
5.1.2. SAMPLE PREPARATION .....	92
5.1.3. CHITOSAN NANOPARTICLES DEVELOPMENT AND OPTIMIZATION.....	92

5.1.4.	ENCAPSULATION OF SAGE, SAVORY AND ROSMARINIC ACID INTO CHITOSAN NANOPARTICLES.....	93
5.1.5.	ANTIOXIDANT CAPACITY ASSESSMENT.....	93
5.1.5.1.	<i>2,2-azinobis (3-ethylbenzothiazoline-6-sulphonic acid) method</i> .....	93
5.1.5.2.	<i>Oxygen radical absorbance capacity</i> .....	94
5.1.6.	STATISTICAL ANALYSIS .....	94
<b>5.2.</b>	<b>RESULTS AND DISCUSSION .....</b>	<b>94</b>
5.2.1.	ANTIOXIDANT ACTIVITY MEASUREMENT .....	94
<b>5.3.</b>	<b>CONCLUSION .....</b>	<b>97</b>
<b>PART V</b> .....		<b>99</b>
<b>ABSTRACT</b> .....		<b>101</b>
	CHAPTER 6 - IN VITRO EVALUATION OF CYTOTOXICITY, MUCOADHESION AND OCULAR PERMEABILITY OF ROSMARINIC ACID INTO CHITOSAN-BASED NANOPARTICLES .....	103
<b>6.</b>	<b>INTRODUCTION.....</b>	<b>105</b>
<b>6.1.</b>	<b>EXPERIMENTAL.....</b>	<b>106</b>
6.1.1.	MATERIALS AND CELLS .....	106
6.1.2.	PREPARATION AND CHARACTERIZATION OF ANTIOXIDANT-CONTAINING CHITOSAN NANOPARTICLES.....	107
6.1.3.	SIZE AND SURFACE CHARGE.....	107
6.1.4.	ASSOCIATION EFFICIENCY.....	107
6.1.5.	MUCOADHESION PROPRIETIES EVALUATION BY MUCIN INTERACTION METHOD....	108
6.1.6.	CELL VIABILITY AND CYTOTOXICITY OF NANOPARTICLES .....	109
6.1.6.1.	<i>Cytotoxicity test using chorioallantoic membrane</i> .....	110
6.1.7.	PERMEABILITY STUDIES .....	111
6.1.7.1.	<i>Cell monolayers culture</i> .....	111
6.1.7.2.	<i>Transepithelial electrical resistance</i> .....	111
6.1.7.3.	<i>Permeation studies in cell monolayers</i> .....	111
6.1.7.4.	<i>High performance liquid chromatography analysis</i> .....	112
6.1.8.	STATISTICAL ANALYSIS .....	112
<b>6.2.</b>	<b>RESULTS AND DISCUSSION .....</b>	<b>113</b>
6.2.1.	PARTICLE SIZE, POLYDISPERSITY AND ZETA POTENTIAL.....	113
6.2.2.	ASSOCIATION EFFICIENCY AND LOADING CAPACITY .....	114

6.2.3.	MUCOADHESION PROPRIETIES EVALUATION BY MUCIN INTERACTION METHOD ....	115
6.2.4.	CELL VIABILITY STUDIES .....	116
6.2.5.	PERMEABILITY ASSAYS .....	121
<b>6.3.</b>	<b>CONCLUSION .....</b>	<b>125</b>
	CHAPTER 7 - THERAPEUTICAL POTENTIAL EVALUATION IN ISCHEMIA-REPERFUSION ANIMAL MODEL OF CHITOSAN BASED-NANOPARTICLES .....	127
<b>7.</b>	<b>INTRODUCTION.....</b>	<b>129</b>
<b>7.1.</b>	<b>EXPERIMENTAL.....</b>	<b>130</b>
7.1.1.	ANIMALS AND DRUG ADMINISTRATION .....	130
7.1.2.	INTRAVITREAL ADMINISTRATION OF ROSMARINIC ACID .....	130
7.1.3.	ELECTRORETINOGRAM RECORDINGS .....	130
7.1.4.	RETINAL ISCHEMIA-REPERFUSION INJURY .....	131
7.1.5.	PREPARATION OF FROZEN RETINAL SECTIONS .....	131
7.1.6.	TERMINAL DEOXYNUCLEOTIDYL TRANSFERASE-MEDIATED DUTP NICK END LABELING (TUNEL) ASSAY .....	132
7.1.7.	IMMUNOHISTOCHEMISTRY .....	132
7.1.8.	IMAGE ANALYSIS.....	133
<b>7.2.</b>	<b>RESULTS AND DISCUSSION .....</b>	<b>133</b>
7.2.1.	DIFFERENTIAL EFFECTS OF ROSMARINIC ACID ON ELECTRORETINOGRAMS .....	133
7.2.2.	EFFECT OF ROSMARINIC ACID ON RETINAL ISCHEMIA-REPERFUSION INJURY RAT MODEL - MICROGLIAL REACTIVITY .....	135
7.2.3.	EFFECT OF ROSMARINIC ACID ON CELL DEATH AND RETINAL GANGLION CELL LOSS 137	
<b>7.3.</b>	<b>CONCLUSION .....</b>	<b>138</b>
<b>PART VI.....</b>		<b>141</b>
	CHAPTER 8 - GENERAL CONCLUSIONS.....	143
	8. <i>Conclusions</i> .....	145
	9. <i>Future prospects</i> .....	151
<b>REFERENCES.....</b>		<b>153</b>

## List of figures

Figure 1. 1. Structure and molecular formula of chitosan.....	9
Figure 1. 2. Schematic illustration of eye structure and subsequent critical biological barriers that drugs need to overcome after topical administration onto the eye surface. .	28
Figure 1. 3. Schematic view of the ocular permeability, physiological barriers, and transport pathways of a drug applied topically onto the eye.....	29
Figure 1. 4. Classification of antioxidants and characterization of some nanostructures. Highlights to real benefits of antioxidants encapsulation considering its liberation, absorption, distribution, metabolism, elimination and response. ....	31
Figure 3. 1. Representative chromatogram of: (i). rosmarinic acid (retention time: $48.9 \pm 0.1$ min) and (ii). quercetin (retention time: $57.9 \pm 0.6$ min); (a). in standard solutions; (b). in sage extracts; (c). and savory extracts. ....	60
Figure 4. 1. Schematic illustration of ionic gelation process of antioxidant-chitosan based nanoparticles.....	71
Figure 4. 2. TEM micrographs of fresh chitosan-based nanoparticles loaded: (a). commercial rosmarinic acid; (b). sage; and (c). savory. ....	77
Figure 4. 3. SEM micrographs of lyophilized chitosan-based nanoparticles loaded: (a). commercial rosmarinic acid; (b). sage; and (c). savory. ....	78
Figure 4. 4. Rosmarinic acid <i>in vitro</i> release from rosmarinic acid, sage and savory chitosan-based nanoparticles.....	81
Figure 4. 5. Thermogram of: I.(a). chitosan empty nanoparticles; (b). free rosmarinic acid; (c). rosmarinic acid and chitosan physical mixture (mixing ratio 1:1); (d). rosmarinic acid encapsulated in chitosan nanoparticles (at a theoretical 40% loading) (d). II.(a). chitosan empty nanoparticles; (b). free sage; (c). sage and chitosan physical mixture (mixing ratio 1:1); (d). sage encapsulated in chitosan nanoparticles (at a theoretical 50% loading). III.(a). chitosan empty nanoparticles; (b). free savory; (c). savory and chitosan physical mixture (mixing ratio 1:1); (d). savory encapsulated in chitosan nanoparticles (at a theoretical 50% loading).....	84

Figure 4. 6. Spectrum of: I. (a). chitosan empty nanoparticles; (b). rosmarinic acid in a free form; (c). physical mixture between chitosan unloaded nanoparticles and rosmarinic acid (mixing ratio 1:1); (d). rosmarinic acid encapsulation into chitosan nanoparticles. II.(a). chitosan empty nanoparticles; (b). sage in a free form; (c). physical mixture between chitosan unloaded nanoparticles and sage (mixing ratio 1:1); (d). sage encapsulation into chitosan nanoparticles. III.(a). chitosan empty nanoparticles; (b). savory in a free form; (c). physical mixture between chitosan unloaded nanoparticles and savory (mixing ratio 1:1); (d). savory encapsulation into chitosan nanoparticles..... 87

Figure 6. 1. Effect of rosmarinic acid, sage and savory-loaded chitosan nanoparticles on cell cytotoxicity of ARPE (A, C and E) and HCE (B, D and F) cell lines after 4 h (black bar) and 24 h (white bar) of incubation. DMEM+cells and DMSO were used as controls. The formulation concentration used was displayed in the tables, relatively to rosmarinic acid (A, B), sage (C, D) and savory (E, F) (results were the mean of 6 replicates, bars represent standard deviation)..... 117

Figure 6. 2. Effect of rosmarinic acid, sage and savory-loaded chitosan nanoparticles on viability of ARPE (A, C and E) and HCE (B, D and F) cell lines after 4 h (black bar) and 24 h (white bar) of incubation. DMEM+cells and DMSO were used as controls. The formulation concentration used was displayed in the tables, relatively to rosmarinic acid (A, B), sage (C, D) and savory (E, F) (results were the mean of 6 replicates, bars represent standard deviation)..... 119

Figure 6. 3. Cumulative transport and TEER cell monolayer measurements of rosmarinic acid loaded chitosan-based nanoparticles and free in solution across HCE-T model cells (Values were means of 6 replicates, bars represent standard deviation). ..... 124

Figure 6. 4. Cumulative transport and TEER cell monolayer measurements of rosmarinic acid loaded chitosan-based nanoparticles and free in solution across ARPE-19 model cells (Values were means of 6 replicates, bars represent standard deviation). ..... 125

Figure 7. 1. Electroretinogram of mixture response of both rods and cones cell populations either in photopic or scotopic conditions ( $\alpha$  and  $\beta$  – waves) recordings of rosmarinic acid administration effect. Left eye: representative traces of individual ERG recorded 24 h before treatment injection (Baseline ERG – blue line) and 24 h after intravitreal injection in I-R model (red line); Right eye: representative traces of individual ERG recorded 24 h

before treatment injection (Baseline ERG – blue line) and 24 h after intravitreal injection (red line)..... 134

Figure 7. 2. Rosmarinic acid effect on activated microglia induced by I-R injury at 24 h of reperfusion retinal. Retinal sections were stained with antibodies against Iba1 (green) and OX-6 (red). Nuclei were stained with DAPI (blue). Representative images were depicted in: Activated microglia/macrophages (Iba 1 - OX-6 immunoreactive cells), comparing with saline ischemial..... 136

Figure 7. 3. Rosmarinic acid administration did not altered the cell death induced by I-R injury at 24 h of reperfusion. Cell death was assayed with TUNEL assay. Nuclei were stained with DAPI (blue). Representative images were depicted in: TUNEL+ cells (green) comparing with saline intravitreal and ischemial..... 138

## List of tables

Table 1. 1. Principal properties of chitosan in relation to its use in biomedical applications. .....	10
Table 1. 2. Recent published data of antioxidants nanoencapsulation for several applications. ....	33
Table 3. 1. Results of precision tests for the determination of rosmarinic acid and quercetin in standard solutions. ....	56
Table 3. 2. Accuracy results for different levels of rosmarinic acid and quercetin in standard solutions. ....	58
Table 4. 1. Average hydrodynamic diameter ( <i>Z</i> ), polydispersity index ( <i>Pdl</i> ), zeta potential and the association efficiency considering the different loading (%) of rosmarinic acid, sage and savory nanoparticles (n = 3). ....	76
Table 4. 2. Association efficiency, theoretical loading, and final rosmarinic acid content in chitosan nanoparticles. ....	80
Table 4. 3. Peak temperatures in the DSC thermograms collected from chitosan, rosmarinic acid, sage and savory, physical mixtures, and nanoparticles. ....	82
Table 5. 1. Antioxidant activity measurements by ABTS and ORAC, considering the 50% loading ( <i>m/m</i> ) sage and savory nanoparticles; and 40% loading ( <i>m/m</i> ) of and rosmarinic acid nanoparticles for (n = 3). ....	96
Table 6. 1. Average hydrodynamic diameter ( <i>Z</i> ), polydispersity index ( <i>Pdl</i> ) and zeta potential of chitosan nanoparticles loaded rosmarinic acid, sage and savory. ....	114
Table 6. 2. Average hydrodynamic diameter ( <i>Z</i> ), polydispersity index ( <i>Pdl</i> ) and zeta potential of chitosan nanoparticles loaded rosmarinic acid before and after mucin interaction (n = 3). ....	116
Table 6. 3. Cytotoxicity of rosmarinic acid, sage and savory-loaded chitosan nanoparticles for development of irritation symptoms such as vasoconstriction, hemorrhage and coagulation. ....	121

## List of abbreviations

**ABTS** - 2,2-Azinobis (3-Ethylbenzothiazoline-6-Sulphonic) Acid

**AE** - Association Efficiency

**AGE** - Advanced Glycation End Products

**AMD** - Age Macular Degeneration

**ANOVA** - One-Way Analysis of Variance

**ARVO** - Association for Research in Vision and Ophthalmology

**BAB** - Blood-Aqueous Barrier

**BRB** - Blood-Retinal Barrier

**CAT** - Catalase

**CBQF** - Centro de Biotecnologia e Química Fina

**Copper** - Cu

**Da** - Dalton

**DAPI** - 4',6-Diamidino-2-Phenylindole

**DD** - Deacetylation Degree

**DL** - Detection Limit

**DMEM** - Dulbecco's Modified Eagle's Medium

**DMSO** - Dimethyl Sulfoxide

**DNA** - Desoxyribonucleic Acid

**DPPH** - Diphenyl-1-Picrylhydrazyl

**DSC** - Differential Scanning Calorimetry

**EMA** - European Medicines Agency

**ERG** - Electroretinograms

**FDA** - Food and Drug Administration

**FFUP** - Faculdade de Farmácia da Universidade do Porto

**FTIR** - Fourier Transform Infrared

**GCL** - Ganglion Cell Layer

**GNP** - Gold Nanoparticles

**GPx** - Glutathione peroxidase

**GSH** - Glutathione

**HBA** - p - Hydroxybenzyl Alcohol

**HBSS** - Hanks' Balanced Salt Solution

**HCE-T** - Human Cornea Cell Line

**HET-CAM** - Chorioallantoic Membrane Test



**HPLC** - High Performance Liquid Chromatography  
**HPOX** - Hydroxybenzyl Alcohol Incorporated Copolyoxalate  
**IBILI** - Institute for Biomedical Imaging and Life Sciences  
**INEB** - Instituto de Engenharia Biomédica  
**INL** - Inner Nuclear Layer  
**IOBA – NHC** - Immortalized Epithelial Cell Line from Human Conjunctiva  
**IOP** - Intraocular Pressure  
**IPL** - Inner Plexiform Layer  
**I-R** - Ischemia-Reperfusion  
**ISCS-N** - Instituto Superior de Ciências da Saúde – Norte  
**LCPUFA** - Long-Chain Polyunsaturated Fatty Acid  
**LDH** - Lactate Dehydrogenase  
**MNP** - Magnetically Responsive Nanoparticles  
**MnSOD** - Superoxide Dismutase  
**MSc** - Master of Science  
**MTT** - Thiazolyl Blue Tetrazolium Bromide  
**MW** - Molecular Weight  
**NR** - Rosmarinic Acid Nanoparticles  
**NSG** - *Satureja montana* Nanoparticles  
**NSV** - *Salvia officinalis* Nanoparticles  
**OCT** - Optimal Cutting Temperature  
**ORAC** - Oxygen Radical Absorbance Capacity  
**OS** - Oxidative Stress  
**Papp** - Apparent Permeability Coefficient  
**PBS** - Phosphate Buffer Saline  
**PdI** - Polydispersity Index  
**PhD** - Philosophiæ Doctor  
**PLA** - Polylactic Acid  
**PP** - Polypropylene  
**PUFA** - Polyunsaturated Fatty Acid  
**PVA** - Poly (Vinyl Alcohol)  
**QL** - Quantification Limit  
**QUEN** - Quercetin Nanoparticles  
**RGC** - Retinal Ganglion Cells  
**ROS** - Reactive Oxygen Species

**RPE** - Retina Pigment Epithelium  
**rpm** - Rotations per Minute  
**RSD** - Relative Standard Deviation  
**SD** - Standard Deviation  
**SEM** - Scanning Electron Microscopy  
**SiNPs** - Silicate Nanoparticles  
**SOD** - Superoxide dismutase  
**TEM** - Transmission Electron Microscopy  
**TPP** - Tripolyphosphate  
**TUNNEL** - Terminal Deoxynucleotidyl Transferase (TdT)-Mediated dUTP Nick End Labeling  
**UV** - Ultra-Violet  
**v** - Volume  
**VEGF** - Vascular Endothelial Growth Factor  
**w** - Weight  
**Zn** - Zinc

# PART I - Introduction

---

*“Somewhere, something incredible is waiting to be known”*

Carl Sagan



## *CHAPTER 1 - State of art*

---



## 1. Introduction

In pharmaceutical science there is a continuous blockbuster drug development, and nowadays biomolecules as active agents, are widely explored to develop new therapeutics. Nevertheless, most of these new active compounds are unstable and must be protected from degradation in the physiological environment, due to the poor absorption that constrains the transport across biological barriers. Thus, the efficacy of most drugs clearly depends on the design of appropriate carriers for their physical protection, delivery and controlled release (1). Among the different approaches explored so far, colloidal carriers are particularly interesting, especially those made of mucoadhesive polymers to assure their epithelium permanence (2, 3). For this application, chitosan has had quite impact in the association and delivery of labile macromolecular compounds (4). Chitosan carriers have an exceptional potential for drug delivery, especially for mucosal, since these systems are stable in contact with physiological fluids and barriers. They are also able to control drug release and protect against adverse conditions like mucosal enzymes and biological protective fluids. Due to its mucoadhesion, particle size, particle surface chemistries, charge and the unique absorption enhancing properties, the chitosan potential in the medical field is widely promising. Different formulations such as films, tablets, hydrogels, micro and nanosystems are expected to optimize, characterize and select the drug performance, improved properties and increase stability for great specific applications. Pharmacokinetics and toxicological relevance of chitosan systems are guaranteed by *in vitro* model systems in molecular, subcellular and cellular levels, as well as their therapeutic efficacy and safety performance should also be proven *in vivo*. One category of compounds in which these chitosan carriers may be a key for success, are the antioxidants. Considering the biology definition, antioxidants are chemical compounds or a substance that inhibits oxidation, counteracting the damage of free radicals effects in a living organism, and for this reason are reactive species (5). Antioxidants are widespread virtually in plant foods, often at high levels, and include phenols, phenolic acids and flavonoids (6). Rosmarinic acid ( $\alpha$ -O-caffeoyl-3,4-dihydroxyphenyllactic acid) (7) is a phenolic compound, which can provide protection against cancer (7) and have other multitude biological activities, namely adstringent, anti-inflammatory, anti-mutagen, antibacterial and antiviral (7, 8). The latter activity has been tested in the therapy of Herpes simplex infections with rosmarinic acid-containing extracts of *Melissa officinalis* (7). It is also one of the efficient natural antioxidants (9) since rosmarinic acid displays a

huge potential radical scavenging activity, higher than trolox (a derivative of  $\alpha$ -tocopherol) (10-12). Rosmarinic acid has also an anti-angiogenic activity to retinal neovascularization in a mouse model of retinopathy (13). Significantly inhibited the proliferation of retinal endothelial cells in a dose-dependent manner, and inhibited *in vitro* angiogenesis of tube formation. Moreover, rosmarinic acid showed no retinal toxicity. These data suggest rosmarinic acid could be a potent inhibitor of retinal neovascularization and may be applied in the treatment of vasoproliferative retinopathies (13). It is the major component of *Salvia officinalis* (sage) and *Satureja montana* (savory) natural extracts. These are plants often used in traditional medicine, and which grow in the poor soils of the Mediterranean basin (14). Besides application as condiment, sage and savory have been used as an anti-diarrhea vector, digestion adjuvant, contribute to heal wounds, play an anti-inflammatory role, disinfectant, fight insomnia and decrease blood pressure. Some of these biological activities have been associated with its high contents of rosmarinic acid and the presence of other relevant phenolic compounds such as quercetin and rutin (9, 14). Beyond the biological huge benefits, antioxidants are extremely sensitive to light, oxygen, are highly reactive with other compounds, in some cases possess poor solubility, inefficient permeability, and are extremely unstable (15-17). For all these reasons their delivery using the conventional dosage forms is a challenge (18). In this context, alternative carriers are being considered, regarding the optimization of pharmacokinetics and pharmacodynamics of antioxidant molecules. Chitosan nanoparticles, due to their proper properties, are on the raw. For this concern the nanotechnology is expected to increase the ability, to retain the antioxidant activity during the preparation process, to optimize the release of the compound from the carrier system, and to ensure a good control of their physical-chemical properties increasing their stability. If these nanocarriers may improve the efficacy performance of the antioxidants, several diseases like cancer, diabetes, hypertension, arterio-sclerosis, cardiovascular disease or ocular anomalous conditions that have a clinical impairment with oxidation processes, may be prevented or better controlled (19). Considering the eye disorders, there are many types of retinopathies conditions that may have an oxidative etiology (20, 21), like retinitis pigmentosa, glaucoma, macular degeneration, retinoblastoma and diabetic retinopathy (19, 21). Multiple factors have been also proposed to explain retinopathies, including genetic disorders, infections by microbial agents, sorbitol pathway hyperactivity, accumulation of advanced glycation end products (AGEs) (22) and protein kinase C activation (23). Nevertheless the precise pathological mechanism remains to be elucidated. Which is clear is the collateral damage of these disorders, that may result on



reflectivity changes, bifurcations, tortuosity neovascularization as well as other patterns of blood vessels and even blindness (19, 21). In the case of ocular pathologies the oxidative stress (OS) clinical impairment has a significant impact, since the ocular globe is the organ most affected by OS. Its constantly expose to light and oxygen and its high polyunsaturated fatty acid (PUFA) content that is prone to lipid peroxidation, may be some prominent reasons (24). OS is also associated with increased vascular permeability, disruption of blood-retinal barrier, apoptotic loss of retinal capillary cells, microvascular abnormalities and neovascularization (25). High levels of OS are also usually associated with increased levels of oxidative modified desoxyribonucleic acid (DNA) and nitrosylated proteins, and antioxidant defense enzymes impair (26). When such damages are presented, without effective medical treatment, cells and tissues of the retina become malnourished and progressively degenerate, which leads to damage in cells responsible for vision, leading to its inevitable loss (21). Due to this intimate relationship between OS and the pathogenesis of retinopathies, the use of appropriate antioxidants may have potential on the metabolic and functional abnormalities in retinopathies (27). Nevertheless, for antioxidants assure these conditions they need the nanocarrier support to take them to the right place without losing their functional activity.

## 2. Chitosan proprieties and biomedical application

Chitosan is an alkaline-deacetylated chitin biodegradable polysaccharide commonly derived from the exoskeletons shells of crustaceans and insects (28). Its extraction is a cost-effective way to valorise seafood wastes and it is produced with different deacetylation degrees (DD) (29, 30), and molecular weights (MW) (31). Chitin is synthesized by an enormous number of living organisms and considering the amount of chitin produced annually in the world, it is the most abundant polymer after cellulose (29). Chitin is obtained on an industrial scale from shrimp and crustaceans in general. The pupae of silkworms are also an alternative source of chitin and, consequently, of chitosan (32). Other sources include the production of chitosan from fungi by fermentation (33), from chrysalides (a by-product from the silk industry) (32), or from sources of chitin (e.g.  $\beta$ -chitin) obtained from squid pens (4). However, the most commonly obtained form of chitosan is the  $\alpha$ -chitosan from crustacean, which represents approximately 70% of the organic compounds in such shells (4).

For the chitin isolation from the raw materials and subsequent chitosan production, the original sources in solid form are washed with water, desiccated at room temperature and cut into small pieces. Demineralization is carried out at room temperature using hydrochloric acid and the de-proteinization should also be performed (32).

There are small differences in the chemical structure of chitin and chitosan, but these differences are extremely important when drug delivery is thought (34). Considering the similar structures of chitin and chitosan with cellulose, both are made by linear  $\beta$ -(1-4)-linked monosaccharides. However, the functional groups connected to the second carbon in the repeating units differ from one to another (35). Chitin is a linear homopolymer composed of  $\beta$ -(1,4)-linked *N*-acetyl-glucosamine units (34), while chitosan is a linear copolymer polysaccharide consisting of  $\beta$ -(1-4)-linked 2-amino-2-deoxy-D-glucose (D-glucosamine) and 2-acetamido-2-deoxy-D-glucose (*N*-acetyl-D-glucosamine) units, as depicted in Figure 1.1 (4). Chitin is insoluble in water and most common organic solvents used in pharmaceutical technology and consequently not useful in the development of drug delivery systems (36). In contrast, chitosan is rather insoluble in water and organic solvents, but soluble in dilute aqueous acidic solution (pH < 6.5), which can convert the glucosamine units into a soluble protonated amine form (34). It is readily soluble in dilute organic acids such as acetic, citric and malic acid as well as hydrochloric acid (37). This positive charge of chitosan is very useful since enables negative interaction with polyanions (36). Chitosan is usually characterized in terms of MW, which commonly ranges

from ca. 10 to 1000 kDa, and DD, in the range of 50 to 95% (38). The biodegradability and biological properties of chitosan are frequently dependent on the relative proportions of N-acetyl-D-glucosamine and D-glucosamine residues (4) as well as on the MW.

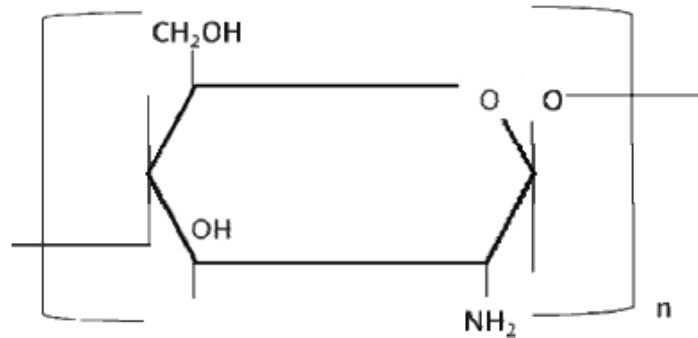


**Figure 1. 1.** Structure and molecular formula of chitosan.

Chitosan has biological properties (28, 39), unique and exceptional, that promote its use as a drug carrier (1, 3, 40), particularly to enhance transiently the permeability of mucosal barriers (36), increasing the effect on cell permeability (41), biocompatibility and biodegradability (42), being simultaneously non-toxic, non-antigenic (43) and mucoadhesive (2, 42). Previous reports also indicated that chitosan possess various biological activities, such as antitumor effects (44), anti-hypercholesterolemia (45) and antimicrobial activity against several pathogen and spoilage bacteria that has already been widely demonstrated (46). Currently, chitosan is widely used as a supporting material for tissue engineering applications, cell culture and nerve regeneration (47).

Table 1.1, summarizes the main potential biomedical properties of chitosan and associated characteristics. The better understanding of this unique cationic polymer invites new and several applications.

**Table 1. 1.** Principal properties of chitosan in relation to its use in biomedical applications.

Potential biomedical applications	Principal characteristics
Surgical sutures	Biocompatible
Dental implants	Biodegradable
Artificial skin	Nontoxic, biological tolerance
Bone rebuilding	Non-antigenic
Corneal contact lenses	Mucoadhesiveness
Time-control release drugs for animals and humans	Renewable
Encapsulating material	Film forming
Tissue engineering	Hydrating agent
Cell culture	Hydrolyzed by lysozyme
Nerve regeneration	Efficient against bacteria, viruses, fungi
	Anti-tumor
	Anti-hypercholesterolemia

## 2.1. Chitosan-based drug delivery systems

Controlled release technology emerged during the 1980s with a remarkable and increasing importance. This pharmaceutical technology that allows the predictable and reproducible release of a drug into a specific environment over an extended period of time, creating an optimal response, with minimum side-effects and prolonged efficacy, is a borderline of science (48).

The cationic nature of chitosan has been conveniently exploited for the development of new drug delivery systems and actually, a variety of chitosan-based delivery carriers have been described for pharmaceutical field as well as for other medical applications (1). In addition, the further chemical modification of chitosan is a powerful tool to control the interaction of the polymer with drugs, to enhance the load capability and to tailor the release profile of the particles (1). Hence, chemically modified chitosan improves its bulk properties for the preparation of sustained drug release systems (1), which enhance its versatility in the biomedical and biotechnological fields (49).

Chitosan can be employed to formulate a variety of pharmaceutical dosage forms, namely solutions, hydrogels, films, tablets, micro and nanoparticles. It is also a protagonist in

other advanced fields, like non-viral vector for DNA and gene delivery (49, 50). Drug delivery applications include oral, nasal, parenteral and transdermal administration, implants and gene delivery. The transmucosal administration of drugs is being largely exploited by chitosan-based systems (30).

### **2.1.1. Chitosan solutions**

The study of chitosan solutions and related properties has much merit considering the multi-potential of the polymer and its many applications in the biomedical field. The preparation of the aqueous solution is also a mandatory step before obtaining any type of secondary materials such as films, gels, sponges, fibers, or particles. Despite this, most of the properties such as flocculation, adsorption and biological activities are accomplished in aqueous solution, the interactions between molecules of chitosan and metal ions, proteins, cells and bacteria have been widely studied in solutions (51). The gross conformation of chitosan in solution may be spherical shape, random coil and rod shape, which is manipulated by two sets of parameters: structure parameters such as MW and DD, and solution parameters such as ionic strength, solvent, temperature and pH. Molecular weight can induce a conformation transitions — the conformations of small MW chitosans are stiffer and more extended than those of higher MW. In general, an increase of ionic strength makes the molecule contract (51). These parameters are obtained from the plots of log intrinsic viscosity, sedimentation coefficient, diffusion coefficient, radius of gyration and log MW of the polymer (51). The most widely used methods to characterize the conformation transition are capillary viscosity, analytical ultracentrifugation, static and dynamic light scattering (51). Commonly, chitosan solutions are easily prepared dissolving chitosan in organic acid like acetic or lactic acid.

Chitosan solutions have demonstrated most of their applications in the mucosal absorption, mainly due to the transiently ability of chitosan molecules to open tight junction of epithelial cells. Globally, it can be concluded that chitosan is able to enhance the paracellular route of absorption by tight junction disruption, inducing the translocation of tight junction proteins from the membrane to the cytoskeleton (52). Regarding the effect of chitosan salts on drug intestinal permeability *in vitro*, there is general agreement that these polymers are potent absorption enhancers for poorly absorbed drugs such as atenolol and peptides (52). Studies with buserelin, 9-deglycinamide, 8-arginine

vasopressin and insulin have evidenced a strong increase in the transport of these drugs in the presence of chitosan glutamate and chitosan hydrochloride (acidic environment) (52). Studies using chitosan glutamate and western blotting of Caco-2 cells fractions, observed translocation of tight junction proteins (ZO-1 protein) from the membrane to the cytoskeleton in response to treatment with chitosan (53).

Yu and his collaborators (54) developed a chitosan solution for nasal insulin delivery. They reported that chitosan concentration, osmolarity, medium and absorption enhancing ability of chitosan solution have significant effect on nasal insulin absorption. This may represent a new administration of insulin, safer, convenient for diabetic patients and with good applicability.

Recent research has also exploited the ability of chitosan solutions to control the spread of cytokine and improve the immunoadjuvant properties in vaccine applications (55). Sustained, local delivery of immunomodulatory cytokines in chitosan solution is under investigation for its ability to enhance vaccine and anti-tumor responses, both pre-clinically and clinically. In short, the study concluded that the chitosan solution maintained a deposit of bioactive antigen and cytokines, induced a cell expansion of the lymph nodes, including an increase in dendritic cells and antigen presenting cells. The resulting increase in the capacity of antigen presentation was exploited to improve both the humoral and cellular responses to the vaccine. The ability of chitosan to form deposits of antigens and cytokines, in addition to its safety profile and inherent versatility makes it a promising platform for the delivery of vaccines and cytokines (55).

### **2.1.2. Films**

Use of porous biomaterials in the film development attracts scientists in particular concerning the biomedicine applications (47). In the field of tissue engineering, porous polymer scaffolds can provide a framework for the seeded cells until they are well organized into a functioning tissue, especially in bone regenerative therapy (47). In the field of surgical, the porous biomaterial is usually used as wound dressing to absorb wound fluid and promote healing (47). On the other side, films, erodible and non-erodible inserts, rods and shields are the most logical delivery systems aimed at remaining for a long resident time in contact with physiologic surfaces like skin and the mucosal (56). Films by themselves or acting as drug carriers have been particularly considered worldwide (31). Porous membrane materials based on chitosan, add advantages of

biocompatibility, barrier properties, non-toxicity, non-polluting and low cost (31, 47). Besides biological activities, chitosan has attracted notable interest due to its good mechanical and oxygen barrier properties, becoming a promising edible film component (44) applicable to pharmaceutical and food industries. The functional properties of chitosan-based films can be improved by combining them with other hydrocolloids (57). The cationic properties of chitosan offer good opportunities to take advantages of electron interactions with numerous compounds (mainly macromolecules) and incorporate specific properties into the material (44). Examples are chitosan blends with hyaluronic acid, alginate, rice, collagen and oleic acid (35). Several aspects of the chitosan film-forming properties have been described, including the effect of solvent, concentration, storage effects and the influence of important structural characteristics such as the MW of chitosan and its DD (58).

To produce chitosan films, usually chitosan is dissolved in acetic acid or hydrochloric acid and then the solvent is removed by drying and final dry film is collected. Another methodologies involves the precipitation of chitosan by common coagulating agents (e.g., sodium hydroxide) and finally made into film (35). Other preparation techniques (e.g. casting and extrusion) and drying conditions may have influence on film properties. Mechanical film properties can be modified by controlling chain polymer orientation (44). The relevant applications of these chitosan films include bone cell adhesion and growth, blood compatibility and cell adhesion (35).

Since chitosan was reported to have intragastric floating characteristics and prolonged retention of the dosage form in the stomach, novel citrate cross-linked chitosan film was prepared by dipping chitosan film into citrate solution in order to improve it for site-specific drug delivery in the stomach (59). The results indicated that the citrate-chitosan film was useful in drug delivery such as for the site-specific drug controlled release in stomach.

Another study demonstrated the use and potential of chitosan films for production of mono and bilayer chitosan films containing corticosteroids as a drug carrier and controlled release in the eye (56). Corticosteroids are most common use in eye drops for inflammation following eye surgery, such as after cataract surgery and corneal operations and others. Mono and bilayer corticosteroids chitosan films were successfully obtained and results suggested that these films are potential sustained release carriers for corticosteroids. The monolayer corticosteroids chitosan film might be a promising ocular delivery carrier for corticosteroids in few hours and bilayer corticosteroids-chitosan film in weeks. The importance and application of chitosan films also cover the local drug delivery system of antibiotics (60). Local antibiotic delivery is another area of study designed to

provide alternative methods of treatment to clinicians for compromised wound sites where avascular zones can prevent the delivery of antibiotics to the infected tissue. A recent study demonstrated that incorporating antibiotics in chitosan films could provide alternative methods of treating musculoskeletal infections (60).

Novel chitosan based polyelectrolyte complexes were developed and optimized in order to obtain films possessing the optimal functional properties (flexibility, resistance, water vapor transmission rate and bioadhesion) to be applied on skin (61). The development was based on the combination of chitosan and two polyacrylic acid polymers with different cross-linkers and crosslinking densities. The optimized film, including adhesive property, has shown very good properties for application in the skin and represents a very promising formulation for further incorporation of drugs for topical and transdermal administration.

### **2.1.3. Tablets**

Various studies with chitosan regarding controlled release delivery systems have been conducted for oral dosage forms, from film coated pellets, tablets or capsules to more sophisticated and complicated delivery systems such as osmotically driven systems, systems controlled by ion exchange mechanism, systems using three dimensional printing technology and systems using electrostatic deposition technology (62). The most common controlled delivery system have been tablets and granules because of its effectiveness, low cost, ease of manufacturing and prolonged delivery time period, where the drug is uniformly dissolved or dispersed throughout the polymer (62). The tableting process is associated with relatively high pressure in order to form suitable compacts. However, not only the tableting excipients are deformed during the process of tablet formation, but also the tablet itself. This can lead to total or partial damage to such materials, namely loss of biological activity of proteins and enzymes, polymorphic transformation of excipients or damage of the coating material. Most recently, different excipients were tested in order to prevent such damages. Amongst others, polysaccharides like chitosan and carrageenan have shown to be advantageous because of their elastic tableting behavior (63). Several reports have been published on the use of chitosan as tablet excipients. It was applied as a carrier for sustained release tablets, a direct compressible diluent, a tablet disintegrate and a tablet binder (37). As a diluent, chitosan was used for preparation of direct compressed tablets (64, 65) where drug release was controlled. Studies using chitosan as



directly compressible tablet excipient showed its potential for use in modified release drug delivery systems without the need for additional adjuvants (64). Chitosan also showed higher binder efficiency than other tablet binders such as methylcellulose and sodium carboxymethylcellulose (66) and used as a binder for colon specific drug delivery tablets with slow drug release compared with other polysaccharides or synthetic polymers (67). Chitosan was utilized as tablets disintegrate (66) and showed bioadhesive properties in mixture with sodium alginate and in the form of thiolated chitosan derivative with slow drug release for intra-oral drug delivery tablets (68). Furthermore, the solubilizing and amorphizing properties of low MW chitosan toward naproxin made it an optimal carrier for developing fast release oral tablet (69). Depending mainly on ionic interaction, chitosan was also used for the preparation of tablets matrix to control drug release (70, 71).

When used in a matrix-type tablet formulation, chitosan forms a gel-barrier in an acid environment that can modulate or constrain drug release. Furthermore, at acidic pH amines of chitosan are protonated and can therefore interact with oppositely charged drug ions, serving as excipient for modified release of drug delivery systems (65).

Chitosan was studied as excipient in the preparation of prolonged theophylline tablets. These tablets showed higher drug bioavailability than of the commercial ones, which becomes a new potential formulation to respiratory problems (66).

The biological potential of chitosan adds also clear benefits to the tablet formulation and process. In a recent research five different polysaccharides with potential antioxidant activity for extended-release matrix tablets were compared (72). The results suggest that chitosan would be potentially useful in an extended-release tablet with the higher antioxidant activity, able to catch the most diverse and natural oxidative species, usually involved in different pathologies.

A new study concerning vaginal infections and inflammations were evaluated using chitosan tablets (73). Topical administration of the antibacterial metronidazole represents the most common therapy in the treatment of bacterial vaginosis caused by *Trichomonas vaginalis*. The formulations generally available for such therapy are creams, gels, vaginal lavages and vaginal suppositories. In this study, a new dosage form, containing metronidazole was developed with the aim to realize vaginal mucoadhesive tablets by including bioadhesive polymers as chitosan. This kind of delivery systems suitable for formulating metronidazole for topical application represents a good alternative to traditional dosage forms for vaginal topical administration in the treatment of infections or inflammations. These solutions overlap the limitations of conventional therapies that are

not suitable to assure drug permanence on the vaginal mucosa surface for adequate time assuring the complete elimination of bacteria and pathology eradication.

Nonetheless, all applications of chitosan as tablet excipient were not in its derivative forms. However, attempts have been made to improve chitosan property by developing derivative salts. Chitosan derivatives such as glutamate, aspartate and hydrochloride salts have been used for colon-specific drug delivery and to enhance the delivery of therapeutic peptide across intestinal epithelia (37).

#### **2.1.4. Hydrogels**

Hydrogels are networks of hydrophilic polymers that can absorb large quantities of water without dissolution. Due to their physical properties resembling human tissue and its excellent tissue compatibility, hydrogels have been extensively studied for biomedical applications. They can be used as soft contact lenses (74), tissue engineering scaffolds (75), drugs carriers and controlled-release systems (76). In addition, hydrogels have the potential for further healing (77). They can absorb excess wound exudates, protect the wound from secondary infection and effectively promote the healing process by providing an environment for moist wound healing (78). Even can also be removed without causing trauma to the wound (78).

Several models of hydrogels have been studied, including chitosan, poly (vinyl alcohol) (PVA) that is a water-soluble polyhydroxy polymer and alginate. However, chitosan has been widely exploited in hydrogel formulation and in practical applications because of its easy manipulation, excellent chemical resistance, physical properties, biodegradability and low price (78). This polymer is used to produce hydrogels with well-known properties that are used for delivery of proteins and synthetic drugs. Since this compound is also polyelectrolyte, its ionic form produces complexes through hydrogen bonding or electrostatic interactions. Besides this, another interesting property of chitosan is its ability to gel in contact with specific polyanions. This gelation process is due to the formation of inter- and intramolecular bonding mediated by these polyanions (1). In the last decade, different chitosan hydrogels were produced for drug delivery in micro or nano-scale using the polyelectrolyte complexation technique. There are many factors that affect the relevant properties of the capsules of chitosan, in particular the composition, MW and DD of chitosan. Several methods have been developed in which the particle size of chitosan

hydrogel and its related properties are quite distinct, according to the method of preparation and the reaction conditions that are employed. One of the major factors that may influence the final properties is the method of preparing hydrogel. Moreover, few attempts were made to correlate statistically the reaction conditions with the final properties of chitosan hydrogel. Liu and his collaborators (79) evaluated the influence of chitosan MW and its concentration, along with pH, upon the swelling behavior of microcapsules of chitosan-alginate, and postulated that all factors have an effect on the behavior of the hydrogel swelling. The alginate-chitosan hydrogels are commonly prepared by ionic complexation using alginate as a gel core (80) and then characterized by the vibration modes of their main groups using FTIR. Other hydrogels formulation procedures can be performed by UV crosslinking. In this method, lactose moieties are introduced into chitosan to obtain much better water-soluble chitosan at neutral pH, and photoreactive azide groups are added to provide the ability to form a gel through crosslinking azide groups with amino groups (81). This photocrosslinkable chitosan is then exposed to UV irradiation to form an insoluble and adhesive hydrogel within 60 s. Hydrogel has the consistency of transparent and soft rubber (81).

The crosslinking can also be performed by high temperature. It is based on the neutralization of a chitosan solution with a polyol counterionic dibase salt such as  $\beta$ -glycerophosphate. Chitosan/glycerophosphate is a thermosensitive solution, which is liquid at room temperature and solidifies into a white hydrogel at body temperature (81).

In addition, crosslinking can be achieved by high pH, employing the pH-sensitive property of chitosan solutions at low pH. Once injected into the body, these polymer solutions face different environmental pH conditions and form gels (81).

The chitosan hydrogel formulation can also be made by, freezing, thawing or chemical methods. Irradiation has the advantages of easy control of processing, without adding initiators or cross-linkers that can be harmful and difficult to remove and also has the option of combining the hydrogel formation and sterilization in one technological step. The main disadvantage of hydrogels prepared by irradiation is its poor mechanical strength. However, hydrogels prepared by freeze-thaw for example, of aqueous solutions of PVA has good mechanical strength, are stable at room temperature and does not require initiators or cross-linkers. The main disadvantage of this type of hydrogel is its opaque appearance and limited expansion capability (78).

The hydrogel yields are evaluated through the weight difference, placing the washed hydrogels into pre-weighed flasks and then into a stove at 50 °C until dryness. The chitosan hydrogel particles can then be visualized and characterized by particle size and

size distribution using an inverted optical microscope (80) as well as, by solubility, X-ray diffraction, thermal analysis, and solvent uptake (82).

An ophthalmic delivery system with improved mechanical and mucoadhesive properties that could provide prolonged retention time for the treatment of ocular diseases were evaluated considering chitosan hydrogel formulation. For this, an *in situ* forming gel was developed by the combination of a thermosetting polymer, poly (ethylene oxide)–poly (propylene oxide)–poly (ethylene oxide) with chitosan. Therefore, the final formulation presented adequate mechanical and sensory properties and remained in contact with the eye surface for a prolonged time. In conclusion, the *in situ* forming gel comprised of poloxamer/chitosan is a promising tool for the topical treatment of ocular diseases (83).

To overlap the limitation of topical delivery of antimicrobial agents and to prolong active drug concentrations in the oral cavity, it was designed a hydrogel formulation containing chitosan for delivery of chlorhexidine gluconate to the oral cavity (84). Chitosan prolongs the adhesion time of oral gels and drug release also inhibiting the adhesion of *Candida albicans* to human buccal cells since it has antifungal activity (84). The antifungal agent, chlorhexidine gluconate also induces the reduction of *Candida albicans* adhesion to oral mucosal cells.

The preparation and characterization of thiol-modified chitosan, which formed crosslinked hydrogels, was also described to characterize *in vitro* release kinetics of insulin encapsulated in different chitosan MW hydrogels and evaluated for their potential use as a scaffold for the culture of NIH 3T3 cells (85). The results demonstrated that insulin is not immobilized locally within the gel network. Since the incorporation into the gel has no impact on insulin stability it may be assumed that the chitosan thermogelling system is an attractive delivery system for peptides and proteins.

The main goal of other study was to developed a chitosan bioadhesive gel for nasal delivery of insulin (86). The proposed gel formulation could be useful preparation for controlled delivery of insulin through the nasal route and may represent an alternative treatment to diabetes.

Mucoadhesive chitosan lactate gels were developed intended for the controlled release of lactic acid onto vaginal mucosa (87). The conclusions finding makes it reasonable to envisage a complete release of lactate from the tested formulations in vaginal environment. A recent research reports an *in situ* gelling chitosan-based hydrogel system that sustains the release of a potential anti-cancer gene (pigment epithelium-derived factor) to the tumor site. A significant reduction of the primary osteosarcoma in a clinically relevant orthotopic model was measured. The combination of plasmid treatment and

chemotherapy together with the use of this delivery system led to the highest suppression of tumor growth without side effects. The results obtained from this study demonstrate the potential application of a hydrogel system as an anti-cancer drug delivery for successful chemo-gene therapy (88).

Another notorious study focuses on the current use of injectable to form *in situ* chitosan hydrogels in cancer treatment (81). Formulation protocols for *in situ* hydrogel systems, their cytotoxic properties, loading and *in vitro* release of drugs, their *in vitro* effect on cell growth, the inhibition of tumor growth *in vivo* using mouse models, and future directions to enhance this technology were discussed. In conclusion, chitosan gelling systems due to their antibacterial, biocompatible, biodegradable and mucoadhesive properties are a potential carrier for various cancer treatments.

These hydrogels may also be useful to detect the localized growth of cells (81), which can also be directed to innovative methods of diagnosis.

#### **2.1.5. Microparticles**

Microparticles are defined as multiparticulate delivery systems, usually spherical with size varying from 1 to 1000  $\mu\text{m}$ , containing a core active substance (48). The terms microcapsules and microspheres are often used synonymously. Spheres and spherical particles are also used for a large size and rigid morphology (48).

The use of microparticles-based therapy allows drug release to be carefully tailored to the specific treatment site through the choice and formulation of various drug–polymer combinations. The total dose of medication and the kinetics of release are the variables, which can be manipulated to achieve the desired result. Using innovative microencapsulation technologies, and by varying the copolymer ratio, MW of the polymer among other parameters, microparticles can be developed into an optimal drug delivery system, which will provide the desired release profile (34).

Chitosan with different MW and concentration, degradation rate of chitosan particles and drug concentration interfere on microparticle properties (1). Chitosan microparticles are used to provide controlled release of many drugs and to improve the bioavailability of degradable substances such as protein or enhance the uptake of hydrophilic substances across the epithelial layers (34). Having in mind bio/mucoadhesive properties of natural biopolymers, chitosan microparticles have potential for colon targeting. In order to achieve localization and prolonged residence time in the colon, matrices should have optimal

particle size, between 4 and 15  $\mu\text{m}$  (89). Carrier systems in that size range are able to attach more efficiently to the mucus layer and accumulate in the affected region without the need for macrophage uptake. This novel formulation will offer efficient treatment of colon inflammatory diseases like ulcerative colitis and Chron's disease (89), increasing therapeutic concentration (at the site of inflammation) and activity and minimizing side effects that occur by conventional systemic absorption. Chitosan microparticulate carrier systems are also efficient in the treatment of inflammatory bowel diseases (89). Budesonide is one of the most used drug substances in the treatment of active inflammatory bowel diseases. Chitosan microparticles loaded with budesonide were produced using novel one step spray-drying procedure. Coated microparticles were suitable candidates for oral delivery of budesonide with controlled release properties for local treatment of inflammatory bowel diseases.

Chitosan microparticles also represents a promising polymer in nasal peptide delivery (90) prolonging the residence time of nasal drug delivery systems at the site of drug absorption. Additionally, chitosan improves the absorption of peptides by opening transiently the tight junctions.

Oral administration of the nonsteroidal anti-estrogen tamoxifen is the treatment of choice for metastatic estrogen receptor-positive breast cancer. Chitosan microparticles were developed for tamoxifen delivery into the lymphatic system (91), improving tamoxifen oral bioavailability and decreasing its side effects. These data underline other potential therapies to this serious cancer condition.

It was also reported the importance of chitosan microparticles in the purification of immunoglobulin G from human plasma by affinity chromatography using linoleic acid attached chitosan microparticles (92). It was concluded that the microparticles allowed just one-step purification of immunoglobulin G from human plasma.

Chitosan and its derivative N-trimethyl chitosan chloride, given as microparticles associated to the non-toxic mucosal adjuvant LTK63, were evaluated for intranasal immunization with the group C meningococcal conjugated vaccine. The bactericidal activity measured in serum of mice immunized intranasally with the conjugated vaccine formulated with this delivery system and the LT mutant was superior to the activity in serum of mice immunized sub-cutaneous. Importantly, intranasal but not parenteral immunization, induced bactericidal antibodies at the nasal level, when formulated with both delivery system and adjuvant (93).

In another study, it was evaluated the ability of chitosan microparticles to enhance both the systemic and local immune responses against diphtheria toxoid after oral and nasal

administration in mice. Significant systemic humoral immune responses were also found after nasal vaccination with diphtheria toxoid associated to chitosan microparticles. Diphtheria toxoid associated to chitosan microparticles results in protective systemic and local immune response against this toxoid after oral vaccination and in significant enhancement of immunoglobulin G production after nasal administration. Hence, these *in vivo* experiments demonstrate that chitosan microparticles are very promising mucosal vaccine delivery system (94). Other similar studies considered the chitosan microparticles as encapsulating agent of large amounts of antigens such as ovalbumin, or tetanus toxoid (95). Besides chitosan particles are a promising candidate for mucosal vaccine delivery, mucosal vaccination not only reduces costs and increases patient compliance, but also limits the invasion of pathogens through mucosal sites.

#### **2.1.6. Nanoparticles**

Nanoparticles are defined as a microscopic particle whose size is in the nanoscale, varying from 1 to 1000 nm, able to deliver drugs (2) to the right place, at appropriate times and at the right dosage, also improving their bioavailability, efficiency and reducing cytotoxicity associated to other systemic drugs carriers, actually becomes one of the most attractive areas of research in drug delivery (2). These submicron particles containing entrapped drugs are intended for enteral or parenteral administration, which may prevent or minimize the drug degradation and metabolism as well as cellular efflux, extending the shelf-life (50). Some researchers have also observed that the number of nanoparticles, which cross the intestinal epithelium is greater than that of the microparticles and hydrophilic nanoparticles generally have longer resident time in blood than microspheres (96). With their easy accessibility in the body, nanoparticles can also be transported via the circulation to different body sites. These particulate delivery systems have been shown to enhance the immune response following mucosal application. Nanoparticles have been made of safe materials, including synthetic biodegradable polymers, natural biopolymers, lipids and polysaccharides and have the potential for overcoming important mucosal barriers, such as the intestinal, nasal and ocular barriers (50). Chitosan based nanoparticles show great potential for delivering macromolecular therapeutics (in particular drugs and genes) and control the complete release of the drugs in their native forms across biological barriers (41). Important advantages of these nanoparticles include

their rapid preparation under extremely mild conditions and also their ability to incorporate bioactive compounds (45). Chitosan nanoparticles topically applied into the eye has been proven to increase the residence time of drugs in the precorneal area due to their adhesive properties and, therefore, could prolong the penetration of drugs into the intraocular structures (2). An important research shows that a chitosan derivative can be used to prepare norcantharidin-associated nanoparticles by taking advantage of the ionic cross-linkage between the drug molecule and of the chitosan carrier for anti-hepatocarcinoma medicine (97).

The potential of nanoparticles as a vaccine delivery has also been demonstrated in several studies (98-100). Nanoparticle-mediated gene delivery is an alternative to viral gene delivery. Nanoparticles offer the potential for safe, targeted and efficient gene delivery in a variety of organs (101).

Borges et al. (102), recently described a delivery system that is composed of a nanoparticulate chitosan core to which the hepatitis B surface antigen (AgHBs) was adsorbed and subsequently coated with sodium alginate. The enhancement of the immune response observed with the antigen-loaded nanoparticles demonstrated that chitosan is a promising platform for parenteral delivery of this antigen, since it resulted in a mixed Th1/Th2 type immune response.

Chitosan nanoparticles have been also produced as a carrier system for the nasal delivery of a monovalent influenza subunit vaccine (103). The intranasal administered antigen-chitosan nanoparticles induced higher immune responses compared to the other intranasal antigen formulations, and these responses were enhanced by intranasal booster vaccinations. Moreover, among the tested formulations only intranasal administered antigen-containing chitosan nanoparticles induced significant immunoglobulin A levels in nasal washes of all mice tested, demonstrating that chitosan nanoparticles are a potent new delivery system for intranasal administered influenza antigens.

Another study indicate that chitosan nanoparticles are a good carrier for DNA vaccines against tuberculosis by pulmonary delivery, which may provide an advantageous delivery route compared to intramuscular immunization, due increasing higher immunogenicity (104).

Chitosan nanoparticles have been also introduced as a useful carrier for peptide oral delivery, because they can protect these compounds from degradation. Insulin, like other peptides, has low therapeutic activity when administered orally due to degradation by proteolytic enzymes (105).



Sarmento et al. (106) developed chitosan nanoparticles as drug carrier of insulin. Insulin was entrapped in different polyanion/chitosan nanoparticulate systems with high efficiency, to study morphologic and physical properties of resulting nanoparticulate complexes and to investigate insulin release behavior under gastrointestinal conditions (106). These nanoparticulate complexes appear to possess good properties for oral protein delivery, particularly those containing dextran sulfate/chitosan polyelectrolytes, which provided highest insulin association efficiency and retention of insulin in gastric simulated conditions. However alginate/chitosan nanoparticles also appear as promising in oral delivery system for insulin and potentially for other therapeutical proteins (107). Moreover, it was demonstrated that blood glucose levels of diabetic rats can be effectively controlled by insulin-loaded chitosan nanoparticle administration, following either single or multiple oral administration. In addition, the hypoglycemic effect was observed for more than 24 h (108).

## **2.2. Clinical trial - Safety and tolerability of chitosa-n-acetylcysteine eye drops in healthy young volunteers**

There are many definitions of clinical trials, generally are studies of biomedical and health research related to human beings following a pre-defined protocol (109). These tests can only take place when quality and safety of the test are guaranteed by the Health Authority or the Ethics Committee recognized by the country, which will run the clinical trial. The randomized controlled trial is commonly accepted as the gold standard research method for evaluating health care interventions (110). In any clinical trial it is desirable not only to achieve similar numbers of patients in each treatment group, but also to ensure that patient groups are similar with respect to prognostic factors such as age or stage of disease (110). Nowadays, many studies have come and explore the multi-potential of chitosan as a carrier for drug delivery and release (109).

The "dry eye syndrome" DES is a highly prevalent ocular disease, particularly in the elderly population and that current therapy is the use of topically administered lubricants, no "ideal" formulation has yet been found. Recently, Croma Pharma has introduced chitosan-n-acetylcysteine eye drops (111), designed for treatment of symptoms related to "dry eye syndrome". The new formulation comprises n-acetylcysteine, which has been used in ophthalmology because of its mucolytic properties for several years. Based on theoretical considerations, one can hypothesize that the new chitosan derivative may

prove an increased adhesion to mucins of the ocular surface and may therefore be particularly beneficial in reducing the symptoms associated with DES.

Men and women aged between 18 and 45 years healthy with normal physical examination/laboratory values, medical history and with normal ophthalmic findings, were considered. Exclusion criteria were: patients who participated in a clinical trial in the 3 weeks preceding the study; abuse of alcoholic beverages; symptoms of a clinically relevant illness in the 3 weeks before the first study day; ametropia and pregnancy. The study was completely and successful based on the differences found between the treated and the non-treated eye with chitosan-n-acetylcysteine eye drops.

The study resulted in two subsequent studies in similar collaboration with Croma-Pharma: Evaluation of the corneal residence time of chitosan-n-acetylcysteine eye drops in patients with dry eye syndrome after single and multiple instillation; and the assessment of safety and tolerability of chitosan-n-acetylcysteine eye drops in subjects while wearing contact lenses before and insertion of contact lenses. The studies were successfully completed in Phase II and Phase I, respectively.

The emergence of innovative medicines demands effective strategies to enhance drug permeation and bioavailability. A better understanding of the mechanisms of action of these novel drugs carriers will provide their further optimization, opening exciting opportunities to improve the administration of macromolecules, such as proteins, peptides, genes, vaccines, antigens and synthetic compounds, which allows the treatment of several diseases.

Therefore, useful knowledge for future adaptation is provided for pharmaceutical industry, medical assistance and human health care.

### **3. Oxidative products and the clinical importance of antioxidants**

The reactive oxygen species (ROS) like superoxide anion radical ( $\bullet\text{O}^{2-}$ ), hydrogen peroxide ( $\text{H}_2\text{O}_2$ ) and hydroxyl radical ( $\bullet\text{OH}$ ), are also ubiquitous, highly reactive, diffusible molecules that are generated within the cell as by-products of aerobic respiration and metabolism resulting in a very reactive unpaired electron state, within and out of the cell (112). Indeed, ( $\bullet\text{O}^{2-}$ ) radical is the precursor of most ROS and could be a mediator in oxidative chain reactions (112).

Cellular damage or oxidative injury arising from free radicals or ROS now appears the fundamental mechanism underlying a number of human neurodegenerative disorders,

diabetes, inflammation, viral infections, autoimmune pathologies, atherosclerosis, coronary heart disease, digestive system disorders and cancer (113). Free radicals are constantly generated through normal metabolism, degradation of drugs, environmental chemicals and other xenobiotics as well as endogenous chemicals, especially stress hormones (adrenalin and noradrenalin) (113).

Antioxidants may control this OS imbalance by acting at different levels: scavenge free radicals, inhibiting their formation or otherwise preventing the damage caused by them and increasing antioxidant defense (15-17).

The global market of antioxidants is increasing rapidly, because of the increased health risk in a constantly polluting environment. However, there are not many antioxidants listed in pharmacopoeias and extensive research is being carried out globally on these agents, most of them demonstrating their pharmacological effect (18). For instance, the role of several active infusions in the prevention and cure of disease has been attributed, at least in part, to antioxidant properties and to its constituents that are widely known as polyphenols. These phenolic compounds are commonly found in both edible and inedible plants, and display a variety of biological effects, including anti-inflammatory properties (114), regulation of cholesterol, vascular problems healing, promotes blood circulation, relieves blood stasis and have huge antioxidant activity (14, 115, 116). In this regard, antioxidants are seen as compounds that protect cells against OS, which could lead to cell damage, cancer, neurodegenerative diseases and vision problems (115).

However, all these antioxidant compounds are labile macromolecules that are light and oxygen sensitive, with a high index of reactivity with other compounds and in some cases with poor solubility and low mucosa permeability (15-17).

### **3.1.1. Types of antioxidants agents**

Antioxidant is any substance which when present at low concentrations compared with those of an oxidizable substrate, significantly decreases in oxidation of substrate, preventing oxidative complications (113). The term 'oxidizable substrate' includes almost everything found in the living cells including proteins, lipids, DNA and carbohydrates (113). Antioxidants may interact and eliminate ROS before they react with biologic targets, preventing chain reactions or preventing the activation of oxygen to highly reactive products (117). Antioxidants can be classified into enzymatic and non-enzymatic antioxidants, since they are endogenously produced or exogenously obtained (118). Antioxidants that are endogenously produced include enzymes, low molecular weight

molecules and enzyme cofactors (119). Enzymes are known to afford more effective protection against acute massive oxidative damage, such as hyperoxia or inflammation (18). The enzymatic antioxidant systems, such as Copper (Cu), Zinc (Zn), manganese superoxide dismutase (MnSOD), glutathione peroxidase (GPx), glutathione reductase (GR) and catalase may remove the ROS directly or sequentially, preventing their excessive accumulation and consequent adverse effects (113). Non-enzymatic antioxidants are obtained exogenously, mainly from dietary sources such as vitamins, carotenoids, organosulfural compounds, minerals, lipoic acid, and polyphenols (120). Polyphenols are the major and most important class which includes phenolic acids and flavonoids (121). A polyphenol is any compound that contains more than two (–OH) groups attached to a benzene ring (119). Naturally occurring in vegetables, fruits and plant derived beverages such as tea, red wine, and extra virgin olive oil, are a wide variety of organic molecules (122). Commonly flavonoids are catechins, resveratrol, quercetin, anthocyanins and hesperitin derivatives, and phenolic acids such as phytic, caffeic and chlorogenic acids (112).

Vitamin E, fat-soluble antioxidants, is a family of four tocotrienols ( $\alpha$ - $\beta$ - $\delta$ - $\gamma$ -tocopherols) (123). Vitamin E is generally thought to be the most important inhibitor of lipid peroxidation. There are some reports showing that vitamin E intake prevents the generation of free radicals (119). The most active form of vitamin C (ascorbic acid), a water soluble antioxidant, interacts with the tocopheroxyl radical and regenerates the reduced tocopherol, scavenging ROS and protects the DNA damage (119).

Carotenoids are fat-soluble antioxidants, including  $\beta$ -carotene, lutein,  $\alpha$ -carotene, zeaxanthin, cryptoxanthin and lycopene (112).

Trace elements also have indirect antioxidant and detoxifying properties and are therefore essential in the defense systems against ROS-induced cellular damage. Indeed, copper (Cu), zinc (Zn), manganese (Mn), selenium (Se) are particularly of utmost importance as they are essential constituents of enzymatic antioxidant systems (112).

Plant extracts and their constituents are a natural source of antioxidants. There are several different plant organs such as seeds (soybean, peanut, cottonseed, mustard, rapeseed, rice and sesame seed), fruits (grape, citrus, black, pepper and olive), leaves (tea, rosemary, thyme and oregano) and others (sweet potato, onion and oat seedling) (113).

Numerous naturally compounds are useful as antioxidants in plant extracts, namely  $\alpha$ -tocopherol and  $\beta$ -carotene, phenolic compounds (tannins, flavonoids, anthocyanins, chalcones, xanthones, lignans, depsides, and depsidones), terpenes (sesquiterpens and

diterpenes), alkaloids, and organic sulfur compounds (124). Rosmarinic acid, (a-O-caffeoyl-3,4-dihydroxyphenyllactic acid), is a phenolic compound generally admitted as a free radical scavenger (125). The high biological activity is related to its chemical structure, in particular the two catechol moieties. Catechol is an important sub-structure for the potent antioxidant activity of phenolic antioxidants (125). The general antioxidant mechanism of phenolic compounds is thought to be divided into two stages: radical catching stage and radical conclusion stage (126). The structure of the final product would afford important information about the antioxidant mechanism of the phenolics (126). Rosmarinic acid can have many beneficial functionalities like its potent antioxidant activity associated to its huge potential radical scavenging activity, higher than trolox (a derivative of  $\alpha$ -tocopherol), commonly used as control (10-12). It is also well documented its antibacterial and antiviral activity (7, 8), anti-inflammatory activity (127), anti-mutagenicity character (128), capability to reduce atopic dermatitis symptoms (129), prevention of Alzheimer's disease (130) and apoptosis induction of colorectal cancer cells (131). Rosmarinic acid has also an anti-angiogenic activity to retinal neovascularization in a mouse model of retinopathy. Rosmarinic acid is suggested as potent inhibitor of retinal neovascularization and that may be applied in the treatment of vasoproliferative retinopathies (13). It is reported that rosmarinic acid may inhibit the proliferation of retinal endothelial cells and inhibited *in vitro* angiogenesis of tube formation. It also has showed no retinal toxicity.

### **3.1.2. Physiology and pathobiology of reactive oxygen species in retinopathies**

The retina is a thin, transparent, highly organized structure of neurons, glial cells, and blood vessels (118) (Figure 1.2). Of all structures within the eye, the neurosensory retina has been the most widely studied. Retina is organized into neural retina and retinal pigment epithelium (RPE) (132), being the first involved in signal transduction, leading to vision. Light enters through the retinal ganglion cell layer and penetrates all the deeper layers where the transduced signal is taken by several retinal neurons to the optic nerve and forward to the brain, where it is registered and formed an image. RPE, on the other hand, is a single cell layer that separates the outer surface of the choroid and neural retina and appears as a uniform, continuous layer that extends through the retina and a have an essential role in the viability of the neural retina (132).

There are two barriers that form the blood–ocular barrier which limit the permeation into the retina, the blood–aqueous barrier (BAB) and blood–retina barrier (BRB) (Figure 1.3) (132).

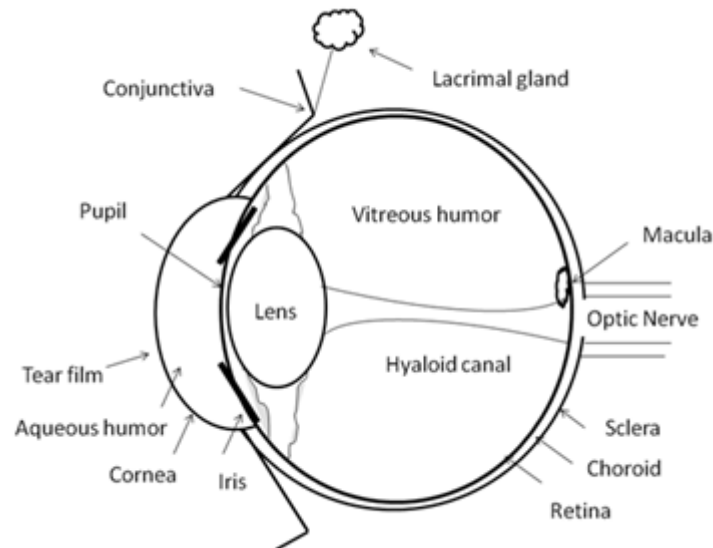


**Figure 1. 2.** Schematic illustration of eye structure and subsequent critical biological barriers that drugs need to overcome after topical administration onto the eye surface, in: (118).

In addition to the physical barriers, ocular tissues contain metabolic enzymes, such as esterases, aldehyde and ketone reductases (133, 134), which may degrade drugs or infectious agents that reach the eye, reducing their efficacy, pathogenicity or even eliminating them. As a result of these anatomical and physiological constraints after topical or local application, a major fraction of the administered drug is lost by different mechanisms, resulting in very low ocular bioavailability (Figure 1.3) (135). This justifies the poor effectiveness of topical administrations in ocular globe, and the need to treat several diseases by invasive methods as the intra-vitreous injections or surgeries.

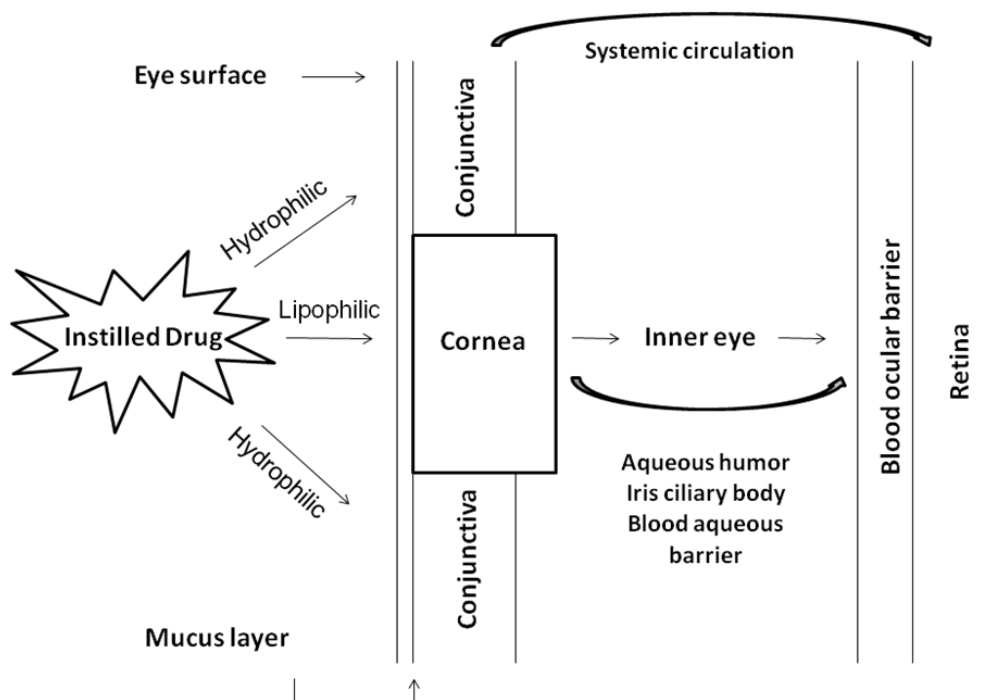


**Figure 1. 3.** Schematic view of the ocular permeability, physiological barriers, and transport pathways of a drug applied topically onto the eye, in: (27).

Nevertheless, human antioxidant defense is set with enzymatic scavengers like superoxide dismutase (SOD), catalase (CAT) and glutathione peroxidase (GPx), hydrophilic scavengers like urate, ascorbate, glutathione (GSH) and flavonoids, lipophilic radical scavengers such as tocopherols, carotenoids and ubiquinol (18). In addition, defense also comprises enzymes responsible for the reduction of oxidized forms of molecular antioxidants like glutathione reductase and dehydroascorbate reductase.

In eye pathologies, the defense against ROS is weakened or damaged and the oxidant load increases. In such conditions, external supply of antioxidants is essential to countervail the deleterious consequences of OS (136). The OS imbalance, potentially leads to retinal cell damage, and degenerates lipids, proteins, enzymes, carbohydrates and DNA in cells and tissues, resulting in membrane damage (25). These consequences of OS construct the molecular basis in the development of degenerative eye diseases.

### 3.1.3. Oxidative stress imbalance and retinal affected diseases

The clinical impair of OS and ocular diseases are particularly due to some factors, namely: the retina natural high content of PUFA, the oxygen uptake and glucose oxidation higher than any other tissue (15), the eye structurally subjected to light, atmospheric

oxygen, environmental chemicals and physical abrasion (137, 138). Protective components like water-soluble antioxidants, lipid-soluble antioxidants and highly specialized enzymes are thought to serve as a frontline defense for the ocular surface tear film and underlying tissues (118). If the antioxidants are depleted or acting inefficiently, an imbalance between the high increased production of ROS and the sharp reduction in antioxidant defenses will alter cellular redox status (136). In retinopathy, OS has been widely involved in decreased retinal blood flow (139), increased vascular permeability, disruption of BRB (140) and the appearance of cellular capillaries from the apoptotic loss of retinal capillary cells (141). OS has also been linked to microvascular abnormalities in retinopathies, degenerative process of retinal neovascularization and the suppression of antioxidants systems (25).

#### **4. Nanotechnology applied to antioxidants protection**

Nanoparticles have been made of safe materials, including synthetic bio-degradable polymers, natural biopolymers, lipids and polysaccharides and have the potential for overcoming important mucosal barriers, such as ocular barriers (50). Nanoparticles may be obtained via different preparation protocols and have been widely studied in recent years as carriers for therapeutic agents with varying degree of effectiveness (142). Different preparation of micro/nanoparticles can be considered, mainly physical methods, chemical crosslinking methods and miscellaneous. Physical methodologies involve ionotropic gelation, emulsification and ionotropic gelation, modified emulsification and ionotropic gelation, floating hollow chitosan microspheres obtained by ionic interaction with sodium dioctyl sulfosuccinate, coacervation and complex-coacervation (34). Crosslinking with other chemicals are used for emulsion crosslinking method, multiple emulsion method, precipitation–chemical crosslinking and crosslinking with a naturally occurring agent (34). Miscellaneous methods include thermal crosslinking, solvent evaporation method, spray drying and interfacial acylation (34). Nanocarriers can be applied to improve the solubility, permeability, stability of the compounds and some can even surpass the first pass metabolism (Figure 1.4). These delivery systems have been beneficial to the pharmaceutical industries as it is a strategic tool for expanding drug market and patent life. Novel drug delivery systems would make antioxidant reach site of action and improve the efficacy of therapy, generally by improving the bioavailability, which are of prime importance when antioxidants intended for prophylactic purpose (116).



Implication of novel delivery systems for antioxidants is ruled by physical-chemical characteristics, biopharmaceutics and pharmacokinetic parameters of the antioxidant to be formulated (116). Recently, chemical modifications, coupling agents, liposomes, microparticles, nanoparticles and gel-based systems have been explored to overcome difficulties in the development of new products for the improvement of human healthcare (18).

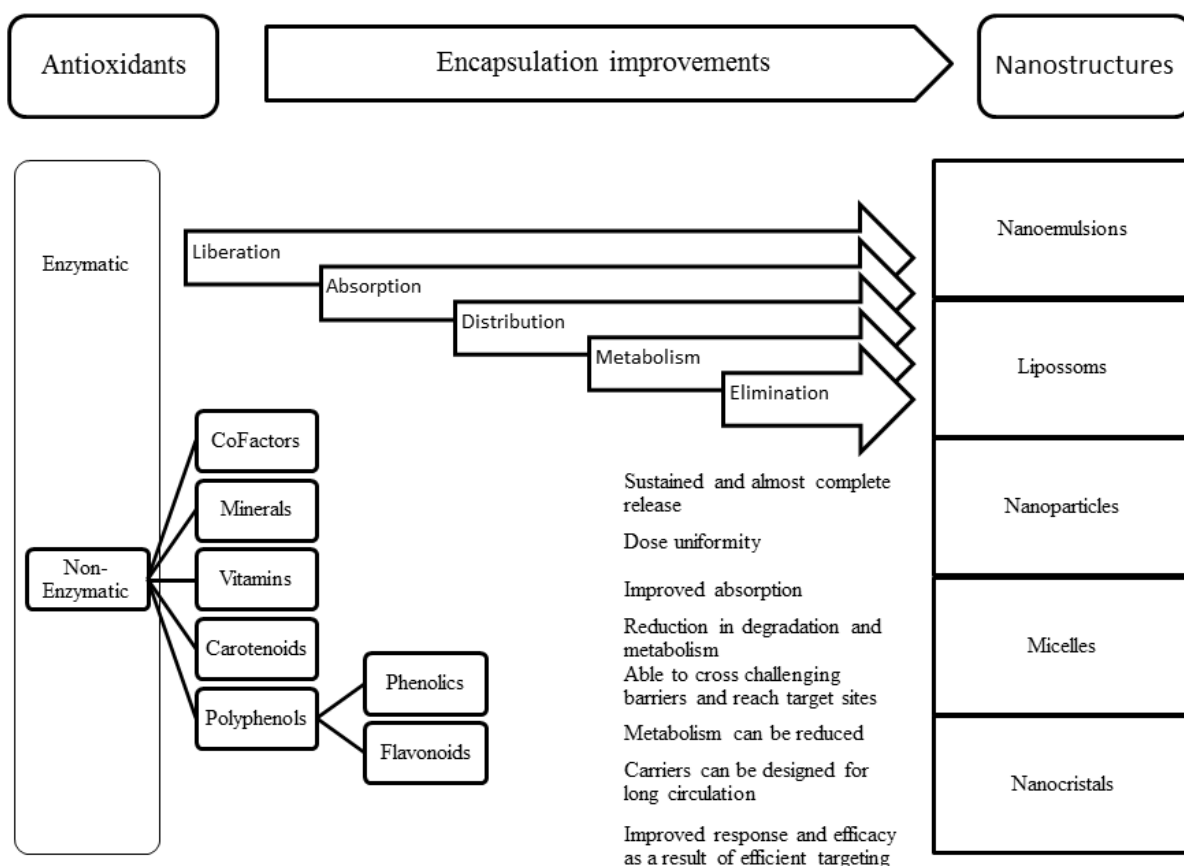


**Figure 1. 4.** Classification of antioxidants and characterization of some nanostructures. Highlights to real benefits of antioxidants encapsulation considering its liberation, absorption, distribution, metabolism, elimination and response, adapted from (18).

Nevertheless, it may be highlighted the huge importance of nanotechnology and nanocarriers to be applied in common delivery systems, like immunoglobulin's deliver to

the retina. In particular, the injecting vascular endothelial growth factor (VEGF) to neutralize the antibodies into the vitreous. Silicate nanoparticles (SiNPs) have been demonstrated efficiency in inhibition of VEGF-induced angiogenesis. Via suppression of VEGF receptor-2 phosphorylation induced by VEGF, SiNPs blocked ERK 1/2 activation (143). Intravitreal injection of gold nanoparticle (GNP) also has shown an inhibition of retinal neovascularization in a mouse model of retinopathy of prematurity. GNP not affected the cellular viability of retinal microvascular endothelial cells and not induced retinal toxicity. GNP can be used in a variable vaso-proliferative retinopathies mediated by VEGF (144).

A molecule with ideal solubility and permeability profile can be administered with a minimum effective dose and with no presystemic loss due to mucosas, physical barriers or enzymatic degradation (18). For antioxidants assure these conditions they need nanocarriers to take them to the right place without losing their functional activity. Therefore, considering the therapeutic potential of the antioxidants, there is every need to implicate novel drug delivery technologies to improve their performance. Nanoparticles are expected to develop and improve protection, stability, bioavailability and therefore the therapeutic efficacy of antioxidants, without compromising the safety performance of the drug. The Age-Related Eye Disease Study (AREDS) (145), an National Eye Institute-sponsored, multicenter, controlled, randomized clinical trial, demonstrated that the combination of oral supplements consisting of antioxidant vitamins C (500 mg), E (400 international units), and  $\beta$ -carotene (15 mg), and minerals, ZN (80 mg of zinc oxide) with Cu (2 mg cupric oxide). This reduced the 5-year risk of developing advanced age macular degeneration (AMD) in eyes with intermediate AMD by 25% (estimated probability of progression was 28% for placebo vs 20% for antioxidants plus zinc). The primary purpose of the Age-Related Eye Disease Study 2 (AREDS2) (145) was to evaluate the efficacy and safety of lutein plus zeaxanthin and/or  $\omega$ -3 long-chain polyunsaturated fatty acid (LCPUFA) supplementation, reducing the risk of developing advanced AMD. Nevertheless and besides the promising effect of this huge antioxidant supplementary, it would be expectable that this effect could be also potentiated by the protection of these antioxidants using the nanotechnology. The protection may be crucial in order to guarantee the safe antioxidant performance, bioavailability and absorption, over the several barriers of the digestive system (such as the biological fluids and enzymatic pathways). Other studies have been performed to maintain or even increase the activity and stability of antioxidants using nanotechnology (Table 1.2). These are evidences that antioxidant nanoparticles

may be used for therapy of several diseases, however further studies are needed to prove their efficacy in the prevention and treatment of retinopathies.

**Table 1. 2.** Recent published data of antioxidants nanoencapsulation for several applications.

Antioxidant	Method	Results	Application	References
3,5-di-tert-butyl-4-hydroxycinnamic acid	A nanosilica-immobilized antioxidant was prepared and incorporated into polypropylene (PP) by melt compounding	The antioxidant efficiency of the nanosilica-immobilized antioxidant was superior to the corresponding low molecular counterpart (AO). The thermal oxidative stability of PP/nanosilica-immobilized antioxidant was much higher than that of PP/AO compound during the long-term accelerated thermal aging	Application not described	(146)
Antioxidant enzymes (catalase and superoxide dismutase)	Magnetically responsive nanoparticles (MNP) formed by precipitation of calcium oleate in the presence of magnetite-based ferrofluid (controlled aggregation/precipitation)	Catalase stably associated with MNP was protected from proteolysis and retained 20% of its initial enzymatic activity after 24 h of exposure to pronase. Under magnetic guidance catalase-loaded MNP were rapidly taken up by cultured endothelial cells providing increased resistance to OS ( $62 \pm 12\%$ ) cells rescued from hydrogen peroxide induced cell death vs. $10 \pm 4\%$ under non-magnetic conditions	Can be highly relevant for the treatment of vascular disease	(147)
Antioxidants of <i>Salvia miltiorrhiza</i> (salvianolic acid B, cryptotanshinone, tanshinone I and tanshinone IIA)	The dried roots of <i>S. miltiorrhiza</i> were ground by the atomizer and further sprayed granulating with the aid of floating bed. The resulting materials were dried to form the nanoparticles under the dry processes	Stronger antioxidant bioactivities were observed for the extracts prepared using nanotechnology in all tested assays. The polar active constituent in the nanoparticles samples was released faster compared to the traditionally powdered samples	Application not described	(116)
Idebenone	Co-drying with chitosan (Ch) or N-carboxymethylchitosan (N-CMCh) cross-linked with tripolyphosphate (TPP)	Nanoparticles showed a 10-fold increase of drug stability in comparison with free drug and preserved antioxidant activity <i>in vitro</i> . Compared with the severely irritative free form of idebenone, the nanoparticle formulation showed decreased mucous membrane irritation	These nanoparticles have potential roles as carriers for hydrophobic and irritative drugs such as the antioxidant idebenone for topical or nasal use	(148)

Natural antioxidants extracted from <i>Ilex paraguariensis</i> (ILE)	Nanoparticles were prepared by ionic gelation of chitosan hydrochloride and sodium tripolyphosphate. The active components were added to the sodium tripolyphosphate solution and this was added dropwise to the chitosan hydrochloride solution while stirring	Chitosan hydrochloride–TPP nanoparticles maintain the antioxidant activity of ILE-polyphenols. Nanoparticles released 100% of ILE-polyphenols loaded after 15 min in two buffers with different pH values (pH 5.7 and 6.5)	This method is a promising technique for nutraceutical and cosmetic applications	(149)
p-Hydroxybenzyl alcohol (HBA)	HBA-incorporated copolyoxalate (HPOX)	HBA released from HPOX demonstrated excellent antioxidant activity, such as inhibition of nitric oxide (NO) production by suppressing iNOS (inducible nitric oxide synthases) expression in lipopolysaccharide (LPS)-activated RAW 264.7 cells. HPOX nanoparticles delivered intranasally significantly reduced pulmonary inflammation and suppressed the iNOS expression	HPOX nanoparticles are highly potent for the treatment of oxidative damage-related diseases, such as asthma	(150)
Quercetin	Nanoprecipitation technique with Eudragit® E (EE) and PVA as carriers	Particle distribution with polydispersity index <0.3, and its yield and encapsulation efficiency were over 99%. The release of the drug from the quercetin-loaded nanoparticles (QUEN) was 74-fold higher compared with the pure drug. The antioxidant activity of the QUEN was more effective than pure quercetin on diphenyl-1-picrylhydrazyl (DPPH) scavenging, anti-superoxide formation, superoxide anion scavenging, and anti-lipid peroxidation	These nanoparticles may be applied in clinical setting	(151)
Quercitrin ( <i>Albizia chinensis</i> isolated antioxidant)	Quercitrin has been encapsulated on PLA nanoparticles by solvent evaporation method	The encapsulation efficiency of nanoencapsulated quercitrin evaluated by HPLC and antioxidant assay is 40%. The <i>in vitro</i> release kinetics of quercitrin under physiological condition reveals initial burst release followed by sustained release. Less fluorescence quenching is observed with equimolar concentration of PLA encapsulated quercitrin than free quercitrin. The presence of quercitrin specific peaks on FTIR of five times washed quercitrin loaded PLA nanoparticles provides an extra evidence for the encapsulation of quercitrin into PLA nanoparticles	Potential use for therapeutic of intestinal anti-inflammatory effect and nutraceutical compounds	(152)
$\alpha$ -tocopherol (vitamin E)	Gold nanoparticles prepared with 2,2-DPPH	Chromanol groups on gold nanoparticles could efficiently enhance the activity of the vitamin E-derived antioxidant	Potential strategy for antioxidant design with several applications	(153)

#### 4.1. Nanoantioxidants pharmacotherapy

Drugs topically administered in the eye have low probability of reaching the posterior segment in significant amounts, as they have to pass through several metabolic and physical barriers to reach the retina, namely the corneal and conjunctival epithelium, then aqueous humor, and lens (132). One of the main problems encountered with the topical administration of liquid forms is the rapid and extensive loss of drugs to the limited capacity of drug retention in the ocular surface and also as a result of the blinking process, which normally is stimulated after instillation (118). The BRB and the extra ocular epithelia represent the obstacle in the drug delivery to the choroid, retina and vitreous. Only a fraction of the drug administered orally or by subcutaneous or intramuscular routes reaches the retina, requiring large doses to be therapeutically effective (118). Presently, there are several antioxidant products on market which have been formulated into these conventional dosage forms, with vitamins leading the group. Vitamins have been formulated mainly into tablets and capsules. Generally, these agents were found in combinations rather than individual products (18). A possible approach to improve retinal drug delivery is to facilitate localized delivery to the posterior segment of the eye by using Anopore™ nanoporous filter. Catalase and vitamin C were delivered using these inorganic nanoporous filter, which is made up of aluminum oxide filter with pores of 20 nm size, as a semipermeable membrane to separate two compartments *in vitro*. The data shown represented the possibility of biocompatible capsules based on nanoporous filters, which are able to provide controlled delivery of antioxidant molecules (154). Several nanocarriers may be consider as nanoantioxidants transporters as self-emulsifying drug delivery systems, which offer the potential for enhancing the absorption of poorly soluble and/or poorly permeable compounds. For drugs that are poorly soluble and/or poorly permeable, a significant improvement in reproducibility in performance and bioavailability might be achieved with these nanocarriers. Lutein is a well-known antioxidant and anti-free radical used in cosmetic, nutraceutical industry with potential application in pharmaceuticals as supportive antioxidant in treatments. However, lutein is a lipophilic molecule which is poorly soluble in water and has a low bioavailability. The lutein nanosuspension was converted into pellets and filled into hard gelatin capsules for nutraceutical use, yielding a superior *in vitro* release (155). However, there are some limitations associated with these formulations, including stability, manufacturing methods, interaction of the fill with the gelatin shell and limited solubility of some drugs in lipid solvents (18). Liposomes are potential systems for drug delivery because of their size,

hydrophilic and hydrophobic character and biocompatibility (156). The term liposomes with antioxidants could be liposomes containing lipid-soluble, water-soluble or enzymatic antioxidants. Antioxidant liposomes hold great promise in the treatment of many diseases in which OS plays a significant role (157). A major problem associated with conventional liposomes is that they are recognized by the immune system as foreign substances and rapidly removed by phagocytic cells of the reticuloendothelial system (18). Nanoparticles have been explored as drug delivery systems for encapsulation of different drugs or incorporation either into lipid or polymeric particles. The nanoencapsulation can help deliver drugs with poor aqueous solubility and permeability. In biodegradable polymeric nanoparticles the drug is dissolved, adsorbed, attached or encapsulated in the polymeric matrix of nanometer size. Depending upon the method of preparation, nanospheres or nanocapsules are obtained with different release and surface properties (158). Nanoparticles are also being explored for targeted drug delivery (159). Polymeric nanocarriers are attractive vehicles for vascular drug delivery as well, but remained a waif technology for antioxidant enzymes due to poor loading and inactivation of proteins during formulation (159). Microparticles have also been designed and evaluated as delivery systems for antioxidants produced endogenously and exogenously. The matrix is generally a polymer which sustains the release of drug. These particles are either matrix type entrapping the active moiety or capsule type encapsulating the drugs (18). The need to improve the ocular drug bioavailability, effectiveness and higher retention time becomes an emerging field in medicine, considering ocular conditions. Although there are not any antioxidant nanoparticles agent approved by European Medicines Agency (EMA) and Food and Drug Administration (FDA) there are at least 60 agents in the clinic touted as anti-angiogenic, many more potential anti-angiogenic candidates are currently in preclinical development, with the distinct possibility of moving into ocular clinical studies (160, 161). Recent data from very important multicenter clinical trials have emphasized the importance of new and evolutionary therapies.

#### **4.2. Safety issues of antioxidant nanoparticles**

Despite of nanoparticles with antioxidants are known to be from natural sources, then safe, biocompatible and biodegradable with no toxicity effects or collateral damages, pharmacokinetics and toxicological analyses should not be dispensable. This safety

performance should guarantee the molecular, subcellular and cellular behavior of nanoparticles in ocular tissues and in the systemic circulation. The development of *in vitro* cell culture models for studying ocular barriers undoubtedly provides a platform to investigate the impact of pharmaceutical trafficking on ophthalmic diseases (162). The human corneal epithelium HCE-T model, formed by transfection of human corneal epithelial cells from a 47-year-old female donor with a recombinant SV40-adenovirus, represents a standard tool for drug permeation, bioavailability prescreening, and toxicity assessment (163), should be used to simulate the corneal absorption of antioxidants. The cell line has good growth characteristics and shows a cobblestone-like appearance. The IOBA-NHC cell line, a nontransfected, spontaneously immortalized epithelial cell line derived from human conjunctiva (164), should be used for predicting the conjunctival absorption of antioxidants. The IOBA-NHC cells demonstrated high proliferative ability *in vitro* and typical epithelial morphology. Furthermore, cytokeratins, mannose, and sialic acid residues are immunologically detected, therefore appears that this cell line can be a useful experimental tool in the field of ocular surface cell biology. Immortalized human cells ARPE-19 cells are particularly important in the retinopathies studies, since they simulate the retinal behavior and may indicate the absorption of antioxidants. These cells are fully characterized regarding their morphology, the expression of retina specific marker, and their barrier properties (162, 165). Monolayers of ARPE-19 cells have become a well-established *in vitro* model of the outer BRB. Moreover, monolayers of ARPE-19 cells are used by researchers for a variety of other *in vitro* experiments, including studies of the regulation of gene expression, polarized distribution and secretion of proteins, delivery of genes and antisense oligonucleotides, for toxicity studies, and as models of retinal diseases (162, 166, 167). The fate of nanoparticles loaded with natural antioxidants must be followed with a minimum required amount of *in vivo* experiments using topical routes of administration. The therapeutic efficacy and safety *in vivo* in rabbits should be monitored by means of physiological and behavioral parameters, complemented by toxicological and monitoring of conjunctival tissue.

## 5. Summary

The physical-chemical properties of chitosan, such as inter- and intramolecular hydrogen bonding and the cationic charge in acidic medium in addition with its several bioactivities such as nontoxicity, biocompatibility, biodegradability and transmucosal absorption allows chitosan to become an excellent candidate for drug carrier and excipient for controlled release systems. A number of chitosan-based colloidal systems have been explored for bioactive molecules carriers, like films, tablets, hydrogel, micro and nanoparticle. In these formulations chitosan can reach the target sites with low collateral damages, toxicity and higher efficiency. The antioxidant therapy major problem in ocular treatments is the difficult to maintain an effective drug concentration at the site of action for an appropriate period of time, in order to achieve the expected pharmacological response. This suboptimal delivery can be overcome by different novel delivery strategies. Innovative nanomedicines with antioxidants pharmacotherapy could be seen as the key factor for eye diseases, since the use of topical nano-antioxidants to treat or delaying OS-related ocular manifestations is still unexplored, while current retinopathies therapy includes invasive method like laser photocoagulation or surgery, which may also increase risk of endophthalmitis, cataract formation and retinal detachment. Besides the development of laser for retinopathy, there have been no major advances in treatment for the disease, despite numerous clinical trials. Drugs applied directly to the eye represent a non-invasive and safe methodology, increasing the effectiveness of treatment and reducing toxicity associated with systemic administration. An ideal anti-angiogenic agent should be developed for neovascularization control and regression. It may inhibit and stabilize the disease, to prevent the vision loss, retinal scarring and detachment with no toxicity as well as the formulation should be for long term drug delivery. Agents should also be classified into early and late acting, specific and non-specific, and reversible and irreversible. The understanding of where a drug falls into these classes may help in the comprehension of the potential and/or limitation of the drug when used in the clinic, as well as how to predict potential serious adverse events. The nano-antioxidants are expected to be early acting, especially for prophylaxis. Considering this, there are a number of challenges associated to the treatment of ocular diseases. Thus, successful alternatives for ocular therapies are needed and they should provide non-invasive and a cost effective treatment reaching every economic status. Therefore, useful knowledge for future adaptation is provided for pharmaceutical industry, medical assistance and human health care.



## PART II - Aims and goals

---

*“There is a world of advantages of nanotechnology application in different fields ...  
are all a part of its own disadvantages!”*

*Jacques de la Palice*



## *CHAPTER 2 - Aims and organization of the Thesis*

---



## 2. Aims and organization of the Thesis

Considering the antioxidants biological potential, there is every need to implicate novel drug delivery technologies to improve their performance. Chitosan drug delivery systems would achieve this goal by making antioxidants reach the site of action and improve the efficacy, generally by enhancing their bioavailability, which is of prime importance when antioxidants are intended for prophylactic purpose (116).

Implication of novel delivery systems for antioxidants is ruled by physical-chemical characteristics, biopharmaceutics and pharmacokinetic parameters of the antioxidant to be formulated (116). Chitosan-based nanosystems are expected to increase the ability, to retain the drug activity during the preparation process, to optimize the release of the compound from the carrier system, and to ensure good control of their physical-chemical properties, their stability and the crucial ocular mucoadhesion (168).

Presently, the pharmaceutical research in the field of antioxidants is not going so fast as the research concerning the role of free radicals ocular diseases, despite the fact that there are various antioxidants in conventional products on the pharmaceutical market (18).

Chitosan nanoparticles are known to be new natural drug delivery systems that may incorporate antioxidants, being safe, biocompatible and biodegradable systems with no toxicity effects or collateral damages. Moreover pharmacokinetics and toxicological analyses should not be dispensable. The safety performance should guarantee the molecular and cellular behavior of nanoparticles in ocular tissues and in the systemic circulation. The development of *in vitro* cell culture models for studying ocular barriers undoubtedly provides a platform to investigate the impact of pharmaceutical trafficking on ophthalmic diseases (162).

Throughout this thesis, it was expected to:

Characterize, quantify and compare the antioxidant potential of *Salvia officinalis* and *Satureja montana* extracts and their major pure antioxidant compound: rosmarinic acid;

Encapsulate antioxidant compounds into chitosan-based nanoparticles, optimize nanoparticulate systems after deep physical-chemical characterization;

Evaluate the potential absence of cytotoxicity of the developed and optimized aforementioned nanoparticles;

Evaluate the mucoadhesion, permeability, and stability of rosmarinic acid into chitosan-based nanoparticles on the ocular surface by *in vitro* cell cultures, human cornea (HCE-T) and retina pigment epithelium (ARPE-19) (162, 165);

To study the actual effects of the antioxidant power in the elimination of free radicals and decreased vascularity in the retinal, as well as, to evaluate the toxicity, bioavailability and effectiveness (e.g. HCE-T and ARPE-19) (162, 166, 167);

Measure the neuroprotection effect of rosmarinic acid after intravitreal injection in an I-R animal model by monitoring retina morphology and biological parameters.

Pharmacokinetics and toxicological relevance of nanoparticles were guaranteed by *in vitro* model systems to mimic as close as possible the biological conditions. The development of *in vitro* cell culture models (e.g. HCE-T and ARPE-19) for studying ocular barriers undoubtedly provided a platform to investigate the impact of pharmaceutical handling on ophthalmic diseases (162). Nevertheless a number of *in vivo* tests were required in order to validate the antioxidant biological potential; in this way the I-R animal model was chosen to monitor the rosmarinic acid therapeutical potential due to its intimate relationship with glaucoma, and other ocular diseases. Moreover the I-R model allows the control of the magnitude and duration of ischemia, as well as the duration of reperfusion, which are very important parameters concerning retinal ganglion cell death (169). Even though it does not directly track the exact pathophysiology that occurs in human glaucoma, but it induces a specific insult to retinal cells, which is fundamental for the study (169).

The project casts light on the improved therapeutic utilization of the antioxidants loaded in novel, pharmaceutically acceptable nanoparticles. Therefore, useful knowledge for future adaptation is provided for pharmaceutical industry. The development of this project provided a further insight on ocular delivery, benefiting from the advantages of the eye for drug delivery and, additionally, offered new potential applications of chitosan as drug carrier and of natural antioxidants for ocular diseases prevention.

## PART III

---

*“A journey of a thousand miles begins with a single step!”*

*Confucius*





## Abstract

Introduction: *Salvia officinalis* and *Satureja montana* (sage and savory, respectively) are plants used in traditional medicine. The quality control of their herbal formulations is of paramount concern to guarantee the expected biological activity of their antioxidant compounds.

Objectives: To establish a simple and effective HPLC method to evaluate simultaneously quercetin and rosmarinic acid, in a pure form, in natural extracts (sage and savory), and encapsulated into chitosan-based nanoparticles (in the next sections).

Methodology: Chromatography was performed on a RP C18 column, in a gradient mode with a mobile phase comprising methanol:formic acid:water 92.5:2.5:5 (v/v) at a flow rate of 0.75 mL/min and at detection wavelength of 280 nm.

Results: The method was specific, linear in the range of 0.05-1.0 mg/mL ( $R^2 = 1.00$ ), precise at the intra-day and inter-day levels, accurate (recovery rate percentage of  $90.5 \pm 0.6$ ), and robust to changes in equipment conditions.

Conclusion: The established method was effective for quercetin and rosmarinic acid characterization in natural extracts and in chitosan nanoparticles, allowing the loading capacity determination, the association efficiency as well as its *in vitro* release.



## *CHAPTER 3 - High-performance liquid chromatography method validation*

---



### 3. Introduction

During the last decade, scientific evidences have proved that plant phenolics are an important class of defense antioxidants. These compounds are virtually widespread in all plant foods, often at high levels, and include phenols, phenolic acids, flavonoids, tannins, and lignans (6). Sage and savory are plants used in traditional medicine, and grow in the poor soils of the Mediterranean basin (14). Besides application as condiments, sage and savory have been used in folk medicine for their anti-diarrheal, digestive, wound healing, anti-inflammatory, disinfectant, anti-hypertensive and sedative properties. Some of these activities have been associated with their high contents of rosmarinic acid and the presence of other relevant phenolic compounds such as, quercetin, rutin and rosmarinic acid (9, 14). Rosmarinic acid ( $\alpha$ -O-caffeoyl-3,4-dihydroxyphenyllactic acid) is a phenolic compound that has been claimed to provide protection against cancer (7), among other biological activities, namely astringent, anti-inflammatory, antimutagen, antibacterial and antiviral (7, 8). It is also an efficient natural antioxidant (9). Quercetin (3,3',4',5,7-pentahydroxyflavone) is a major representative of the flavonol subclass (170). In its natural sources it exists mainly in the form of glycosides and can be found in vegetables, fruits, herbs, or red wine (151, 171). It has been demonstrated a variety of quercetin biological activities and pharmacological actions, such as dilating coronary arteries, decreasing blood lipid, anti-platelet aggregation, anti-cancer, antioxidant, anti-anemia, anti-inflammation, anti-anaphylaxis and hepatoprotective effects (151). Several studies have also reported that quercetin can inhibit the proliferation of multiple cancer cell types (lung, colon, prostate, pancreatic carcinoma cells) (171-173). Accurate identification and quantification in final formulations or plant extracts is essential to guarantee the expected biological activity. The aim of this study was to validate a HPLC method for simultaneous quantification of rosmarinic acid and quercetin in natural extracts and in polymeric nanoparticles to assess the content, the association efficiency, the *in vitro* release and permeability profile further evaluated in the next chapters.

### **3.1. Experimental**

#### **3.1.1. Materials**

Two plants were selected as extract source namely sage and savory, both provided by ERVITAL (Castro Daire, Portugal), from a previous study involving 48 medicinal plants made by our research group (115). These plants had been cultivated as organic products, and were supplied in their commercial form of dried leaves: ca. 4 g was then crushed (using a coffee mill) for 1 min, so as to obtain the corresponding powder. A fraction (ca. 1 g) was contacted, under uniform stirring, with 100 mL of boiling distilled water. After the powder deposition, samples were filtered, frozen at -80 °C and lyophilized for further procedures (Heto Holten A/S Drywinner). Then solutions (1%) of lyophilized powder were prepared in methanol for chromatographic analyses. Before injections, samples were filtered through a 0.45 µm filter. Rosmarinic acid (96.5 w/w, HPLC), quercetin dehydrate (99.0% w/w, HPLC), methanol CHROMASOLV<sup>®</sup> (HPLC ≥ 99.9%) and formic acid (HPLC ≥ 98.0%) were purchased from Sigma-Aldrich (Missouri, USA).

#### **3.1.2. Equipment and chromatographic conditions**

All HPLC runs were performed using a Waters Series 600 HPLC and results were acquired and processed with Empower<sup>®</sup> Software 2002 for data acquisition (Mildford MA, USA). HPLC analysis was conducted by using a Nova-Pack<sup>®</sup> RP C18 column (250 x 4.6 mm i.d., 5 µm particle size and 125 Å pore size) from Waters. Chromatographic analysis was performed in gradient mode. The mobile phase consisted of methanol: formic acid:ultra-pure water in the ratio of 92.5:2.5:5 (v/v). Stationary phase was made with the same components in the ratio of 5:2.5:92.5, respectively. The phases were filtered through 0.22 µm filter and degassed. Eluent was pumped at a flow rate of 0.75 mL/min, the injection volume was 20 µL and detection wavelength was set to 280 nm. All experiments occurred at room temperature and the total area of peak was used to quantify the rosmarinic acid and quercetin compounds. The conditions were investigated to provide a simple procedure with the best peak resolution regarding symmetry and tailing, reduced run time and cost-effective analysis.

### 3.1.3. Preparation of standard and sample solutions

Stock standard solutions of 2 mg/mL of rosmarinic acid and quercetin were prepared with methanol. The calibration curve was made from the dilution of stock solutions in methanol of seven standards: 0.05, 0.1, 0.2, 0.3, 0.5, 0.8 and 1.0 mg/mL.

### 3.1.4. Method validation

The HPLC method was validated according to the International Conference on Harmonization (ICH) guidelines (174), using the following analytical parameters: linearity, precision, accuracy, specificity, range, robustness, detection and quantification limits. Linearity was evaluated by calculation of a regression line using least squares method. Calibration curves were obtained from seven different concentrations analyzed three times. Precision was assessed by testing the repeatability of three different standard solutions ten times (intra-day) and by intermediate precision analyzing the same three standard solutions, three times on different days (inter-day). Accuracy was tested by percentage recovery of mean of three determinations of rosmarinic acid and quercetin at three different concentrations precisely prepared and by determination of the relative standard deviation (RSD). Specificity was determined by comparing rosmarinic acid and quercetin samples under different stress conditions that may common affect natural extracts and antioxidant activity as the temperatures of (60, 20 and 1 °C) for 24 and 72 h. The solutions were also subjected to the effect of light and air in the same period of time. Range was derived from linearity, accuracy, and precision studies. Robustness was evaluated by testing the same chromatography conditions in different HPLC equipment (Merck-Hitachi Interface D-7000). Detection limit (DL) and quantification limit (QL) were determined based on the standard deviation of the response and on the slope of the calibration curve, using the following expressions:

$$DL = \frac{3.3\sigma}{S}$$

$$QL = \frac{10\sigma}{S}$$

where  $\sigma$  is the standard deviation of the response and  $S$  is the slope of the calibration curve.

### **3.1.5. Method applicability**

Applicability of the method was governed with the simultaneous determination of two antioxidant compounds with great impact on health. The determination could be made for each independent compound or combined, since the presence of both does not affect their quantification, also it could be made in natural extracts or even in the nanoparticulate systems. This HPLC method was also developed, optimized and validated for the best precise results regarding, rosmarinic acid association efficiency in chitosan-based nanoparticles, rosmarinic acid *in vitro* release from the aforementioned nanoparticles and its permeability profile in cell monolayers, assays developed and characterized in the next chapters.

## **3.2. Results and discussion**

### **3.2.1. Application of the chromatographic method**

An HPLC method for the assessment of rosmarinic acid and quercetin has been proposed. Previous experiences were exploited to provide a simple procedure with the best chromatographic peak resolution, reduced run time and cost-effective analysis. All these factors contribute to the establishment of an analytical method which permits the analysis of a large series of samples. A typical chromatogram for the proposed method was depicted in Figure 3.1. The rosmarinic acid and quercetin peak retention time was  $48.9 \pm 0.1$  min (i) and  $57.9 \pm 0.6$  min (ii), respectively. These retention times were not completely straight, but this method may also be useful for the identification and detection of other compounds in natural extracts, which were complex matrixes with different compounds (latest retention time compound at 90 min). However, retention factor parameter ( $k'$ ) was measured in order to evaluate the chromatographic performance



(175). This retention factor was often used to describe the migration rate of an analyte on a column. The retention factor for analyte *A* was defined as:

$$K'A = \frac{tR - tM}{tM}$$

where retention time of the analyte ( $t_R$ ) and retention time of the eluent ( $t_M$ ) were easily obtained from the chromatogram. When the analytic retention factor was less than one, elution was so fast that accurate determination of the retention time was very difficult. High retention factors (greater than twenty) mean that elution takes a very long time. Ideally, the retention factor for an analyte was between two and ten (175). The retention factors of both compounds were 0.918 and 0.930, for rosmarinic acid and quercetin, respectively. Both compound parameters were in the optimal range ( $k' < 10$ ), which means that the migration rate of the analytes were adequate and so was the method. A good experimental design is crucial, and this seems particular important in herbal medicines in order to obtain an optimal separation, since these natural matrixes may entail hundreds of natural compounds (176).

### 3.2.2. Linearity

Linearity was studied in the concentration range of 0.05-1.0 mg/mL by visual inspection of a calibration curve plotting ( $n = 21$ ) and by calculating the regression equation and the correlation coefficient ( $R^2$ ) by the method of least squares. A primary stock solution was accurately prepared followed by rigorous dilution to give secondary standard solutions. Each sample was analyzed three times. A good linearity was obtained in the range of study. The calibration curve for rosmarinic acid was:

$$A = 5.44 \times 10^7 (\pm 2.66 \times 10^5) \times C - 6.21 \times 10^5 (\pm 1.43 \times 10^5) (n = 21) R^2 = 1.00$$

and the calibration curve for quercetin was:

$$A = 4.48 \times 10^7 (\pm 2.73 \times 10^5) \times C - 9.75 \times 10^5 (\pm 1.47 \times 10^5) (n = 21) R^2 = 1.00$$

where *A* is the peak area, *C* is the standard solution concentration in mg/mL, and standard deviation values for *A* and *C* are indicated in brackets. The  $R^2$  obtained was higher than 0.999 as frequently recommended (177), indicating a good linearity in the proposed range.

### 3.2.3. Precision

Precision may be considered at three levels: repeatability, intermediate precision and reproducibility (174). The precision of an analytical procedure is usually expressed as the variance, standard deviation or coefficient of variation of a series of measurements. Repeatability was termed intra-day and expresses the precision under the same operating conditions over a short interval of time. Intermediate precision expresses within-laboratories variations like different days, different analysts or different equipment. Reproducibility expresses the precision between laboratories (standardization of methodology) (174). For this validated method the relative standard variation for system repeatability and analysis repeatability was  $\leq 1.476$  and  $\leq 1.456\%$ , respectively since  $RSD \leq 2\%$ . Such results indicate that the proposed method presents good precision (Table 3.1) (178).

**Table 3. 1.** Results of precision tests for the determination of rosmarinic acid and quercetin in standard solutions.

Standard solution	(mg/mL)	Day	Measured concentration	SD (%)	RSD (%)
<b>System repeatability (n = 10)</b>					
Rosmarinic acid	0.800	0	0.776	0.183	0.235
		5	0.776		
		10	0.779		
	0.400	0	0.405	0.030	1.097
		5	0.404		
		10	0.404		
	0.200	0	0.169	0.065	1.476
		5	0.168		
		10	0.168		
Quercetin	0.800	0	0.735	0.444	0.602
		5	0.733		
		10	0.741		
	0.400	0	0.408	0.248	0.610
		5	0.409		
		10	0.404		
	0.200	0	0.213	0.176	0.835
		5	0.209		
		10	0.210		

<b>System repeatability (n = 3)</b>					
Rosmarinic acid	0.800	0	0.775	0.415	0.533
		5	0.782		
		10	0.776		
	0.400	0	0.389	0.394	1.003
		5	0.393		
		10	0.397		
	0.200	0	0.166	0.244	1.456
		5	0.165		
		10	0.170		
Quercetin	0.800	0	0.807	0.320	0.398
		5	0.804		
		10	0.801		
	0.400	0	0.406	0.389	0.950
		5	0.409		
		10	0.413		
	0.200	0	0.207	0.059	0.352
		5	0.208		
		10	0.207		
<b>System repeatability (n = 3)</b>					
Rosmarinic acid	0.800	0	0.776	0.882	1.128
		5	0.778		
		10	0.792		
	0.400	0	0.405	0.030	0.075
		5	0.404		
		10	0.404		
	0.200	0	0.212	0.578	2.813
		5	0.203		
		10	0.201		
Quercetin	0.800	0	0.821	0.968	1.195
		5	0.809		
		10	0.802		
	0.400	0	0.408	0.248	0.610
		5	0.409		
		10	0.404		
	0.200	0	0.206	0.407	1.983
		5	0.209		
		10	0.201		

### 3.2.4. Accuracy

Three standard solutions (0.05, 0.30 and 0.50 mg/mL) were carefully prepared in triplicate and analyzed by the proposed method. The overall recovery percentage was found to be  $90.5 \pm 0.6$ , thus showing strong agreement between experimental and theoretical values. Detailed results for the three tested concentration levels were presented in Table 3.2.

**Table 3. 2.** Accuracy results for different levels of rosmarinic acid and quercetin in standard solutions.

<b>Standard solution</b>	<b>(mg/mL)</b>	<b>Recovery (%)</b>	<b>RSD (%)</b>
<b>System repeatability (n = 3)</b>			
Rosmarinic acid	0.05	87.06	0.16
	0.30	90.76	0.87
	0.50	91.98	1.16
Quercetin	0.05	89.02	0.92
	0.30	95.21	0.38
	0.50	98.70	0.06

### 3.2.5. Specificity

Specificity of method was verified by analyzing four stress conditions (temperature, UV light, pH and oxidation), in accordance with other publish works (175), in order to detect the occurrence of possible interfering peaks at 280 nm, resulting from the degradation of antioxidants. The stress conditions were the most compromising of antioxidant activity were for that helpful tools in establishing degradation pathways and also help validating the power of the proposed method for studying the stability of the compounds (175). It was tested the effect of solutions of rosmarinic acid and quercetin in methanol for the temperatures of (60, 20 and 1 °C) for 24 and 72 h. The solutions were also subjected to the effect of light and air in the same period of time. Overall, obtained data provides evidence that the method can be regarded as specific, since no potential interfering peak was observed in the antioxidants retention times and the recovery percentage for stress condition was  $76.0 \pm 1.4\%$ . The compounds used as matrix for encapsulation (chitosan

and TPP), could also be seen as interfering. However, the method, once more, demonstrates to be specific for the presence of these compounds, since no potential interfering peak was observed in the antioxidants retention times in the association efficiency tests.

### **3.2.6. Range**

The method working range was defined as to fulfill the required versatility, proving to be linear, accurate and precise between 0.05 and 1.0 mg/mL. Therefore, samples presenting these concentration levels may be suitably assayed by the proposed HPLC method.

### **3.2.7. Robustness**

A method is said to be robust when these alterations produce no significant changes in obtained results. The robustness of this HPLC method was verified by the experimental under the same conditions in totally different equipment (Merck-Hitachi Interface D-7000). This was a robust method since no significant changes were observed in recovery percentage and in the retention time of the compounds.

### **3.2.8. Detection limit and quantitation limit**

Several alternatives were described to determine DL and QL (177). In the present work, these parameters were established from the SD of the response and the slope of the calibration curve. Values of SD were calculated from standard deviation of the free terms taken from regression equations of calibration curves obtained using reference samples in the region of DL. DL and QL were found to be 0.02 and 0.08 mg/mL for rosmarinic acid, respectively. For quercetin were found to be 0.03 and 0.09 mg/mL for DL and QL, respectively.

### 3.2.9. Method applicability

The developed method was applied to ensure the analytical identification, quantification and limit control in both, savory and sage extracts, as well as their antioxidant association efficiency and *in vitro* release from chitosan-based nanoparticles in the next chapters. The peaks of rosmarinic acid and quercetin has a retention time of  $48.9 \pm 0.1$  and  $57.9 \pm 0.6$  min, respectively, and for the present study the quantification of both antioxidants were clear and easily performed (Figure 3.1). For natural extracts quantification of the both antioxidants, three independent experiments were made, with different lyophilized powder dissolved in methanol, in a concentration of 10 mg/mL and in triplicate injections. Savory was founded to contain rosmarinic acid and quercetin in a concentration of  $0.52 \pm 0.02$  mg/mL and  $0.50 \pm 0.04$  mg/mL, respectively and sage has only rosmarinic acid, in a concentration of  $1.10 \pm 0.09$  mg/mL. The method can be extended to other applications, namely, dissolution testing, drug products or different drug release from nanoparticulate systems, testing for impurities or interferences and to analyze changes in the synthesis of the drug substance, in the composition of the finished product and in the analytical procedure.

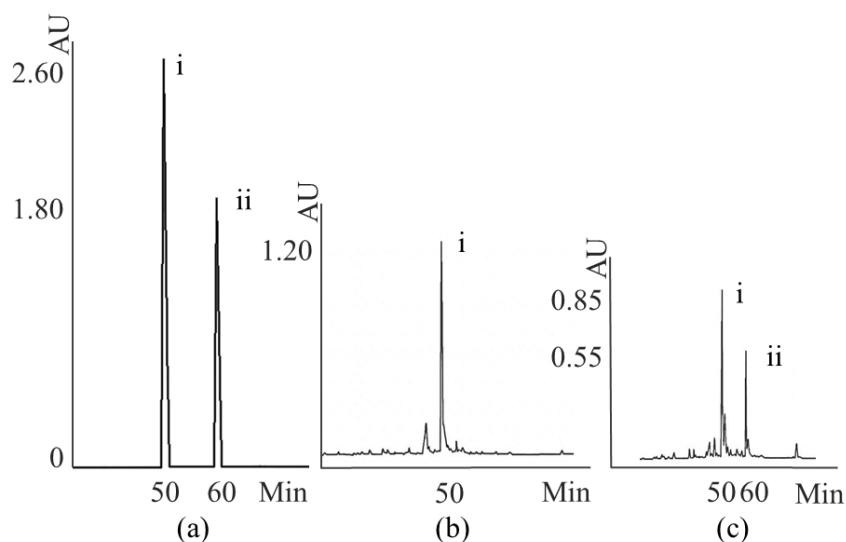


**Figure 3. 1.** Representative chromatogram of: (i). rosmarinic acid (retention time:  $48.9 \pm 0.1$  min) and (ii). quercetin (retention time:  $57.9 \pm 0.6$  min); (a). in standard solutions; (b). in sage extracts; (c). and savory extracts.

### 3.3. Conclusion

In summary, this was the first study to describe a validated HPLC method with UV detection for rosmarinic acid and quercetin determination according to ICH guidelines, in natural extracts and in nanoparticulate systems. All parameters were within the limits proposed by those guidelines for pharmaceutical formulations, indicating that this method was specific, precise, accurate and robust with low detection and quantification limits. Furthermore, suitable application for rosmarinic acid *in vitro* analysis was assumed during formulation development and characterization. The proposed method was used to predict the association efficiency and the release profile of rosmarinic acid from chitosan-based nanoparticles containing sage and savory extracts in the further chapters. Rosmarinic acid and extracts entrapment occurs essentially by reversible ionic interactions, which permits an absence of interaction of polymers on compound determination in the different steps of formulation development.





## PART IV

---

*“Science is a way of thinking much more than it’s a body of knowledge”*

*Carl Sagan*



## Abstract

**Introduction:** Nanotechnology can be applied to deliver and protect antioxidants in order to control the OS phenomena in several chronic pathologies. Chitosan nanoparticles are biodegradable carriers that may protect antioxidants with potent biological activity such as rosmarinic acid in *Salvia officinalis* (sage) and *Satureja montana* (savory) extracts for safe and innovative therapies.

**Objective:** Development, optimization and characterization of chitosan-based nanoparticles as stable and protective vehicle to deliver rosmarinic acid for medical applications using natural extracts as sage and savory.

**Methodology:** Antioxidant-chitosan based nanoparticles were prepared by ionic gelation with sodium tripolyphosphate (TPP), at pH 5.8 with mass ratio of 7:1 (chitosan:TPP), with a theoretical antioxidant-chitosan loading of 40 to 50%. The size and shape of nanoparticles were then characterized by different methods such as: photon correlation spectroscopy, laser Doppler anemometry, scanning electron microscopy (SEM) and transmission electron microscopy (TEM). Chemical interactions between antioxidants and chitosan were assessed by differential scanning calorimetry (DSC) and Fourier-transform infrared (FTIR). HPLC allowed the association efficiency and *in vitro* released measurements. Antioxidant activity was evaluated by 2,2-azinobis (3-ethylbenzothiazoline-6-sulphonic) (ABTS) and oxygen radical absorbance capacity (ORAC) methods before and after lyophilization to assure that antioxidant activity was not compromised after the dried process.

**Results:** Small sizing nanoparticles, around 300 nm, were obtained. SEM and TEM confirmed smooth and spherical nanoparticles. No chemical interactions were found between antioxidants and chitosan, after encapsulation, by DSC and FTIR. The association efficiency was 51.2% for rosmarinic acid (with 40% loading), 96.1 and 98.2%, for sage and savory nanoparticles, respectively (both with 50% loading). The best antioxidant activity results were obtained after nanoparticles lyophilization and by ORAC method, the values for rosmarinic acid, sage and savory nanoparticles were:  $3.6520 \pm 0.1770$ ,  $0.4251 \pm 0.0069$  and  $0.4526 \pm 0.0087$   $\mu\text{mol}/\text{eq}$  Trolox, respectively.

**Conclusion:** The extracts under study were promising vehicles for rosmarinic acid drug delivery in chitosan nanocarriers.



*CHAPTER 4 - Development, optimization and physical-chemical characterization of chitosan-based nanoparticles*

---



#### 4. Introduction

Sage and savory, are plants often used in traditional medicine to improve digestion (179), as disinfectant (180), to decrease blood pressure (7), to prevent premature ejaculation (181), to treat neuropathy (182), urinary and pulmonary infections (183), and other diseases such as Alzheimer's disease (184) and cancer (183). Some of these biological activities have been associated with its high contents in rosmarinic acid (9, 179, 185). Rosmarinic acid, (*a*-*O*-caffeoyl-3,4-dihydroxyphenyllactic acid), is a phenolic compound generally admitted as a free radical scavenger (125). Besides its huge antioxidant activity rosmarinic acid can have many beneficial functionalities like antibacterial and antiviral activity, anti-inflammatory activity (127), anti-mutagenicity character (128), capability to reduce atopic dermatitis symptoms (129), prevention of Alzheimer's disease (130) and apoptosis induction of colorectal cancer cells (131). Nevertheless, besides the poor absorption that constrain the transport across biological barriers, most of the natural antioxidants or other active compounds are unstable and must be protected from degradation in the physiological environment (186). Thus, the efficacy of these drugs clearly depends on the design of appropriate carriers for their delivery, protection and release (1). Among the different approaches explored so far, colloidal carriers have particular interest, especially those made of mucoadhesive polymers to assure drug time retention at the absorption site (2). For this application, chitosan has become of particularly interesting for the association and delivery of labile macromolecular compounds, due to its exceptional potential for drug delivery, especially for mucosal, control drug release and protect against adverse conditions like mucosal enzymes and biological protective fluids (187). The smart symbiosis of these chitosan nanoparticles with a high potent antioxidant could be a hope for future therapies, considering the important effect of OS in several chronic pathologies. In this study chitosan nanoparticles were used, to incorporate natural extracts of sage and savory as a stable and protective vehicle to deliver rosmarinic acid for medical applications. There were no reports in the literature that have demonstrated the good performance of chitosan nanoparticles to incorporate these extracts in order to bring the huge benefits of rosmarinic acid antioxidant, as well as, other compounds that may act synergistically.

## **4.1. Experimental**

### **4.1.1. Materials**

The two selected plants sage and savory were provided by ERVITAL (Castro Daire, Portugal). The plants had been cultivated as organic products, and were supplied in their commercial form of dried leaves. The dried leaves were then kept in the dark at 20 °C. Rosmarinic acid (purity 96.5%), methanol CHROMASOLV® (HPLC  $\geq$  99.9%) and formic acid (HPLC  $\geq$  98.0%) were purchased from Sigma-Aldrich (Missouri, USA). Chitosan low molecular weight and sodium tripolyphosphate (TPP) were also purchased from Sigma-Aldrich (Lisbon, Portugal). The degree of deacetylation for the low molecular weight (LMW) chitosan was 85%, with a purity grade of 85%. Pure acetic acid was purchased from Ponalab (Lisbon, Portugal). Sodium hydroxide (NaOH) and hydrochloric acid (HCl) were from Merck (Darmstadt, Germany). Ultra-pure water was obtained in the laboratory using a Millipore™ water purification equipment (Massachusetts, USA).

### **4.1.2. Preparation of chitosan-based nanoparticles**

Optimized conditions to obtain chitosan nanoparticles were based on previously studies (188), and was schematically described in Figure 4.1. The chitosan nanoparticles were obtained by inducing the gelation of a chitosan solution with TPP. Chitosan was dissolved in acetic acid aqueous solutions at various chitosan concentrations: 0.05, 0.5, 1, 2, 3 and 5% (*w/v*), the pH value was adjusted to 5.8 with 1M NaOH. The concentration of acetic acid was, in all cases, 1.75 higher than chitosan. Then, TPP was dissolved in purified water at 0.05, 0.1, 0.2, 0.5, 1 and 2% (*w/v*). For the study of the best ratio chitosan:TPP, a volume of the TPP solution of 2 was added to 5 mL of the chitosan solution under magnetic stirring at room temperature, thus achieving a final concentration of 2 mg/mL and 0.28 mg/mL of chitosan and TPP respectively (7:1). Stock solution of chitosan (1%) and TPP (0.1%) were maintained at 4 °C for a period of 1 month.



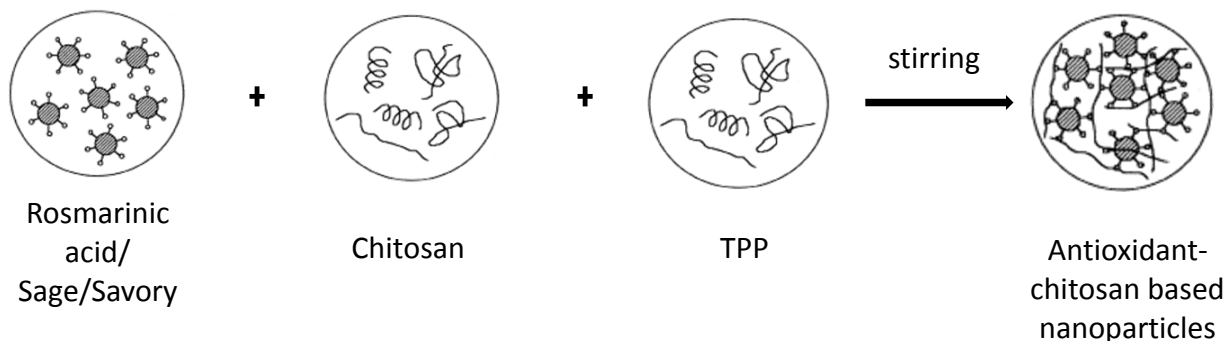


**Figure 4. 1.** Schematic illustration of ionic gelation process of antioxidant-chitosan based nanoparticles.

#### **4.1.3. Encapsulation of sage, savory and rosmarinic acid into chitosan-based nanoparticles**

The addition of 1% extracts aqueous solution and a 1% of aqueous rosmarinic acid solution was added to chitosan previously dissolved in acetic acid at a pH value adjusted to 5.8, in different volumes in order to guarantee the best concentration ratio between chitosan and the different compounds. The encapsulation of rosmarinic acid, sage and savory were tested in different theoretical loadings (5, 10, 15, 20, 30, 40 and 50%) fairly to the initial concentration of chitosan (2 mg/mL). All the tests were made for the 7 batches, considering the two plants and the antioxidant pure. Some of the final batches were then lyophilized (Heto Holten A/S Drywinner) and maintained at -20 °C for 1-2 months for further analysis.

#### **4.1.4. Size and surface charge**

Size and polydispersity (size distribution) of freshly loaded nanoparticles were determined by photon correlation spectroscopy using ZetaPALS (Brookhaven, New York, USA). A sample of 1.6 mL was gently homogenized, placed into analyzer chamber and measured. Collective 6 readings were performed three times on a sample of particles at 25 °C with a detection angle of 90°. The zeta potential was determined by laser Doppler anemometry,

at 25 °C. Triplicate samples were also analyzed, each sample being measured 6 times, and the arithmetic mean was adopted.

#### **4.1.5. Morphology**

In order to characterize the nanoparticles morphology and confirm their size distribution, nanoparticles were also observed by transmission electron microscopy (TEM, Joel JEM 1400) using an acceleration voltage of 120 kV. For sample preparation, fresh nanoparticles were diluted in MilliQ-water, placed on copper coated grids, and contrasted with uranyl acetate. In each step, the excess of water was removed using a filter paper, and finally, grids were left at room temperature for a few minutes to dry before the imaging. Lyophilized nanoparticles morphology such as shape and occurrence of aggregation phenomena was studied by scanning electron microscopy (SEM). Samples of nanoparticles were mounted on metal stubs, gold coated under vacuum and then examined on a JEOL-5600 Lv microscope (Japan). SEM was operated at the low vacuum mode, using a spot size of 27-28 and a potential of 30 kV. All analyses were performed at room temperature (20 °C).

#### **4.1.6. Association efficiency**

Association efficiency (AE) was evaluated considering the amount of rosmarinic acid associated with the particles. For this purpose the particles were centrifuged (20.000 × g/45 min) and suspended in 7 mL of ultra-pure water. The AE was then calculated by the difference between the total rosmarinic acid used to prepare the particles, and the amount of residual rosmarinic acid in the supernatant. AE of rosmarinic acid in rosmarinic acid nanoparticles sage and savory nanoparticles were obtained according to the following equation:

$$AE\% = \frac{\text{Total amount of rosmarinic acid} - \text{Free amount of rosmarinic acid in supernatant}}{\text{Total amount of rosmarinic acid}} \times 100$$

#### **4.1.7. *In vitro* release of rosmarinic acid from chitosan nanoparticles**

The release of rosmarinic acid from chitosan nanoparticles was tracked to predict the diffusion and kinetic behavior of the nanosystems in simulated physiological conditions. The osmolarity was correct to these release tests, to better simulate the topical ocular administration and to study the release profile of rosmarinic acid from chitosan-based nanoparticles in biological settings. The loaded nanoparticles obtained after centrifugation were suspended in 10 mL of a phosphate-buffered saline (PBS) solution, pH 7.4 to also best simulate tear physiological conditions. The PBS ionic strength was 0.075 M which is in the optimal range (e.g. 0.025 to 0.15 M) for physiological environment proof-of-concept testing and characterization (189). Osmolarity of nanoparticles dispersions in PBS, was determined at room temperature using a Micro-Osmometer Type 15 (Löser Messtechnik, Berlin, Germany). Plastic eppendorfs containing 200  $\mu$ L of nanoparticles dispersions were placed in the osmometer and osmolarity values read directly from the equipment. Osmolarity was adjusted 300 mOsm / L, which is the tear film normal osmolarity, with NaCl solution (Merck - Darmstadt, Germany). The nanoparticle suspension was transferred to clean eppendorfs and placed in a water bath at 37 °C under stirring, to fake the blinking process. After 0.5, 1 and 2 h, samples were collected from the bath and centrifuged at 14.000 rpm for 5 min (BOECO, Hamburg, Germany). Supernatants were analyzed by HPLC and used to calculate the amount of rosmarinic acid released from the nanoparticles over the specified time. Triplicate samples were analyzed at each time. It must be highlighted regarding this *in vitro* assays and taking into account the ionic nature of the particles that it would be expected a rapid release of rosmarinic acid, and thus the trial was designed for last only 1 h. However, due to the nanoparticles trapped properties it would not be predictable such a rapid release profile, so more sampling times could be considered (preferably before 15 min). Nonetheless, this test was planned to best simulate the physiological ocular conditions and to study the consequente chitosan-based nanoparticles behavior over a spaced period of time.

#### **4.1.8. High performance liquid chromatography analysis and rosmarinic acid quantification**

Chromatographic analysis were performed as previously described (190), using the Waters Series 600 HPLC and results acquired and processed with Empower® Software

2002 for data acquisition (Mildford MA, USA), on a Nova-Pack® RP C18 column (250 x 4.6 mm i.d., 5 µm particle size and 125 Å pore size) from Waters, in a gradient mode with a mobile phase comprising methanol:formic acid:water 92.5:2.5:5 (v/v) at a flow rate of 0.75 mL/min. The injection volume was 20 µL and detection wavelength was 280 nm. For analysis and quantification of rosmarinic acid content in the extracts, stock standard solutions of 2 mg/mL of rosmarinic acid were prepared with methanol. The calibration curve was made from the dilution of stock solutions in methanol of seven standard (0.05; 0.1; 0.2; 0.3; 0.5; 0.8; 1.0) mg/mL. The HPLC method was validated in chapter 3, according to the International Conference on Harmonization (ICH) guidelines (174).

#### **4.1.9. Differential scanning calorimetry analysis**

Thermograms were obtained using a DSC (DSC-60, Shimadzu, Columbia, USA). Samples were lyophilized, and 2.0 mg of the lyophilized powder were crimped in a standard aluminum pan and heated from 20 to 350 °C at a heating constant rate of 10 °C/min under constant purging of nitrogen at 20 mL/min. All samples were run in triplicate and data presented were the average of the three measurements.

#### **4.1.10. Fourier-transform infrared analysis**

Infrared spectroscopy analysis were performed in a ABB MB3000 FTIR spectrometer (ABB, Switzerland) equipped with a horizontal attenuated total reflectance (ATR) sampling accessory (PIKE Technologies, USA), the Horizon MBTM FTIR software and a diamond/ZnSe crystal. All spectra were acquired using 200 scans and a 4 cm<sup>-1</sup> resolution in the region of 4000-700 cm<sup>-1</sup>. In order to perform the spectra comparison, spectra were truncated at 1800 and 700 cm<sup>-1</sup>, since this region displays typical absorption bands for the used compounds. In addition, baseline - point adjustment and spectra normalization was performed. All samples used were previously lyophilized and run in triplicate, and the data presented were the average of the three measurements.

#### **4.1.11. Statistical analysis**

Statistical analysis was performed using IBM SPSS Statistics v 19.0.0 (Illinois, USA). The one-way analysis of variance (ANOVA) was used with Scheffé post hoc test comparison of groups with normal distribution, and Mann-Whitney test for groups with non-normal distribution. Differences were considered to be significant at a level of  $P < 0.05$ .

## **4.2. Results and discussion**

### **4.2.1. Particle size, polydispersity and zeta potential**

Particle size and size distribution are important parameters towards development of suitable nanomedicines for therapeutic purposes, they influence *in vivo* distribution, biological fate, toxicity and the targeting ability of nanoparticle systems (191). In addition, they can also influence the drug loading, drug release and stability of drug inside nanoparticles (192). Considering the nanoparticles charge it is known that the highest value of zeta potential represents the greater electrostatic repulsive interactions among the particles, the stability will increase as well as the size distribution will be more homogenous. Zeta potential values of  $\pm 30$  mV indicates that the colloidal system are stable in time and that amino groups of chitosan are on the surface, which was also documented in some similar studies of antioxidants encapsulation in chitosan nanoparticles (193). The loaded nanoparticles under study, ranging from 200-300 nm, and with zeta potential from 20-30 (Table 4.1) showed no significant differences ( $P > 0.05$ ) between the different theoretical loadings for each formulation and between the two crude extracts, which was in accordance with previously reports (190). Rosmarinic acid-nanoparticles at 50% theoretical loading were the only exception, since their higher size ( $1218.0 \pm 136.2$  nm) was not in the range of nanoscale, and as consequence not considered for the following tests. The extracts do not seem to interfere in the size or zeta potential of the nanoparticles being a good vehicle for rosmarinic acid incorporation. The obtained nanoparticles also showed values of polydispersity between 0.1 and 0.2 (Table 4.1) corresponding to a narrow particle size distribution, and to monodispersed particles.

These results similar with other research works using similar antioxidant nanoparticles (194).

**Table 4. 1.** Average hydrodynamic diameter ( $Z$ ), polydispersity index ( $Pdl$ ), zeta potential and the association efficiency considering the different loading (%) of rosmarinic acid, sage and savory nanoparticles (n = 3).

Nano	Loading (%)	Z-average (nm)	$Pdl$	Zeta potential (mV)	Free amount ( $\mu\text{g/mL}$ )	Total amount ( $\mu\text{g/mL}$ )	AE (%)
Rosmarinic acid	5	230.0 $\pm$ 48.8 <sup>a</sup>	0.155 $\pm$ 0.043	23.9 $\pm$ 5.5 <sup>b</sup>	56.6 $\pm$ 3.6	100	43.4 $\pm$ 3.5 <sup>c</sup>
	10	242.4 $\pm$ 112.3 <sup>a</sup>	0.215 $\pm$ 0.126	18.7 $\pm$ 2.3 <sup>b</sup>	94.8 $\pm$ 6.1	200	52.6 $\pm$ 3.1 <sup>c</sup>
	15	229.5 $\pm$ 40.1 <sup>a</sup>	0.142 $\pm$ 0.076	29.9 $\pm$ 9.9 <sup>b</sup>	147.9 $\pm$ 54.8	300	50.7 $\pm$ 18.3 <sup>c</sup>
	20	231.1 $\pm$ 68.3 <sup>a</sup>	0.149 $\pm$ 0.044	32.7 $\pm$ 6.4 <sup>b</sup>	186.4 $\pm$ 52.0	400	53.4 $\pm$ 2.0 <sup>c</sup>
	30	261.8 $\pm$ 50.4 <sup>a</sup>	0.171 $\pm$ 0.027	34.5 $\pm$ 4.5 <sup>b</sup>	306.0 $\pm$ 39.2	600	49.0 $\pm$ 6.5 <sup>c</sup>
	40	244.0 $\pm$ 18.0 <sup>a</sup>	0.193 $\pm$ 0.062	29.5 $\pm$ 1.6 <sup>b</sup>	390.4 $\pm$ 41.0	800	51.2 $\pm$ 3.0 <sup>c</sup>
	50	1218.0 $\pm$ 136.2 <sup>a</sup>	0.294 $\pm$ 0.132	35.0 $\pm$ 7.9 <sup>b</sup>	422.0 $\pm$ 65.0	1000	57.8 $\pm$ 1.3 <sup>c</sup>
Sage	5	330.9 $\pm$ 78.9 <sup>a</sup>	0.137 $\pm$ 0.012	20.8 $\pm$ 0.6 <sup>b</sup>	15.1 $\pm$ 0.4	100	84.9 $\pm$ 0.4 <sup>d</sup>
	10	224.3 $\pm$ 82.1 <sup>a</sup>	0.182 $\pm$ 0.061	24.3 $\pm$ 0.2 <sup>b</sup>	17.6 $\pm$ 0.6	200	91.2 $\pm$ 0.3 <sup>d</sup>
	15	200.0 $\pm$ 15.3 <sup>a</sup>	0.145 $\pm$ 0.018	21.4 $\pm$ 1.1 <sup>b</sup>	22.5 $\pm$ 1.1	300	92.5 $\pm$ 0.4 <sup>d</sup>
	20	243.0 $\pm$ 66.2 <sup>a</sup>	0.170 $\pm$ 0.123	21.7 $\pm$ 0.1 <sup>b</sup>	26.0 $\pm$ 4.0	400	93.5 $\pm$ 1.0 <sup>d</sup>
	30	271.5 $\pm$ 22.3 <sup>a</sup>	0.180 $\pm$ 0.056	27.8 $\pm$ 0.6 <sup>b</sup>	29.4 $\pm$ 3.0	600	95.1 $\pm$ 0.5 <sup>d</sup>
	40	272.9 $\pm$ 58.1 <sup>a</sup>	0.254 $\pm$ 0.099	25.1 $\pm$ 0.0 <sup>b</sup>	39.2 $\pm$ 2.1	800	95.1 $\pm$ 0.3 <sup>d</sup>
	50	278.4 $\pm$ 42.2 <sup>a</sup>	0.268 $\pm$ 0.092	24.9 $\pm$ 0.1 <sup>b</sup>	39.0 $\pm$ 2.6	1000	96.1 $\pm$ 0.2 <sup>d</sup>
Savory	5	233.1 $\pm$ 40.8 <sup>a</sup>	0.171 $\pm$ 0.083	23.8 $\pm$ 1.5 <sup>b</sup>	11.9 $\pm$ 0.0	100	88.1 $\pm$ 0.0 <sup>d</sup>
	10	230.7 $\pm$ 21.2 <sup>a</sup>	0.136 $\pm$ 0.094	27.8 $\pm$ 4.2 <sup>b</sup>	12.0 $\pm$ 0.1	200	94.0 $\pm$ 0.1 <sup>d</sup>
	15	182.7 $\pm$ 24.1 <sup>a</sup>	0.087 $\pm$ 0.075	28.0 $\pm$ 5.8 <sup>b</sup>	12.6 $\pm$ 0.1	300	95.8 $\pm$ 0.0 <sup>d</sup>
	20	220.8 $\pm$ 52.7 <sup>a</sup>	0.092 $\pm$ 0.024	26.7 $\pm$ 1.3 <sup>b</sup>	13.2 $\pm$ 0.2	400	96.7 $\pm$ 0.0 <sup>d</sup>
	30	188.0 $\pm$ 50.6 <sup>a</sup>	0.098 $\pm$ 0.006	28.9 $\pm$ 4.5 <sup>b</sup>	14.4 $\pm$ 0.6	600	97.6 $\pm$ 0.1 <sup>d</sup>
	40	139.4 $\pm$ 16.2 <sup>a</sup>	0.135 $\pm$ 0.088	28.4 $\pm$ 1.6 <sup>b</sup>	15.2 $\pm$ 0.4	800	98.1 $\pm$ 1.1 <sup>d</sup>
	50	229.3 $\pm$ 29.6 <sup>a</sup>	0.149 $\pm$ 0.121	26.5 $\pm$ 3.5 <sup>b</sup>	18.0 $\pm$ 0.2	1000	98.2 $\pm$ 0.1 <sup>d</sup>

#### 4.2.2. Morphology

TEM images can directly provide information on the particle size and morphology, also allowing an easy confirmation of photon correlation spectroscopy measurements. The micrograph - Figure 4.2 (a, b and c), showed TEM images of rosmarinic acid, sage and savory nanoparticles respectively (prepared freshly). The microstructural analysis confirmed a mono-disperse population of isolated, smooth and spherical particles with well-defined sizes, which were at all times lower than 500 nm, corroborating the previously obtained results of chitosan nanoparticles characterization. Moreover, in the micrograph it can be also observed a black 'corona' type of structure surrounding the nanoparticle surface which may indicate the presence of rosmarinic acid either adsorbed or covalently linked to the surface of the nanoparticle. Thus it is possible that at this pH rosmarinic acid may be partially adsorbed or covalently linked to the surface of the nanoparticle, and not completely incorporated into chitosan polymeric network. The effect of pH in chitosan ionic nanoparticles incorporation of iron oxide was reported to be crucial to its encapsulation or partial adsorption (195).

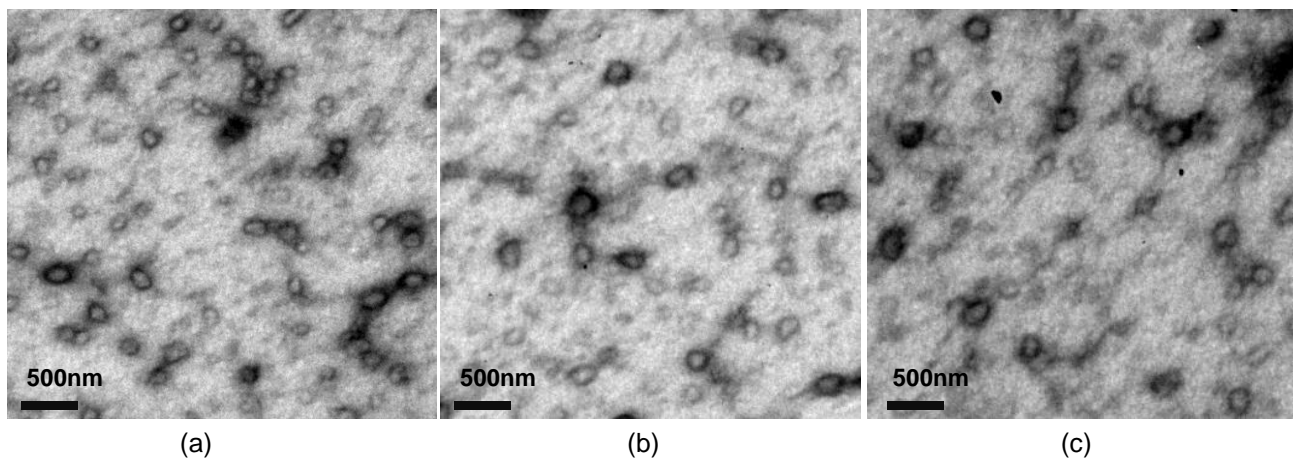


**Figure 4. 2.** TEM micrographs of fresh chitosan-based nanoparticles loaded: (a). commercial rosmarinic acid; (b). sage; and (c). savory.

The size and morphology results were aligned with SEM analyze (Figure 4.3) for the same nanoparticles (196). In this study SEM images were analyzed to prove that the size was

maintained after freeze dried (dehydration process). In the SEM analysis the particles after lyophilization also confirmed smooth and spherical shape with size below 500 nm, even with some aggregation due to the dry process (196). It can be therefore affirmed that rosmarinic acid and extracts encapsulation (either fresh or lyophilized), did not considerably affect particle shape and overall size as it was described above. Figure 4.3 shows the SEM images of lyophilized chitosan nanoparticles prepared by ionic gelation under the same pH conditions, for the encapsulation of rosmarinic acid in a pure form, sage and savory. The lyophilized samples even with some aggregation of the nanoparticles formed by dispersion during freeze drying guarantee the nanoscale particles with the diameters, which was in accordance with other previous studies (197). The microstructural analysis confirmed the morphology and size of the nanoparticles. Other studies reported an increase in the particle size after lyophilization with the unmodified chitosan particles (198). This was resulted from aggregation from the strong inter- and intra-molecular hydrogen bonding, which was not possible to breakdown even by vortex homogenization (198). This particles size increase after lyophilization process was also reported in essentials oils encapsulation (197).

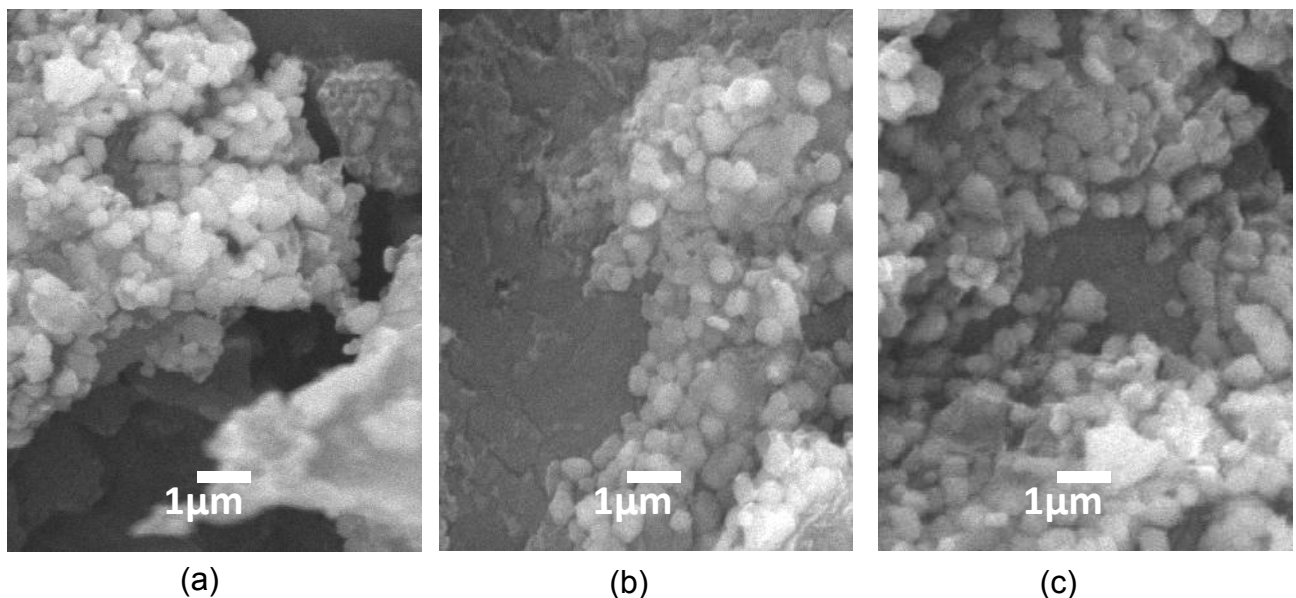


**Figure 4. 3.** SEM micrographs of lyophilized chitosan-based nanoparticles loaded: (a). commercial rosmarinic acid; (b). sage; and (c). savory.



### 4.2.3. Association efficiency and drug loading

It is known that chitosan in acidic media (pKa 6.5) can interact with the negatively charged TPP, forming inter- and intra-molecular cross-linkages, yielding ionically crosslinked chitosan nanoparticles (36). This is a spontaneous method for smaller nanoparticles formation with positive charge, without using any organic solvent or surfactants (198). It is also known that the inter- and intra-molecular linkages created between TPP and the positively charged amino groups of chitosan are responsible for the success of the gelation process (188). In the present study it was described a nanoparticulate system able to encapsulate natural extracts. The particle size was observed to be dependent on both chitosan and TPP concentrations as described in previously studies (188), being the minimum sizes obtained for the lowest chitosan and TPP concentrations. Further experiments were conducted using the mass ratio chitosan:TPP of (7:1), where TPP final concentration was 0.28 mg/mL and chitosan final concentration was 2 mg/mL. Rosmarinic acid was selected as a model antioxidant in order to investigate the feasibility of using chitosan and chitosan nanoparticles for natural extract carriers. Association efficiency and theoretical antioxidant loading of these nanoparticles were displayed in Table 4.2.

The pH of the nanoparticles formation medium was between 5.8 and 6.0, a pH value that favors the interaction of rosmarinic acid and chitosan, thus reaching a maximum leading to the entrapment of high amounts of rosmarinic acid. Among the different samples considering the encapsulation of rosmarinic acid into chitosan nanoparticles, it was observed similar association efficiency around 50% (Table 4.2), for all the different loadings no significant differences were observed ( $P > 0.05$ ). Higher association efficiency was found for rosmarinic acid entrapment in extracts of sage and savory, 96 and 98% respectively with no significant differences observed ( $P > 0.05$ ). This was in accordance with previous reports (190). The higher association efficiency in extracts nanoparticles may be due to the different amount of rosmarinic acid in chitosan nanoparticles and inside the extracts in chitosan nanoparticles (Table 4.2). Since competitive interaction may be happen between phenolic (OH<sup>-</sup>) of rosmarinic acid and (P<sub>3</sub>O<sub>10</sub><sup>5-</sup>) groups of TPP for protonated amino groups of chitosan resulting in low levels of particle formation compared to the chitosan nanoparticles, this may be intensified with the highest amount of rosmarinic acid and phenolic groups (198). This was in accordance with other studies that encapsulate other phenolic compound, such as catechin, in chitosan nanoparticles (198) and in other nanoparticles (199).

**Table 4. 2.** Association efficiency, theoretical loading, and final rosmarinic acid content in chitosan nanoparticles.

Nano	AE (%)	Theoretical Loading (%)	Final content in the chitosan nanoparticles (µg/mL)	Final rosmarinic acid content in chitosan nanoparticles (mg/mL)
Rosmarinic acid	51.2 ± 3.0	40	800	400
Sage	96.1 ± 0.2	50	1000	100
Savory	98.2 ± 0.1	50	1000	50

The association efficiency values were higher than the results for *Ilex paraguariensis* entrapment in calcium alginate nanoparticles coated with chitosan, (around 50%) since active compound was lost during immersion in chitosan (200). The good results for sage and savory association efficiency may be due to the huge affinity of chitosan and this two crude extracts. The results were also higher than a study reported for quercitrin encapsulation into nanoparticles, which was only 40% (152). However the high association efficiency reported in this study, was in accordance to other previously studies with the encapsulation of natural antioxidants extracted from *Ilex paraguariensis* into chitosan nanoparticles (193) and for the encapsulation antioxidant idebenone-loaded into chitosan nanoparticles (201).

#### 4.2.4. *In vitro* rosmarinic acid release from chitosan nanoparticles

All the chitosan-based nanoparticles suspension and the PBS used as medium release were adjusted to the tear normal osmolarity (300 mOsm / L). This normal osmolarity is essential to maintain cellular volume, enzymatic activity, and cellular homeostasis (202). In this *in vitro* release study every effort was made in order to best fate the ocular physiological conditions to test the kinetic nanoparticles behavior in ocular surface. During the experiment a fast release was observed during the *in vitro* release assay which was in accordance with previous data (190). The different rosmarinic acid contents (in rosmarinic acid nanoparticles, sage and savory nanoparticles) were released in all the formulations freshly and lyophilized within 60 min with no significant differences ( $P > 0.05$ ). An initial burst effect was observed in the first 30 min with approximately 80% in sage nanoparticles and almost 100% in rosmarinic acid and savory nanoparticles (Figure 4.4). The results

seem to demonstrate that a significant amount of rosmarinic acid or extracts were initially associated with nanoparticles on their surfaces by weak linkages to chitosan, which did not have the necessary strength to entrap all the compounds. This represents that chitosan nanoparticulate system could retain the primary structure of rosmarinic acid or extracts during encapsulation. The protection release happens only for few minutes due to the polymer network, which was in accordance with other studies, that encapsulate polyphenols from *Ilex paraguariensis* in chitosan nanoparticles prepared also by ionic gelation and a complete release of 100% were demonstrated in the first 15 min (193). In another study for quercetin encapsulation into other nanocarriers, the release within the first 20 min was also 95% (151). Nevertheless, this results were different from other works that demonstrated a complete release of polyphenols from chitosan nanoparticles within 4 h (198). The efficient application of these nanocarriers will certainly depend of the drug purpose. Chitosan nanoparticles maintain their characteristics for this theoretical loadings, and this confers them valuable properties, such as protective and moisturizer, for the encapsulation of active agents for cosmetic or ocular applications, since a rapid released is intentional (193). However for other applications, like oral drug delivery a slower release should be optimized.

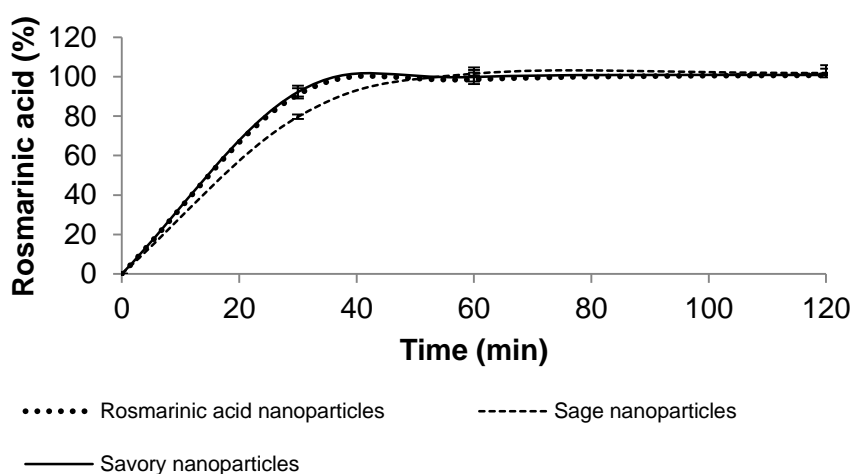


**Figure 4. 4.** Rosmarinic acid *in vitro* release from rosmarinic acid, sage and savory chitosan-based nanoparticles.

#### 4.2.5. Thermal behavior by differential scanning calorimetry analysis

The DSC measurements provide quantitative and qualitative information about physical and chemical changes that involve endothermic or exothermic processes, or changes in heat capacity. Endothermic and exothermic peaks correspond to transitions that absorb or release energy, respectively. DSC was performed to understand the behavior of rosmarinic acid, sage and savory loaded and unloaded chitosan nanoparticles and the thermograms were displayed in Table 4.3.

**Table 4. 3.** Peak temperatures in the DSC thermograms collected from chitosan, rosmarinic acid, sage and savory, physical mixtures, and nanoparticles.

		T (°C)		
		Onset	Peak	EndSet
Nano	Chitosan	102 ± 0.55	122 ± 1.20	131 ± 0.12
	Rosmarinic acid	112 ± 0.61	130 ± 0.73	141 ± 0.24
	Sage	83 ± 0.27	108 ± 0.71	118 ± 0.93
	Savory	103 ± 1.11	124 ± 0.82	137 ± 0.44
Free	Rosmarinic acid	134 ± 0.13	144 ± 0.23	149 ± 0.25
	Sage	140 ± 0.21	141 ± 0.14	145 ± 1.03
	Savory	141 ± 0.53	154 ± 0.51	158 ± 0.81
Physical mixture	Chitosan-Rosmarinic acid	90 ± 0.38	122 ± 0.83	136 ± 0.14
		147 ± 0.14	150 ± 0.70	154 ± 0.13
	Chitosan-Sage	94 ± 0.91	121 ± 0.10	134 ± 0.50
		147 ± 0.67	151 ± 0.63	155 ± 0.84
	Chitosan-Savory	93 ± 0.70	121 ± 0.32	132 ± 0.32
		145 ± 0.28	151 ± 0.64	154 ± 0.24

**Note:** The results were given as mean of triplicate samples.

The same chitosan-based nanoparticles thermal behavior was observed in all thermograms (Figure 4.5Ia, IIa and IIIa). In all chitosan curves, an endothermic peak near 70°C can be ascribed to the loss of water as previously reported (203). The endotherm of rosmarinic acid, sage and savory nanoparticles showed different shift temperatures (Figure 4.5Id, IIId and IIIId, respectively). This may be accounted by the hydrophilic groups

incorporated due to rosmarinic acid that were in different amounts inside the extracts particles. Other previously studies also reported similar shifts in DSC plots of chitosan and chitosan nanoparticles (198, 204). It could also be seen that the peaks of the complexes were shifted from those of physical mixture. Peaks of physical mixture (Figure 4.5Ic, 4.5IIc, 4.5IIIc) appeared to be combinations of each material but they were different from those of nanoparticles, probably because complexation of polyelectrolytes, in accordance with other similar works (205). Also, comparing endothermic peak of antioxidants loaded chitosan nanoparticles to the one obtained with unloaded nanoparticles, the former started at higher temperature, which was a possible evidence of the presence of antioxidants once its decomposition started at higher temperature when comparing to unloaded nanoparticles. The rosmarinic acid, sage and savory loaded sample showed the similar shift of chitosan nanoparticles, which confirms that there were no significant covalent interactions between antioxidants and chitosan after encapsulation and cross-linking (205).

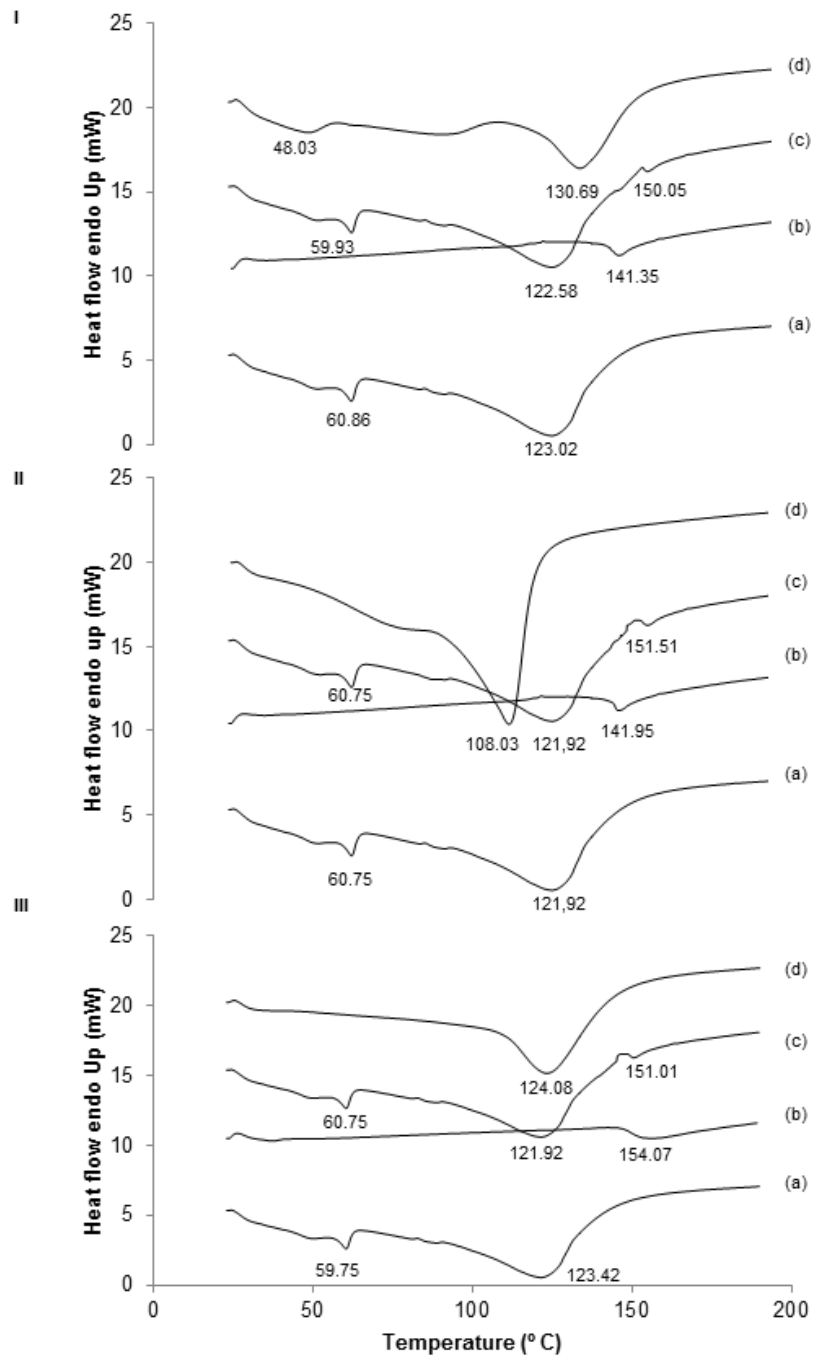


**Figure 4. 5.** Thermogram of: I.(a). chitosan empty nanoparticles; (b). free rosmarinic acid; (c). rosmarinic acid and chitosan physical mixture (mixing ratio 1:1); (d). rosmarinic acid encapsulated in chitosan nanoparticles (at a theoretical 40% loading) (d). II.(a). chitosan

empty nanoparticles; (b). free sage; (c). sage and chitosan physical mixture (mixing ratio 1:1); (d). sage encapsulated in chitosan nanoparticles (at a theoretical 50% loading).  
III.(a). chitosan empty nanoparticles; (b). free savory; (c). savory and chitosan physical mixture (mixing ratio 1:1); (d). savory encapsulated in chitosan nanoparticles (at a theoretical 50% loading).

#### 4.2.6. Spectroscopy by Fourier-transform infrared analysis

Structural features, functional groups that represent backbone produce characteristic and reproducible absorptions in the spectrum, which can be analyzed by FTIR. With these series of experiments it was intended to monitorize the complexation of contrary charged polyelectrolytes at specific pH and stoichiometric relationship between the polyelectrolytes and antioxidants in nanocarriers. For this concern and to examine this relationship between components of nanoparticulate systems, preliminary concerns were taken over polyelectrolytes interactions and antioxidants entrapment. It is well established that the carboxyl group ( $-\text{COO}$ ) of the anionic polymer may interact with the amino group  $\delta\text{-NH}_3$  of chitosan and form an ionic complex between the two compounds (205). Rosmarinic acid displays a typical vibrational absorption bands with the main bands located between 1800 and 700  $\text{cm}^{-1}$  (206). The three bands around 1605, 1520, and 1445  $\text{cm}^{-1}$  were due to the presence of aromatic rings in the molecule indicating an aromatic ring stretching (206). Other evidences for phenolic groups were delivered through the bands at 1360 and 1180  $\text{cm}^{-1}$  resulting from O-H and C-O stretches (206). Therefore, the band at 1684  $\text{cm}^{-1}$  and the two shoulders recognized with this band result probably from the shifted bands due to the presence of carboxylic acid groups and ester group 1725-1750  $\text{cm}^{-1}$  (207). Figure 4.6 (I, II and III) showed that all the above characteristic peaks appear in the spectra of combined drugs loaded chitosan nanoparticles at the same wavenumber indicating no modification or interaction between the drug and carrier. This was in accordance to previous work (208). Nevertheless, some peaks clearly decreased in intensity, after the preparation of rosmarinic acid, sage and savory nanoparticles. Particularly evident were the phenolic group bands (1360 and 1180  $\text{cm}^{-1}$ ) in rosmarinic acid nanoparticles and this is may be due to the highest amount of rosmarinic acid in these nanoparticles, comparing to the inside content of rosmarinic acid in extracts and into the nanoparticles. This effect was also reported by some authors that developed a new

FTIR method for the characterization of rosmarinic acid in *Lavandula officinalis* cultures (206). Nevertheless it must be underline that this characteristic bands decrease observed in the nanoparticles by FTIR analysis, and the decrease in antioxidant activity, may be due to the partial retention of antioxidant before their complete release (considering the theoretical loadings under studied). This was documented for other antioxidant nanoparticles studies, such as essential oils (197). Also no new peaks appeared in nanoencapsulation spectrum, and chitosan, rosmarinic acid, sage and savory were mixed together physically without any chemical reaction (152).



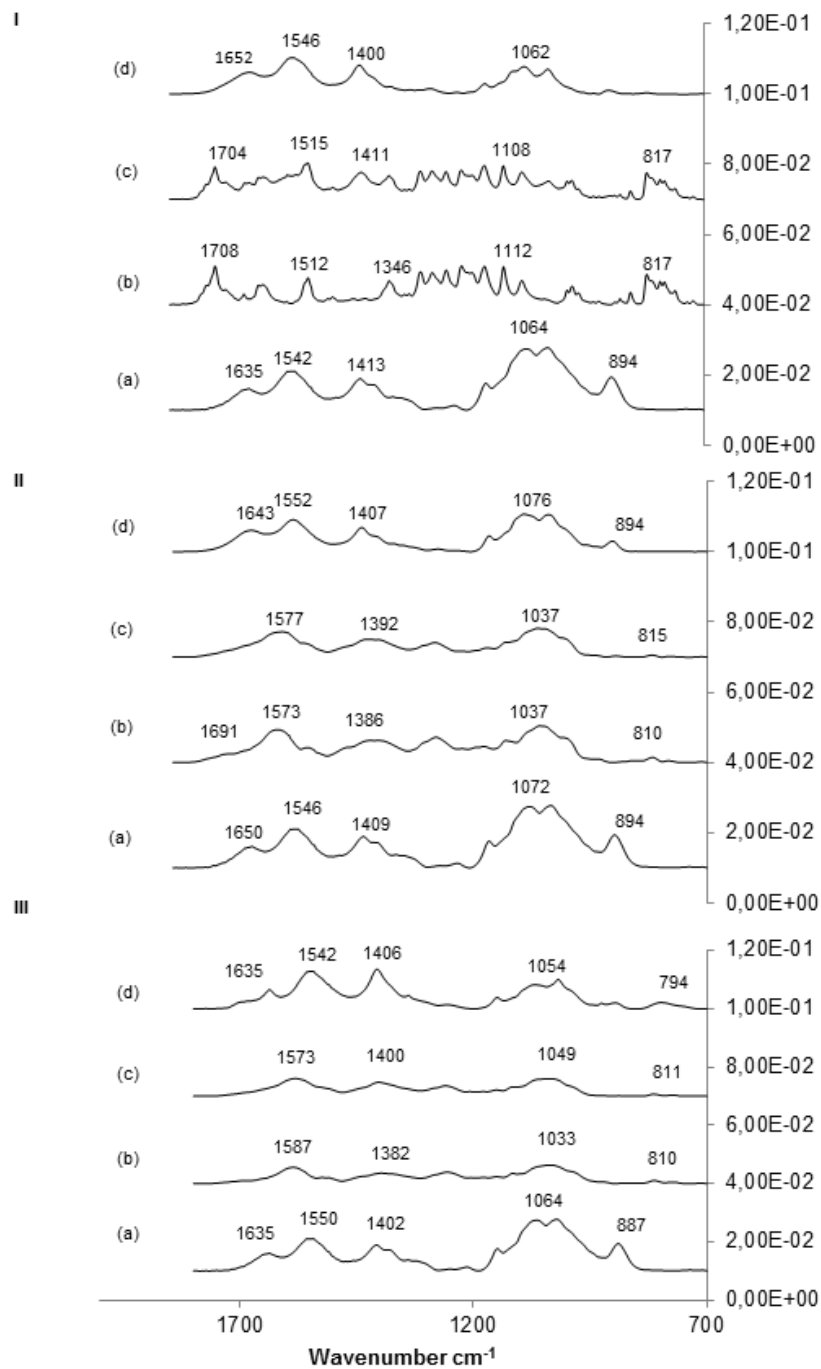


**Figure 4. 6.** Spectrum of: I. (a). chitosan empty nanoparticles; (b). rosmarinic acid in a free form; (c). physical mixture between chitosan unloaded nanoparticles and rosmarinic acid (mixing ratio 1:1); (d). rosmarinic acid encapsulation into chitosan nanoparticles. II.(a). chitosan empty nanoparticles; (b). sage in a free form; (c). physical mixture between

chitosan unloaded nanoparticles and sage (mixing ratio 1:1); (d). sage encapsulation into chitosan nanoparticles. III.(a). chitosan empty nanoparticles; (b). savory in a free form; (c). physical mixture between chitosan unloaded nanoparticles and savory (mixing ratio 1:1); (d). savory encapsulation into chitosan nanoparticles.

### **4.3. Conclusion**

In this study, chitosan nanoparticles incorporating rosmarinic acid, sage and savory were prepared and characterized in order to ensure their best size, efficient encapsulation, thermal stability, and *in vitro* release.

Smooth, spherical and small sizing nanoparticles ca. 300 nm, were obtained. High association efficiency was attained for all the formulations, 51.2% for rosmarinic acid (with 40% loading), 96.1 and 98.2%, for sage and savory nanoparticles, respectively (both with 50% loading). No chemical interactions were found between antioxidants and chitosan, after encapsulation. The chitosan-based nanoparticles released rosmarinic acid in 1 h, which suggested a rapid released profile of the nanosystem, being adequate for ocular applications. The core of this work was to underline the potential application of sage and savory for pharmaceutical or biomedical formulations, considering the benefits of natural extracts containing rosmarinic acid. Bearing in mind that natural nanoparticles offer the most advanced treatment modality for crude extracts incorporation. This could be a fundamental alternative nanomedicine to enhanced antioxidant performance for OS conditions.

*CHAPTER 5 – In vitro assessment of antioxidant activity of chitosan-based nanoparticles*

---



## **5. Introduction**

The oxidative damage plays a causal role in aging and various degenerative diseases, such as heart disease, cataracts, cognitive dysfunction, cancer and ocular diseases (6). Free radicals and ROS in biological systems can be harmful, since they may induce lipid oxidation by attacking the cell membranes, modifying proteins or enzymes in tissues, carbohydrates and even DNA (6). Although organisms already possess their natural antioxidant defense, they seem to be inefficient against the cumulative and continuously attack from ROS. The supplementary delivery of antioxidants using in the conventional dosage forms is a challenge due to their in some cases poor solubility, poor permeability, instability and metabolism before reaching the target (18). In this context, alternative carriers are being considered for pharmacokinetics and pharmacodynamics optimization of antioxidant molecules. For this application, chitosan has come to be particularly interesting for the association and delivery of these labile macromolecular compounds (4). This innovative drug carrier is expected to develop and improve stability and bioavailability, without compromising the safety performance of the antioxidants and target conditions (40). In this study the ability of chitosan-based nanoparticles to maintain the antioxidant activity of rosmarinic acid pure and in natural extracts was evaluated.

### **5.1. Experimental**

#### **5.1.1. Materials**

Materials were described previously in chapter 4. Briefly, the two selected plants sage and savory were provided by ERVITAL (Castro Daire, Portugal). The plants had been cultivated as organic products, and were supplied in their commercial form of dried leaves. The dried leaves were then kept in the dark at 20 °C. Rosmarinic acid (purity 96.5%), methanol CHROMASOLV® (HPLC ≥ 99.9%) and formic acid (HPLC ≥ 98.0%) were purchased from Sigma-Aldrich (Missouri, USA). Chitosan low molecular weight (LMW) and TPP were also purchased from Sigma-Aldrich (Lisbon, Portugal). The degree of deacetylation for chitosan LMW was 85%, with a purity grade of 85%. Pure acetic acid was purchased from Ponalab (Lisbon, Portugal). Sodium hydroxide (NaOH) and

hydrochloric acid (HCl) were from Merck (Darmstadt, Germany). Ultra-pure water was obtained in the laboratory using a Millipore™ water purification equipment (Massachusetts, USA).

### **5.1.2. Sample preparation**

Considering the two plants 1 g of each plant was crushed (using a lab mill) for 1 min, to obtain the corresponding powder. The extraction powder was performed as described in previously reports, via addition of 100 mL boiling water to 1 g of plant powder and after 5 min, the extract was filtered through a 0.45 µm filter (190). This procedure was optimized to obtain the highest potential activity of these plants. After the crude plant sedimentation, samples were filtered and maintained at -80 °C, for lyophilization procedures (Heto Holten A/S Drywinner). Then, solutions of 1% (w/v) of lyophilized powder were dissolved in methanol for chromatographic analyses and in ultra-pure water for antioxidant activity tests. Before injections samples were filtered again through a 0.45 µm filter.

### **5.1.3. Chitosan nanoparticles development and optimization**

Chitosan-based nanoparticles were developed and optimized based on previously studies and as described in previous chapters. The chitosan nanoparticles were obtained by inducing the gelation of a chitosan solution with TPP. For this purpose TPP was dissolved in purified water, and chitosan was dissolved in acetic acid aqueous solutions at various concentrations and pH adjusted to 5.8 with 1 M NaOH. The concentration of acetic acid was, in all cases, 1.75 times higher than that of chitosan, as previously described (188). After several assays considering the variation of concentrations and volumes, an optimal ratio between chitosan:TPP was achieved in chapter 4 (7:1). This optimal ratio was considering to achieve particles ranging (200-300 nm) using ZetaPALS (Brookhaven, New York, USA) and a charge as close as possible of 30 mV by laser Doppler anemometry, at 25°C. A final volume of 2.0 mL of TPP solution was added to 5 mL of the chitosan solution under magnetic stirring at room temperature, thus achieving a final concentration of 2 and 0.28 mg/mL of chitosan and TPP, respectively.

#### 5.1.4. Encapsulation of sage, savory and rosmarinic acid into chitosan nanoparticles

The 1% (w/v) aqueous rosmarinic acid and aqueous extracts solutions were added to chitosan, previously dissolved in acetic acid, in different volumes in order to guarantee the best ratio between chitosan and the different compounds, as previously described in chapter 4 and documented (190). For this concern the encapsulation was tested in different theoretical loadings (5, 10, 15, 20, 30, 40 and 50%) fairly to the initial concentration of chitosan (2 mg/mL). All the tests were made for the 7 batches, considering the two plants and the pure rosmarinic acid. Some of the final batches were then lyophilized (Heto Holten A/S Drywinner) and maintained at -20 °C for 1-2 months for further analysis.

#### 5.1.5. Antioxidant capacity assessment

##### 5.1.5.1. 2,2-azinobis (3-ethylbenzothiazoline-6-sulphonic acid) method

Determination of the antioxidant capacity was performed as described in other research papers (115). The ABTS•+ stock solution was prepared via addition, at 1:1 (v/v), of 7 mM ABTS (2,2-azinobis (3-ethylbenzothiazoline-6-sulphonic) acid) diammonium salt (Sigma-Aldrich, St. Louis, MO, USA) to a solution of 2.45 mM potassium persulphate (Merck, Damstadt, Germany); the developing reaction took place in the dark, for 16 h. In order to obtain an absorbance of  $0.700 \pm 0.020$  at 734 nm, measured with an UV 1203 spectrophotometer (Shimadzu, Tokyo, Japan), the aforementioned stock solution was diluted in ultra-pure water as necessary. A 10 µL aliquot of the sample was assayed for percentage of inhibition (PI), to be between 20% and 80%, to guarantee a linear response of the analytical method, after 6 min of reaction with 1 mL of diluted ABTS•+ solution. The total antioxidant capacity was expressed as percentage of inhibition (PI), according to the equation:

$$PI = \left( Abs_{ABTS \bullet +} - \frac{Abs_{sample}}{Abs_{ABTS \bullet +}} \right) \times 100$$

where AbsABTS<sup>•+</sup> denotes the initial absorbance of diluted ABTS<sup>•+</sup>, and Abs sample denotes the absorbance of the sample by 6 min of reaction. Triplicates of each sample were averaged to generate each datum point (which implies a total of six replicates per sample). The final result was expressed as equivalent concentration of ascorbic acid (in g/L), using a calibration curve.

#### 5.1.5.2. Oxygen radical absorbance capacity

The oxygen radical absorbance capacity (ORAC) assay was employed to evaluate the antioxidant potential of chitosan-antioxidant nanoparticles as described in previously reports (209). All reaction mixtures were prepared in duplicate, and at least three independent measures were performed for each experiment. ORAC-fluorescein (FL) values were expressed in  $\mu\text{mol}$  trolox equivalent per mg hydrolyzed of antioxidant, as purposed elsewhere (210).

#### 5.1.6. **Statistical analysis**

Statistical analysis was performed using IBM SPSS Statistics v 19.0.0 (Illinois, USA). The one-way analysis of variance (ANOVA) was used with Scheffé post hoc test comparison of groups with normal distribution, and Mann-Whitney test for groups with non-normal distribution. Differences were considered to be significant at a level of  $P < 0.05$ .

### 5.2. **Results and discussion**

#### 5.2.1. **Antioxidant activity measurement**

Rosmarinic acid is phenolic compound, with many beneficial functionalities and generally admitted as a free radical scavenger (125). Its high biological activity is particularly related to its two catechol moieties. Catechol is an important sub-structure for the potent antioxidant activity of phenolic antioxidants (125). The general antioxidant mechanism of



phenolic compounds is thought to be divided into two stages: radical catching stage and radical conclusion stage (126). For both methods the antioxidant activity was tested according to the antioxidant activity of rosmarinic acid, either in free solution or encapsulated, both in extracts or in a free form. For both methods no significant differences were found for antioxidant activity between the all nanoformulations, before and after lyophilization processes ( $P > 0.05$ ), except for savory encapsulation. For these nanoparticles a decrease in the antioxidant activity was observed after lyophilization, especially evident in ORAC method. For the loading concentrations of 5 to 15%, no antioxidant activity was found by the ABTS or ORAC methods. This means that the antioxidant activity was clearly compromised for these low theoretical loadings. Considering the both extracts and rosmarinic acid nanoparticles, the highest antioxidant activity was correlated to the highest antioxidants concentrations (or higher loading value) (Table 5.1). Comparing rosmarinic acid, sage and savory in a free form, it can be easily observed that rosmarinic acid has the highest antioxidant activity, followed by sage that has the highest content of rosmarinic acid (10%) and then savory with only (5%) of rosmarinic acid content. By ABTS method, comparing the antioxidant activity before and after the encapsulation process, it was clear a decrease in the antioxidant activity after the encapsulation. This proves that the antioxidant activity were decrease due to the partial entrapment effect of the compounds. Nonetheless the particles still demonstrated good antioxidant activity. This was in accordance to other previously reports that have showed the same good antioxidant effect of Trolox in chitosan nanoparticles (211). Other good results were obtained for the chitosan encapsulation of idebenone antioxidant (201). Furthermore and by ORAC, which is fluorimetric assay and a more sensitive one, it can be easily observed that after the encapsulation process the antioxidant activity was even lower, than the results achieved by ABTS (Table 5.1). These results were consistent with previously studies with the encapsulation of quercetin and rutin (212). This still may be due to the nanoparticles entrapment of rosmarinic acid, in other way because the antioxidant was not completely released. This partial retention means that the compounds will take more time to build up their specific activity. Nevertheless the nanosystems with this entrapment effect still have good antioxidant activity. Although even if the nanosystem antioxidant activity was lower than the unloaded compounds, it is well known that nanocarriers protects the antioxidants for degradation by biological and enzymatic fluids, increasing their bioavailability. The drug release can also be optimized to be even longer, prolonged and controlled in time considering the purpose application of this nanoparticles (187). This makes the nanoencapsulation advantageous and necessary.

**Table 5. 1.** Antioxidant activity measurements by ABTS and ORAC, considering the 50% loading (*m/m*) sage and savory nanoparticles; and 40% loading (*m/m*) of and rosmarinic acid nanoparticles for (*n* = 3).

		ABTS <sup>x</sup>		ORAC <sup>y</sup>	
		(eq [Asc. Ac.]/g/L)/g extract		(μmol/eq Trolox)/g extract	
		Fresh Nanoparticles	Lyophilized Nanoparticles	Fresh Nanoparticles	Lyophilized Nanoparticles
Nano <sup>i</sup>	Rosmarinic acid	0.0348 ± 0.0050 <sup>a</sup>	0.0554 ± 0.0139 <sup>a</sup>	4.8374 ± 0.1719 <sup>b</sup>	3.6520 ± 0.1770 <sup>b</sup>
	Sage	0.0537 ± 0.0015 <sup>c</sup>	0.0440 ± 0.0029 <sup>c</sup>	0.6227 ± 0.0901 <sup>d</sup>	0.4251 ± 0.0069 <sup>d</sup>
	Savory	0.0828 ± 0.0102 <sup>e</sup>	0.0378 ± 0.0015 <sup>f</sup>	1.5315 ± 0.2784 <sup>g</sup>	0.4526 ± 0.0087 <sup>h</sup>
Free <sup>ii</sup>	Rosmarinic acid	0.0917 ± 0.0018		34.1218 ± 2.5733	
	Sage	0.1621 ± 0.0470		19.5924 ± 1.9791	
	Savory	0.1410 ± 0.0087		16.8117 ± 1.3605	

**Note:** The results were given as mean of triplicate samples, each with three measurements. The same letters, in the same line indicate that no significant differences were observed between the fresh and freeze-dried process ( $P > 0.05$ ). The values are significantly different ( $P > 0.05$ ) for the antioxidant methods (<sup>x,y</sup>) and for the encapsulation process (<sup>i,ii</sup>).

Considering the same loading concentrations of the rosmarinic acid and the extracts nanoparticles it was clear that rosmarinic acid in the extracts nanoparticles was in lower concentration than when was purely encapsulated. Rosmarinic acid nanoparticles (40% loading), with 50% efficiency means encapsulate, 0.4 mg/mL of rosmarinic acid. Nevertheless, sage or savory nanoparticles (50% loading), with almost 100% association efficiency (Table 4.2 – chapter 4), the nanosystem encapsulate 1 mg/mL of extract, but only 10 and 5% of rosmarinic acid (Table 4.2 – chapter 4), for sage and savory, respectively. It is also known and documented by our group (179), that these crude extracts (sage and savory) are complex natural matrixes with different antioxidant content (as Protocatechuic acid, coumaric acid, gallic acid, caffeic acid, ferulic acid, naringenin, quercetin, isorhamnetin, chlorogenic acid, prunin, isoorientin, quercitrin and rutin). Nevertheless when natural extracts were encapsulated, the pH value was to allow the great amount of rosmarinic acid interaction with chitosan solution, and then the success of the encapsulation. This means that some phenolic compounds were present in the extracts, but were not negatively charged at formation medium pH, may be lost in encapsulation procedure. However, other antioxidant compounds in extract nanoparticles that have a close pKa of rosmarinic acid were encapsulated adding a synergic antioxidant

activity. This justifies that with lower rosmarinic acid concentrations, the extracts have the same antioxidant activity, being good vehicles of rosmarinic acid and with good antioxidant synergic performance. Furthermore it was important to underline that rosmarinic acid-nanoparticles can encapsulate with only 50% of association efficiency, which means a huge waste of the compound. This could represent that at this moment, for all the tests made for chitosan nanoparticles with sage or savory, they seem to be good vehicles for rosmarinic acid incorporation and represent a more economically process, than nanoparticles with rosmarinic acid pure. Another advantage could be added with the inclusion of biological activities of other natural compounds that were incorporated at this pH value in the nanoparticles. However, *in vitro* tests must be done in order to guarantee that all the biological activities of the extract and of rosmarinic acid were maintained.

### **5.3. Conclusion**

In this study, chitosan nanoparticles incorporating rosmarinic acid, sage and savory were prepared and characterized in order to ensure the highest antioxidant activity performance.

The best antioxidant activity results were obtained for rosmarinic nanoparticles by ORAC method after lyophilization, ca.  $3.6520 \pm 0.1770$   $\mu\text{mol/eq Trolox}$ . Nonetheless, sage and savory showed to be good vehicles for rosmarinic acid regarding the antioxidant activity outline. After nanoparticles lyophilization the obtained values were:  $0.4251 \pm 0.0069$  and  $0.4526 \pm 0.0087$   $\mu\text{mol/eq Trolox}$ , for both sage and savory nanoparticles, respectively. Nevertheless, it is important to underline that the crude extracts have a lower concentration of rosmarinic acid, and the good antioxidant activity results suggested that other synergic compounds may be also encapsulated. Besides a lower antioxidant activity was observed in the nanoparticles comparing to the free compounds due to the partial entrapment effect of the compounds, chitosan-based nanoparticles still maintained the rosmarinic acid good antioxidant activity performance and also allowing its protection and best control its profile release. These results underline the pharmaceutical potential of chitosan-based nanosystems for antioxidants delivery.



## PART V

---

*“Science isn’t about why...it’s about why not?”*

*Unknown*



## Abstract

Introduction: *In vitro* assays are crucial to mimic biological conditions and predict nanoparticles cytotoxicity, mucoadhesion and the encapsulated bioactive permeability profiles. Neuroinflammation is a biological condition intimate related to the glaucoma pathophysiology, increasing the reactivity of microglia and the release of pro-inflammatory mediators.

Objective: The goal of the study was to test the safety performance, mucoadhesiveness and permeability of rosmarinic acid encapsulated into the aforementioned nanoparticles towards ocular cell-based models, and predict their potential to prevent oxidative eye diseases. Nonetheless, it was also intend to evaluate the effect of rosmarinic acid in retinal pro-inflammatory control and infer if it may confer neuroprotection to the retina in an animal model of I-R.

Methodology: Chitosan nanoparticles were evaluated considering mucoadhesiveness and their safety performance and cell permeability by *in vitro* tests using ARPE-19 and HCE-T monolayer cell lines. *In vivo* assays were performed injecting intravitreally rosmarinic acid in an I-R model, the rosmarinic acid neuroprotection was further evaluated by electroretinograms (ERG) and immunohistochemistry.

Results: Nanoparticles previously characterized demonstrated to be safe without relevant cytotoxicity against ARPE-19 and HCE-T cell lines, with no irritancy to the eye. The permeability study in HCE monolayer cell line showed an apparent permeability coefficient  $P_{app}$  of  $3.41 \pm 0.99 \times 10^{-5}$  and  $3.24 \pm 0.79 \times 10^{-5}$  cm/s for rosmarinic acid loaded chitosan nanoparticles and free in solution, respectively. In ARPE-19 monolayer cell line the  $P_{app}$  were  $3.39 \pm 0.18 \times 10^{-5}$  and  $3.60 \pm 0.05 \times 10^{-5}$  cm/s for rosmarinic acid loaded chitosan nanoparticles and free in solution, respectively. Considering the mucin particle method, nanoparticles indicate mucoadhesive proprieties. ERG and immunohistochemistry showed that at this concentration, by intravitreal injection, rosmarinic acid did not have a retina protective effect in I-R studied model.

Conclusion: The natural nanoparticles developed in this study demonstrated to be *in vitro* promising drug delivery systems for ocular application. Nonetheless, the *in vivo* results were not effective regarding retina neuroprotection, which may be due to the acute I-R model, which leads to severe pro-inflammatory damages that antioxidants are not able to revert with a single injection. Despite, this antioxidants pharmacotherapy may be crucial to ocular diseases prophylaxis.



*CHAPTER 6 - In vitro evaluation of cytotoxicity,  
mucoadhesion and ocular permeability of  
rosmarinic acid into chitosan-based nanoparticles*

---



## 6. Introduction

The ocular drug delivery is one of the major challenges in pharmaceutical sciences (213, 214). Topical eye drop is the most convenient and comfortable route for ocular drug administration for patients. Nonetheless, it is well known that the delivery of drugs to targeted posterior ocular tissues is restricted by various precorneal, dynamic and static ocular barriers (3, 215). In the past two decades, ocular drug delivery research was focused on developing novel, safe and patient compliant formulations that may overcome these barriers and maintain higher drug levels in tissues. There are many described categories of ocular diseases, such as retinitis pigmentosa, glaucoma, cataracts, macular degeneration, retinoblastoma and diabetic retinopathy (216). However, the etiology of these degenerative diseases remains poorly explained, thus mainly associated to light-mediated oxidative damage, PUFA content, environmental chemicals and the physical abrasion (217). All these factors contribute to OS that may be seen as the key factor for ocular conditions (218). OS is now associated to the disruption of blood-retinal barrier, apoptotic loss of retinal capillary cells, microvascular abnormalities, retinal neovascularization, oxidative modified DNA, as well as suppression of antioxidants systems (25). For this reason, the use of appropriate antioxidants may have potential on the metabolic and functional abnormalities in retinopathies (219, 220). The delivery of antioxidants using the conventional dosage forms is challenging due to their low permeability, high instability and the losses during metabolism before reaching systemic circulation (18). Nanotechnologies as ocular drug delivery systems are one of the most interesting and challenging endeavors, due to the eye critical environment (214). In the case of ophthalmic nano-drug delivery systems, it is crucial to evaluate an appropriate particle size and a narrow size range, ensuring low irritation, adequate bioavailability and compatibility with ocular tissues (221). Nanotechnologies together with the implementation of optimal, non-invasive and painless administration routes have been deeply studied, considering different biodegradable polymers, their core properties and mucosa interaction (3). Chitosan is a positively charged polysaccharide which binds to negatively charged corneal surface, with potential to improve precorneal residence and decrease clearance (222). However, for using chitosan as a base material to produce nanoparticles with application in biomedical sciences, it is essential to evaluate their bioavailability, cytotoxicity and capacity of transporting bioactive molecules. For this purpose, *in vitro* cell culture models may be considered as the most useful technique to better predict the permeability/absorption of bioactive compounds. Ocular cell-based models (e.g. HCE and

ARPE) have been used for numerous other purposes, such as studying passive and active transport of drugs and endogenous substances, cellular physiology, metabolism and protein expression, development of delivery systems for genes and antisense oligonucleotides, and cytotoxicity (223). Both cell lines have been deeply evaluated for drug permeation studies (224, 225). The main aim of this study was to evaluate the safety performance, mucoadhesiveness, permeability and applicability potential in ocular cell-based models of chitosan nanoparticles encapsulating rosmarinic acid, sage and savory lyophilized extracts as rosmarinic carriers.

## **6.1. Experimental**

### **6.1.1. Materials and cells**

Chitosan LMW ( $\approx 50$  kDa) with deacetylation degree of 86%, and TPP were purchased from Sigma-Aldrich (Portugal). Stock solution of chitosan (1% w/v) were dissolved in 1% (v/v) acetic acid solution and deionized water followed by filtration using a Millipore #2 paper filter and stored at 4 °C. TPP (0.1% w/v) were also dissolved in deionized water and stored in the same conditions. Two plants were selected as extract source namely sage and savory, both provided by ERVITAL (Castro Daire, Portugal). These plants had been cultivated as organic products, and were supplied in their commercial form of dried leaves. After the crude plant sedimentation, samples were filtered and maintained at -80°C, for lyophilization procedures (Heto Holten A/S Drywinner). Then, solutions of 1% (w/v) of lyophilized powder were dissolved in deionized water followed by filtration using a Millipore #2 paper filter and stored at -20 °C, as previously described (190, 196). (190, 196). ARPE-19 and HCE-T human cell lines were obtained from the American Type Culture Collection (ATCC) and used at passages 14-35 and 18-32, respectively. Dulbecco's Modified Eagle Medium (DMEM), fetal bovine serum (FBS), L-glutamine, non-essential amino acids, and 100 U/mL penicillin and 100 mg/mL streptomycin, trypsin-EDTA, Hank's Balanced Salt Solution (HBSS), and wheat germ agglutinin (WGA) were purchased from Gibco (Invitrogen Corporation). Transwell® polycarbonate inserts (6 wells, pore diameter of 3  $\mu\text{m}$  polycarbonate, 4.67  $\text{cm}^2$ ) were purchase from Corning (Madrid, Spain).

### **6.1.2. Preparation and characterization of antioxidant-containing chitosan nanoparticles**

Optimized conditions to obtain antioxidant-containing chitosan nanoparticles were previously documented and described in the above chapters (190, 196). Briefly, chitosan nanoparticles were obtained by inducing the gelation of a chitosan solution with TPP. For the study of the best ratio between chitosan:TPP, a volume of the TPP solution of 2 mL was added to 5 mL of the chitosan solution under magnetic stirring at room temperature, thus achieving a final concentration of 2 mg/mL and 0.28 of chitosan and TPP, respectively (7:1). The 1% (w/v) aqueous rosmarinic acid and aqueous extracts solutions were added to chitosan previously dissolved in acetic acid at a pH value adjusted to 5.8, in different volumes in order to guarantee the best ratio between chitosan and the different compounds, as previously documented (190). For this concern, the theoretical encapsulation was fixed in 40% for rosmarinic acid and 50% for sage and savory nanoparticles, fairly to the initial concentration of chitosan (2 mg/mL). Then, nanoparticles were lyophilized (Heto Holten A/S Drywinner) and kept at -20 °C for 1-2 months

### **6.1.3. Size and surface charge**

Size and polydispersity of freshly unloaded and loaded nanoparticles were determined by photon correlation spectroscopy using ZetaPALS (Brookhaven, New York, USA). A sample of 1.6 mL was gently homogenized, placed into analyzer chamber and measured. Collective 6 readings were performed three times on each sample at 25 °C with a detection angle of 90°. The zeta potential was determined by laser Doppler anemometry, at 25 °C. Triplicate samples were also analyzed, each sample being measured 6 times, and the arithmetic mean was adopted.

### **6.1.4. Association efficiency**

Association efficiency (AE) and loading capacity (LC) was evaluated considering the amount of rosmarinic acid associated with the particles. For this purpose the particles were centrifuged (20.000 g for 45 min) and suspended in 7 mL of ultra-pure water. The AE

and LC were then calculated by the difference between the total rosmarinic acid used to prepare the particles, and the amount of residual rosmarinic acid in the supernatant. AE and LC of rosmarinic acid in rosmarinic acid nanoparticles, sage and savory nanoparticles were obtained according to the following equation:

$$AE\% = \frac{\text{Total amount of rosmarinic acid} - \text{Free amount of rosmarinic acid in supernatant}}{\text{Total amount of rosmarinic acid}} \times 100$$

$$LC\% = \frac{\text{Total amount of rosmarinic acid} - \text{Free amount of rosmarinic acid in supernatant}}{\text{Rosmarinic acid total weight}} \times 100$$

#### **6.1.5. Mucoadhesion proprieties evaluation by mucin interaction method**

An experiment was conducted to determine the chitosan nanoparticles mucoadhesion potential, considering the mucin-particle method. The nanoparticle-mucin interaction was determined measuring the amount of mucin that attaches the nanoparticles, and the success of their connection was evaluated by the variations in size and zeta potential. Particle size, polydispersity and zeta potential of rosmarinic acid-loaded nanoparticles were determined using ZetaPALS (Brookhaven, New York, USA), before and after incubation of nanoparticles in mucin aqueous solution (0.4 mg/mL, incubation conditions: 37 °C, moderate stirring, for 2 h). Mucin activity was stopped by cooling the particles suspension on ice for 45 min. The conditions applied in this experiment were adapted as previously described (226). Loaded nanoparticles before incubation with mucin were used as controls. The interaction of mucin in solution with nanoparticles was also assessed by measuring the transmittance of the dispersion, at 372 nm, measured with an UV 1203 spectrophotometer (Shimadzu, Tokyo, Japan), before and after 45 min of incubation time, at three different pH values, namely 5.8, 5.5 and 7.4. This was performed in order to evaluate particle mucin interaction in ionic gelation, ocular inflammation and the homeostasis pH, respectively. Triplicate samples were analyzed, each sample was measured 6 times, and the arithmetic mean value was adopted.

### 6.1.6. Cell viability and cytotoxicity of nanoparticles

The effect of antioxidant chitosan nanoparticles on cell viability was measured at selected concentrations using the methylthiazolyldiphenyl-tetrazolium bromide conversion (MTT) assay. Cells were seeded in 96-well at  $2 \times 10^5$ /well in 0.3 mL with standard medium, consisted of Dulbecco's Modified Eagle Medium (D-MEM) (1X) (Gibco BRL, Grand Island, NY), 10% Fetal Bovine Serum (Heat Inactivated) (Gibco BRL), 0.1 mg/mL streptomycin, and 1000 IU/mL penicillin (both from Gibco BRL) and incubated 24 h at 37 °C in 5% CO<sub>2</sub> environment. The medium was then changed and the cells were treated with test samples for 4 and 24 h. Each treatment was tested in six individual wells. After time intervals (4 and 24 h), the supernatant was removed and 20 µL of MTT solution (5 mg/mL in HBSS) was added to each well of 96-well plates and then incubated for 2 h at 37°C to allow the formation of formazan crystal. The medium was then removed, and blue formazan was eluted from cells by 150 µL of DMSO. The negative control used, was also DMSO. The plates were shaken on an orbital shaker to solubilize the crystals of formazan. The dark blue crystals were aspirated to another new 96-well plate and measured directly in the plate reader at 570 and 690 nm for background reduction.

The effect of nanoparticles on cell membrane integrity was measured by the lactate dehydrogenase enzyme release (LDH) assays. Ocular cell lines were seeded in 96-well microplates at  $2 \times 10^5$ /well and incubated for 24 h at 37 °C in 5% CO<sub>2</sub> environment. The cultured cells were washed with HBSS (1x) (pre-warmed at 37 °C). Test solution, and controls (DMEM and DMSO) were added in triplicate to the cell culture. Cells were incubated with medium at 37 °C for 4 and 24 h. Afterwards, 100 µL of samples were withdrawn and centrifuged for 2 min at 5000 rpm to remove detached cells from the supernatant. The LDH content of 50 µL supernatant was measured at 490 nm (and 690 nm for background deduction) with spectrophotometer using a commercial test kit (Takara, Shiga, Japan) after incubation for 30 min at room temperature in the dark. Cytotoxicity was measured by following the equation:

$$\text{Cytotoxicity \%} = \frac{\text{Experimental value} - \text{Low control}}{\text{High control} - \text{Low control}} \times 100$$

#### 6.1.6.1. Cytotoxicity test using chorioallantoic membrane

To evaluate the cytotoxicity and biocompatibility of extracts and rosmarinic acid-containing nanoparticles, Hen's Egg Tests (HETs) were performed on the chorioallantoic membrane (CAM) as previously described (227). HET-CAM test method was used for the detection of ocular corrosives and severe irritants, as defined by the U.S. Environmental Protection Agency (EPA 1996), the European Union (EU; EU 2001), and in the United Nations Globally Harmonized System (GHS) of Classification and Labelling of Chemicals (UN 2003). Fertile hen's eggs at 10 days of incubation at 37 °C, obtained from Guaraves Guarabira Aves Ltda, were used in the tests. Five eggs were used for each nanoparticles solution assay. After 10 days of incubation, the egg shell above the air space was removed. The exposed membrane was moistened with a drop of 0.9% physiological saline and the saline was removed, uncovering the chick embryo chorioallantoic membrane (CAM). An aliquot of 200 µL of nanoparticles solution was applied on the CAM. All assays were repeated five times. Signs of vasoconstriction, hemorrhage and coagulation for 5 min were observed evaluate the potential for irritation according to the method of HET-CAM. The time (in seconds) at which the indicated processes began were applied in Equation (228). The time (in seconds) at which the indicated processes began were applied in Equation (228):

$$Het - Cam (IS) = \frac{(301 - h) \times 5}{300} + \frac{(301 - v) \times 7}{300} + \frac{(301 - c) \times 9}{300}$$

After application of the formula above, it was possible to quantify the observed potential for irritation (irritation score-IS) and to obtain means and standard deviations for the analysis as follows: 0-0.9 no irritation, 1-4.9 slight irritation, 5-8.9 moderate irritation and 9-21 severe irritation (228). All procedures with chicken eggs were followed by the regulations and procedures for handling of human or animal materials.



## **6.1.7. Permeability studies**

### **6.1.7.1. Cell monolayers culture**

Immortalization of human corneal epithelium (HCE) and retinal pigment epithelium (ARPE) cells have been described earlier. Polycarbonate Transwell<sup>®</sup> cell culture filters (Corning, 3  $\mu\text{m}$ , 6 wells, USA) were used for permeability assays. Suspension of HCE and ARPE cells were seeded onto the filters at a concentration of 200.000 cells/cm<sup>2</sup>. The cells were grown at 37 °C in humidified air with 5% of CO<sub>2</sub>, in standard culture medium in apical chamber for 21 to 30 days until the cells were confluent. The culture DMEM medium was replaced every two days.

### **6.1.7.2. Transepithelial electrical resistance**

Transepithelial electrical resistance (TEER) was measured at different phases of cell growth (Evom; World Precision Instruments, Sarasota, FL), as an indicator of epithelial differentiation and epithelial tightness. TEER data were corrected for low-background TEER by using a blank filter containing the possible coating materials and culture medium. At the end of each permeability experiment, TEER was measured to detect the condition of the cells.

### **6.1.7.3. Permeation studies in cell monolayers**

The permeation study with different solutions was initiated by washing with HBSS (1x) liquid (without calcium and magnesium) both the basolateral and apical side one time and then adding 2.5 mL of HBSS to the basolateral side (receiver side) and 1.5 mL of HBSS to the apical side (donor side). At different time points, during 60 minutes, aliquots of 100  $\mu\text{L}$  were withdrawn from the receiver chamber and replaced with an equal volume of blank medium. TEER was measure at each time and the plates were incubated with the sample

at 37 °C to sum to the test times.  $P_{app}$  was calculated from the measurement of the flow rate of insulin from the donor to the acceptor chambers:

$$P_{app} (cm/s) = dQ/dt (A \times C_0)$$

where, dQ is the total amount of permeated rosmarinic acid (mg), A is the diffusion area (cm<sup>2</sup>), C<sub>0</sub> is the initial concentration of rosmarinic acid (mg/mL), and dt is the time of experiment in seconds (s). The coefficient dQ/dt represents the steady-state flux of rosmarinic acid across the monolayer.

#### 6.1.7.4. High performance liquid chromatography analysis

The HPLC method was developed and validated, as previously described in chapter 3. Briefly, aliquots of 100 µL were injected at HPLC to quantify which quantity concentration permeates to the basolateral side of the plates. All HPLC runs were performed using a Waters Series 600 HPLC and results were acquired and processed with Empower® Software 2002 for data acquisition (Mildford MA, USA). HPLC analysis was conducted by using a Nova-Pack® RP C18 column (250 x 4.6 mm i.d., 5 µm particle size and 125 Å pore size) from Waters. Chromatographic analysis was performed in gradient mode. The mobile phase consisted of methanol: formic acid: water UP in the ratio 92.5:2.5:5 (v/v). Stationary phase was made with the same components in the ratio of 5:2.5:92.5, respectively. The phases were filtrated through 0.22 µm filter and degassed. Eluent was pumped at a flow rate of 0.75 mL/min, the injection volume was 20 µL and detection wavelength was 280 nm.

#### 6.1.8. **Statistical analysis**

Statistical analysis was performed using IBM SPSS Statistics v 19.0.0 (Illinois, USA). The one-way analysis of variance (ANOVA) was used with Scheffé post hoc test comparison of groups with normal distribution, and Mann-Whitney test for groups with non-normal distribution. Differences were considered to be significant at a level of  $P < 0.05$ .

## 6.2. Results and discussion

### 6.2.1. Particle size, polydispersity and zeta potential

The particle size and mean size distribution are fundamental features that influence the *in vivo* distribution, biological fate, toxicity and the targeting ability of nanoparticles containing therapeutic drugs (191). It is also known that the highest value of zeta potential represents the greater electrostatic repulsive interactions among the particles. Zeta potential values of  $\pm 30$  mV indicates that the colloidal systems are stable in time and that amine groups of chitosan are on the surface (193). The developed nanoparticles ranged from 200-300 nm in size and zeta potential were around 20-30 mV (Table 6.1). It is described that for ultrafine particles the induction of ROS, OS, inflammation and vasculature are a risk (229). In this sense it can be considered that the particles of this study will have no such harmful effects. Moreover, the results are in agreement with similar nanoparticles containing rosmarinic acid we recently developed (230) and with other extracts, also encapsulated in chitosan nanoparticles (193). The results did not show significant differences ( $P > 0.05$ ) in size between the rosmarinic acid and the two crude extracts, as previously described (190, 196). This may be due to the high rosmarinic acid content in extracts composition 10 and 5% in sage and savory, respectively (196). Thus the extracts under study are promising vehicles for rosmarinic acid nano-incorporation, as previously documented (190, 196). The size obtained is also in agreement with ocular drug delivery demands, as particles with size  $\leq 200$  nm were observed to reach the retina, vitreous and trabecular meshwork (231) and have more vitreal half-life compared to huge nanoparticles (232). The obtained nanoparticles also showed values of polydispersity between 0.1 and 0.2 corresponding to a narrow distribution and monodispersed particles. These results are in accordance to other works using similar antioxidant nanoparticles (194).

**Table 6. 1.** Average hydrodynamic diameter ( $Z$ ), polydispersity index ( $Pdl$ ) and zeta potential of chitosan nanoparticles loaded rosmarinic acid, sage and savory.

Nano	Z-average (nm)	$Pdl$	Zeta potential (mV)	Association efficiency (%)	Loading capacity (%)
RA	280.0 ± 16.0 <sup>a</sup>	0.201 ± 0.091 <sup>b</sup>	30.1 ± 1.8 <sup>c</sup>	60.2 ± 1.3 <sup>d</sup>	5.3 ± 0.4 <sup>f</sup>
Sage	302.4 ± 18.2 <sup>a</sup>	0.288 ± 0.074 <sup>b</sup>	27.5 ± 0.9 <sup>c</sup>	96.8 ± 0.2 <sup>e</sup>	8.1 ± 0.6 <sup>g</sup>
Savory	298.3 ± 20.8 <sup>a</sup>	0.214 ± 0.085 <sup>b</sup>	28.2 ± 2.2 <sup>c</sup>	98.0 ± 0.3 <sup>e</sup>	7.8 ± 0.2 <sup>g</sup>

**Note:** Values were means of triplicate samples ± standard deviation; <sup>a,b,c,d,e,f,g</sup> means within the same column, labelled with the same letter, were not statistically different from each other ( $P > 0.05$ ).

### 6.2.2. Association efficiency and loading capacity

Chitosan can interact with the negatively charged TPP, forming inter- and intra-molecular cross-linkages, yielding ionically cross-linked chitosan nanoparticles in acidic media (pKa 6.5) (36). It is also known that the inter- and intra-molecular linkages created between TPP and the positively charged amine groups of chitosan were responsible for the success of the gelation process (188). Among the different sources of rosmarinic acid encapsulated into chitosan nanoparticles, it was observed different loading capacity between free drug and extracts (Table 6.1). This may be correlated to the lower initial amount in rosmarinic acid used to prepare nanocomplexes, as previously described for insulin encapsulation into chitosan-alginate ionotropic nanoparticles (233). The results were in line with previous data for ionic gelation chitosan nanoparticles (234, 235). Higher association efficiency was found for rosmarinic acid entrapment in extracts of sage and savory (with no significant differences observed between them ( $P > 0.05$ ), than in pure rosmarinic acid entrapment in chitosan nanoparticles. The results were on the row with other chitosan idebenone and *ilex paraguensis* encapsulation (193, 201). Other studies showed similar association efficiency for other phenolic compound, such as catechin (198) and epigallocatechin gallate (199). The results also exhibited higher association efficiency than the obtained for quercetin encapsulation in PLA nanoparticles (i.e. 40%) (152). Nevertheless, higher association efficiency for rosmarinic acid nanoparticles were previous described in solid-lipid-nanoparticles (230). Nevertheless, higher association efficiency for rosmarinic acid nanoparticles were previous described in solid-lipid-

nanoparticles (230). Therefore, the association efficiency was highly dependent on the nanosystem used, as well as from the loading and rosmarinic acid amount utilized into the nanoparticles.

### **6.2.3. Mucoadhesion proprieties evaluation by mucin interaction method**

Ocular mucosa may affect the stability chitosan nanoparticles in the presence of mucus components (2). Mucus consists in a heterogeneous tridimensional network, being basically composed of a mucin fibers network, creating an endless system of canals in which particles can diffuse and/or be retained (236, 237). Chitosan is a mucoadhesive polymer that may increase residence time and intimate contact of the delivery vehicle with the mucosa, consequently increasing the drug bioavailability, such proprieties were well documented in literature (168). The chitosan adhesion mechanism is mainly associated to the electrostatic interactions established between protonated amine groups of mucoadhesive chitosan and negatively charged groups of mucin (238). In this study, the nanoparticle-mucin interaction was determined measuring the amount of mucin that attaches the nanoparticles (239). The degree of adsorption of nanoparticles/mucin particles can be determined by the variations in size (240), zeta potential (241) or electrophoretic mobility (242) of formed complexes with mucosal fluids, in particular with mucin. Size can influence the diffusion of drug carriers through the mucin mesh that composes mucus fluids, being the optimal range between 200 and 500 nm to enhance diffusion (243). Higher or smaller diameters may decrease transport through the mucus layer. This is in contrast to the prevailing belief, demonstrate that large nanoparticles, can rapidly penetrate physiological human mucus, and that large nanoparticles can be used for mucosal drug delivery (243). For this purpose, rosmarinic acid containing nanoparticles were evaluated, since chitosan was the only responsible for the mucoadhesion results and rosmarinic acid was the principle active of all the formulations used. As depicted in Table 6.2, the rosmarinic acid nanoparticles obtained in this study were in optimal range mentioned, for the three pHs used. The influence of pH values was intended to demonstrate that the particles were mucoadhesive in different conditions, at the normal ionic gelation pH (5.8), at an inflammation pH (5.0) and in homeostasis pH (7.4). The increased size after mucin incubation suggests that nanoparticles-mucin interaction were forming microaggregates, and decrease in zeta potential values was probably due to the electrostatic interaction between positive charged of chitosan and anionic mucin (241).

Strong ability of those nanoparticles to interact with mucin through electrostatic forces were observed, highlighting their potential as mucoadhesive carriers (226). Other study demonstrated the effect of low, medium and high molar mass chitosan in coated polycaprolactone (PCL) nanoparticles (238). The results were according to mucoadhesive nanoparticles made of thiolated quaternary chitosan crosslinked with hyaluronan (244).

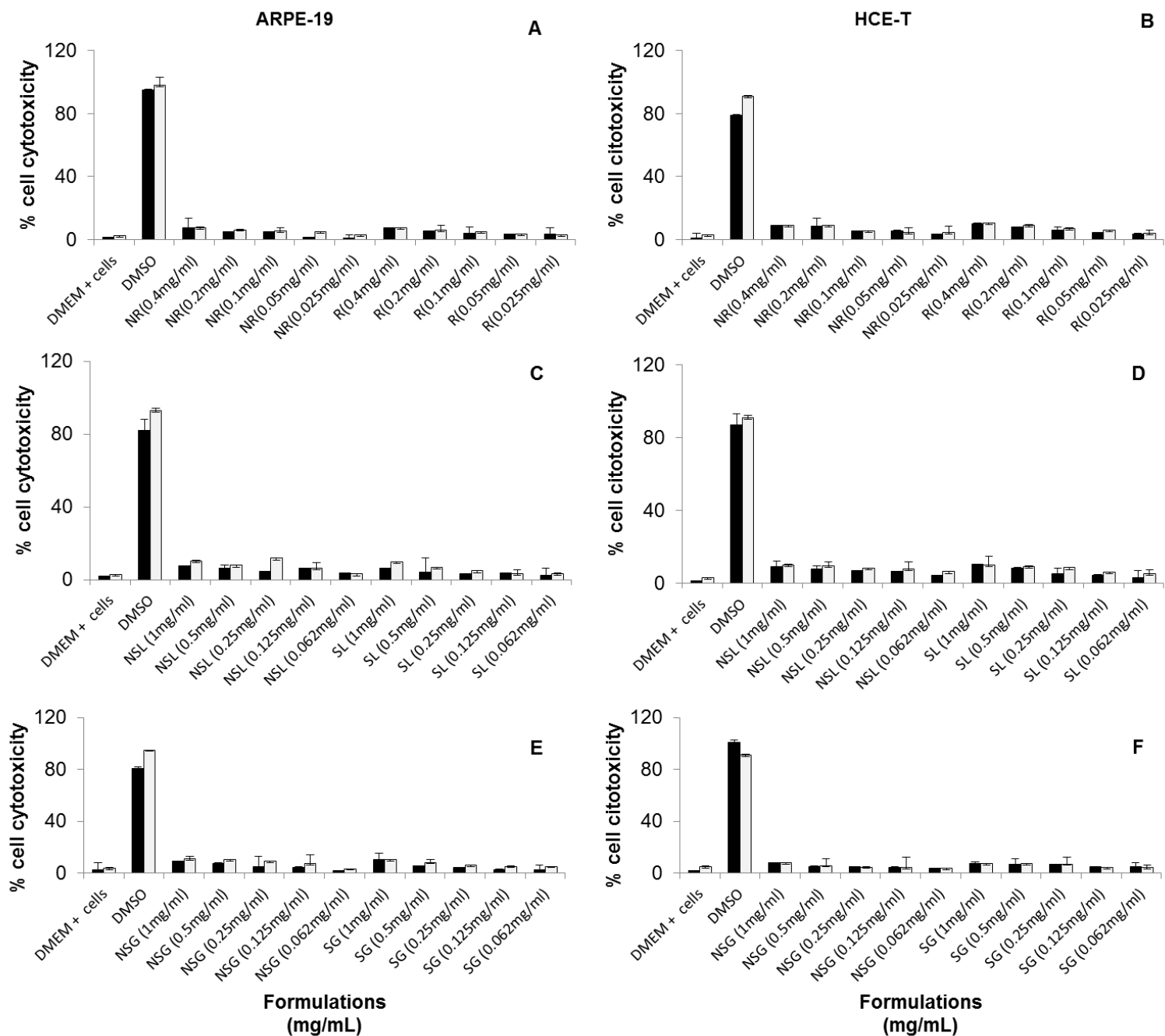
**Table 6. 2.** Average hydrodynamic diameter ( $Z$ ), polydispersity index ( $Pdl$ ) and zeta potential of chitosan nanoparticles loaded rosmarinic acid before and after mucin interaction (n = 3).

Nanoparticles	pH	Z-average (nm)	Pdl	Zeta potential (mV)
Rosmarinic acid	5.8	236.0 ± 7.1 <sup>a</sup>	0.719 ± 0.036	40.1 ± 0.8 <sup>c</sup>
Rosmarinic acid + Mucin	5.0	488.2 ± 30.5 <sup>b</sup>	0.619 ± 0.049	22.5 ± 0.9 <sup>d</sup>
Rosmarinic acid + Mucin	7.4	414.1 ± 32.3 <sup>b</sup>	0.511 ± 0.014	23.1 ± 0.6 <sup>d</sup>

**Note:** Values were means of triplicate samples ± standard deviation; <sup>a, b, c, d</sup> means within the same column, labelled with the same letter, were not statistically different from each other ( $P > 0.05$ ).

#### 6.2.4. Cell viability studies

In order to evaluate any potential cytotoxicity of rosmarinic acid, sage and savory on ARPE-19 and HCE-T cell lines, pure rosmarinic acid and extracts-loaded chitosan nanoparticles were tested for 4 and 24 h. The effect of nanoparticles on membrane integrity was measured by the LDH enzyme release assay and the effect on cell viability was measured using the MTT conversion assay. *In vitro* cytotoxicity results were presented in (Figure 6.1). Results showed that after 4 h the cytotoxicity was below 10% for the tested concentration range, for both cells lines. Moreover, there were no significant differences ( $P > 0.05$ ) between the 4 and 24 h (testing time) considering all formulations and different cell lines.

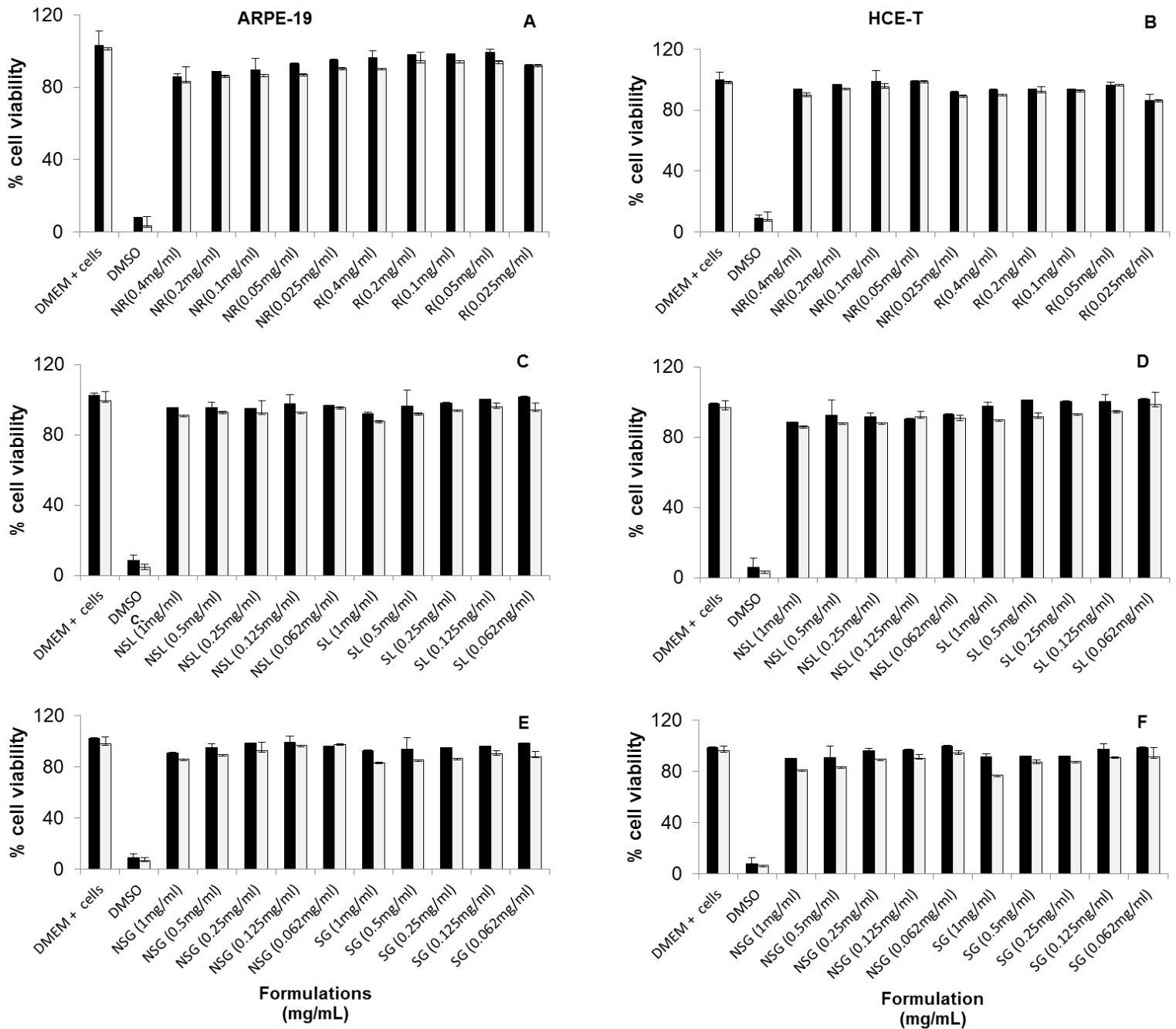


**Note:** NR, R - rosmarinic acid loaded and unloaded chitosan nanoparticles, respectively; NSL, SL – *Salvia officinalis* loaded and unloaded chitosan nanoparticles, respectively; NSG, SG – *Satureja montana* loaded and unloaded chitosan nanoparticles, respectively.

**Figure 6. 1.** Effect of rosmarinic acid, sage and savory-loaded chitosan nanoparticles on cell cytotoxicity of ARPE (A, C and E) and HCE (B, D and F) cell lines after 4 h (black bar) and 24 h (white bar) of incubation. DMEM+cells and DMSO were used as controls. The formulation concentration used was displayed in the tables, relatively to rosmarinic acid (A, B), sage (C, D) and savory (E, F) (results were the mean of 6 replicates, bars represent standard deviation).

Results of cell viability for rosmarinic acid, sage and savory loaded chitosan nanoparticles obtained from the MTT test were shown in Figure 6.2. These were in a good correlation with those from the LDH assay. Antioxidant/chitosan nanoparticles presented a good profile in terms of cell viability of ARPE-19 and HCE-T cells. The results showed that these nanoparticles were not toxic for the cells at concentrations below 1 mg/mL. The results were in line with chitosan cell safety performance regarding its use as drug delivery systems and data show that it was completely safe with no-toxicity effect upon cell lines since chitosan can interact with cell membranes and be uptake with no cytotoxicity and cell collateral damages. The results were in line with previous studies on the use of chitosan in drug delivery systems, (40) regarding its non-toxicity, good cell membrane interaction and cellular uptake with no collateral damages. Moreover, other studies demonstrated that chitosan nanoparticles besides being non-toxic, may have protective effects on cell lines (245-247).





**Note:** NR, R - rosmarinic acid loaded and unloaded chitosan nanoparticles, respectively; NSL, SL – *Salvia officinalis* loaded and unloaded chitosan nanoparticles, respectively; NSG, SG – *Satureja montana* loaded and unloaded chitosan nanoparticles, respectively.

**Figure 6. 2.** Effect of rosmarinic acid, sage and savory-loaded chitosan nanoparticles on viability of ARPE (A, C and E) and HCE (B, D and F) cell lines after 4 h (black bar) and 24 h (white bar) of incubation. DMEM+cells and DMSO were used as controls. The formulation concentration used was displayed in the tables, relatively to rosmarinic acid

(A, B), sage (C, D) and savory (E, F) (results were the mean of 6 replicates, bars represent standard deviation).

The cellular models have been established as promising tools for the investigation of pathological ocular conditions, and the toxicological screening of compounds as alternative to *in vivo* toxicity tests. Animal based experiments are important for pharmacological and toxicological studies while cell models are relevant to mechanistic researches (165). Several animal models including rabbits, pigs, rats and monkeys have been exploited for studies of ocular drug pharmacokinetics and bioavailability. The ethical controversy associated to these biological trials implies the need to develop cell cultures that mimic the action of drugs on the organism. It is now known that the development and validation of *in vitro* tests to replace animal experimentation is among the priorities of the 7th European Community framework program (162, 165). Several studies have been conducted to evaluate the feasibility of using HET-CAM as a complete replacement for the *in vivo* rabbit ocular test (Draize test). This test has several advantages, such as avoiding the ethical concerns, allow high simplicity, rapid, sensitive and easily performance. It is also an economic method to simulate *in vivo* ocular reactions (248). Animal experiments regulation allows protocols that use chick embryos without needing authorization from animal experimentation committees (248). The HET-CAM test has been proposed as a model for a living membrane because it has a functional vasculature, in other words, the acute effects induced by a test substance on the small blood vessels and proteins of this soft tissue membrane are similar to those of the rabbit eye test, while offering the advantages of being a non-animal test, more rapidly and universally acceptable. For that reason, HET-CAM cytotoxicity test was intended to evaluate the development of irritation symptoms. Cytotoxicity of rosmarinic acid, sage and savory-loaded chitosan nanoparticles was then evaluated for hemorrhage, coagulation (intra- and extravascular protein denaturation) and vasoconstriction, when the test substances were added to the membrane and left in contact for 5 min (Table 6.3). The particles were shown to be non-irritating (IS = 0.0) because they did not prompt vasoconstriction, haemorrhage or coagulation in the HET-CAM cells within 5 min of contact. These results were in agreement with the MTT and LDH assays made before, and with those obtained elsewhere for chitosan, chitosan nanoparticles and other nanosystems (227, 249-251).

**Table 6. 3.** Cytotoxicity of rosmarinic acid, sage and savory-loaded chitosan nanoparticles for development of irritation symptoms such as vasoconstriction, hemorrhage and coagulation.

Assays	Nanoparticles			
	Sage	Savory	Rosmarinic acid	SLS 1%
Vasoconstriction	n. o.	n. o.	n. o.	7 ± 0.6
Hemorrhage	n. o.	n. o.	n. o.	49 ± 2.0
Coagulation	n. o.	n. o.	n. o.	68 ± 3.0
Irritation Potential	0.0 ± 0.0	0.0 ± 0.0	0.0 ± 0.0	18 ± 0.5

**Note:** Positive control - sodium lauryl sulfate 1% (SLS). n.o. signs not observed. Non-irritating: 0-0.9; slightly irritating: 1-4.9; Irritating: 5-8.9 and severely irritating: 9-21.

#### 6.2.5. Permeability assays

Only about 1-5% of a topically applied drug dose often reaches the anterior segment of the eye (118). Therefore, the subsequent diffusion of drugs to the posterior segment will often be low. Moreover eye drops in solution are eliminated from the precorneal area within 90 seconds and absorbed systemically through the highly vascular conjunctival stroma and nasolachrymal ducts (252). This means that drugs topically administered have low probability of reaching the posterior segment in significant amounts (due to corneal and conjunctival epithelium, then aqueous humor, and lens physical barriers) (132).

Undoubtedly, the permeation of a molecule is determined by the delicate balance of numerous parameters that are clearly interrelated. In modern pharmacological discovery stage, the study of biological activity and drug physical-chemical profile are crucial. Some of these core properties are the aqueous solubility, lipophilicity and membrane permeability, which will influence the transport, cellular uptake and distribution of chemicals in biological systems (253).

In the ocular system, the drug absorption from the surface of the eye can be summarized in either corneal or noncorneal (254). Mostly drugs are passive diffused across the cornea and this diffusion transport is influenced by solubility, molecular weight, partition coefficient and drug ionization degree (253). In structure, the corneal epithelium is the main limiting barrier for hydrophilic drugs that penetrate through the paracellular pathway, but in another way, hydrophilic compounds may have the diffusion eased in cornea

hydrophilic stroma, which also is the most tightness structure of cornea and represents 85-90% of cornea total mass (162). In the opposite case, the lipophilic compounds are able to permeate through the cornea epithelium via transcellular route, nonetheless, they will deal with a huge difficulty to cross the stroma (27). Having this in mind, chitosan mucoadhesive carriers that increases the retention time in ocular surface may be, in the future, a crucial solution in topical administration.

In this study, after morphological characterization, mucoadhesion, and viability assays, the rosmarinic acid transport study was conducted to track the effect of chitosan nanoparticles on the *in vitro* permeability. The transport of rosmarinic acid (loaded chitosan-based nanoparticles and free in solution) was tracked through the different ocular cell models (e.g. ARPE and HCE), following by the measurement of rosmarinic acid transport across the cells. For these permeability experiments, initial TEER values were  $\approx 300 \Omega\text{cm}^2$ , for both cell lines, at 21 days of post-seeding (90-100% confluence) on the Transwell<sup>®</sup>. The results demonstrated similar  $P_{app}$  after 1 h, for both rosmarinic acid (loaded chitosan-based nanoparticles and free in solution) and for both cell lines, with no significant differences ( $P > 0.05$ ) between wither loaded and free solution or cells. HCE cell line permeability study showed a  $P_{app}$  of  $3.41 \pm 0.99 \times 10^{-5}$  and  $3.24 \pm 0.79 \times 10^{-5}$  cm/s for rosmarinic acid loaded chitosan-based nanoparticles and free in solution, respectively (Figure 6.3). In ARPE-19 cell study the  $P_{app}$  was  $3.39 \pm 0.18 \times 10^{-5}$  and  $3.60 \pm 0.05 \times 10^{-5}$  cm/s for rosmarinic acid loaded chitosan-based nanoparticles and free in solution, respectively (Figure 6.4).  $P_{app}$  was calculated considering only the apical to basolateral direction. No significant differences between formulations neither between cell lines ( $P > 0.05$ ) were observed. Regarding TEER results it has been reported ARPE-19 TEER values of 30, 100 and higher than 200  $\Omega\text{cm}^2$  (223). Thus, the great disparity in the TEER values found in the literature was probably due to differences in post seeding time and percentage of confluence of ARPE-19 cell lines. Regarding the HCE-T cell line, TEER values obtained were expectable and similar to those reported by Nagai et al. (ca. 400  $\Omega\text{cm}^2$ ) (255). The TEER values under studied guarantee that the established monolayers were considered to be tight enough for permeability experiments (162). In the same way as TEER values,  $P_{app}$  values can also depend on various factors such as passage number, age of the cells, the media and growth conditions used and even the own TEER values (256). For this reason, this technique was more precise when a comparative manner with all the compounds assessed in the same assay and under the same conditions. The  $P_{app}$  values may allow the permeability compounds rating into poorly, moderately, and highly permeable ( $P_{app} < 1 \times 10^{-6}$ ,  $1-10 \times 10^{-6}$ , and  $>10 \times 10^{-6}$  cm/s,

respectively) (257, 258). Considering this, and the rosmarinic acid  $P_{app}$  values ( $>10 \times 10^{-6}$  cm/s) it can be predicted that this phenolic acid was highly permeable in ocular cell lines. In fact, the low molecular weight (i.e. 360.31) of this compound was in the range of “non-restricted membrane diffusion” (259). Also, its hydrophilic character and consequent passive diffusion through the paracellular route was predictable. The increase of rosmarinic acid permeability during the time in HCE-T and ARPE-19 cell lines was deeply related with the decrease of tight junction stickiness, tracked by the decrease of TEER values found for the cell culture during the time of the experiment, promoting the paracellular transport of rosmarinic acid (Figure 6.3 and 6.4). It is already known that as the tight junctions open, the TEER values of cell monolayers are significantly reduced, due to ion passages through the paracellular route (260). It was expectable that chitosan enhanced rosmarinic acid cell permeability, due to its ability to open epithelium tight junctions. In addition, the chitosan is also commonly explored for improving precorneal residence of nanoparticles because it is positively charged which hence it binds to negatively charged corneal surface and thereby improves precorneal residence and decreases clearance (261). Nevertheless, chitosan permeation effect was not observed in this study, since no significant differences were detected in permeation between rosmarinic acid loaded chitosan nanoparticles or free in solution. One important fact that may be on the base of the absence of enhancement effect of chitosan nanoparticles was the natural rapid release profile of these particles described previously (190, 196). Since that in the first 15-20 min over 50 to 60% was released at physiological pH, which was the ideal profile when it is not needed to prolong the drug release for several hours, as in the case of ophthalmic solutions. This may be one of the reasons that from this time on, no significant differences could be found between nanoformulation and the free compound. These solutions must ensure the best compromise between efficiency and minimum residence time possible in order to not cause discomfort to the patient. The permeability values were higher than other previous reports considering rosmarinic acid in *Prunella vulgaris* and ursolic acid in *Salvia officinalis* extracts across Caco-2 cell monolayers (262). Moreover, the results were also in the line with those reported in other study, which showed rosmarinic acid intestinal absorption efficiency and evidences of transport mainly via paracellular diffusion (263). Furthermore, it was described that rosmarinic acid appeared to be unsusceptible to hydrolysis by mucosa esterase in Caco-2 cells and further metabolized and degraded into m-coumaric and hydroxylated phenylpropionic acids by gut microflora, which were then efficiently absorbed and distributed by the monocarboxylic acid transporter (MCT) within the body (263). Notwithstanding and

besides no enhancement permeability effect was observed in chitosan encapsulation of rosmarinic acid, it should be underline the chitosan mucoadhesiveness proprieties that are crucial to overcome the drug lost by blinking process that happens in the first 90 s (252). In this sense it is vital the particles adherence and protection of the drug delivery in the first brief minutes, as chitosan particles ensure in this study.

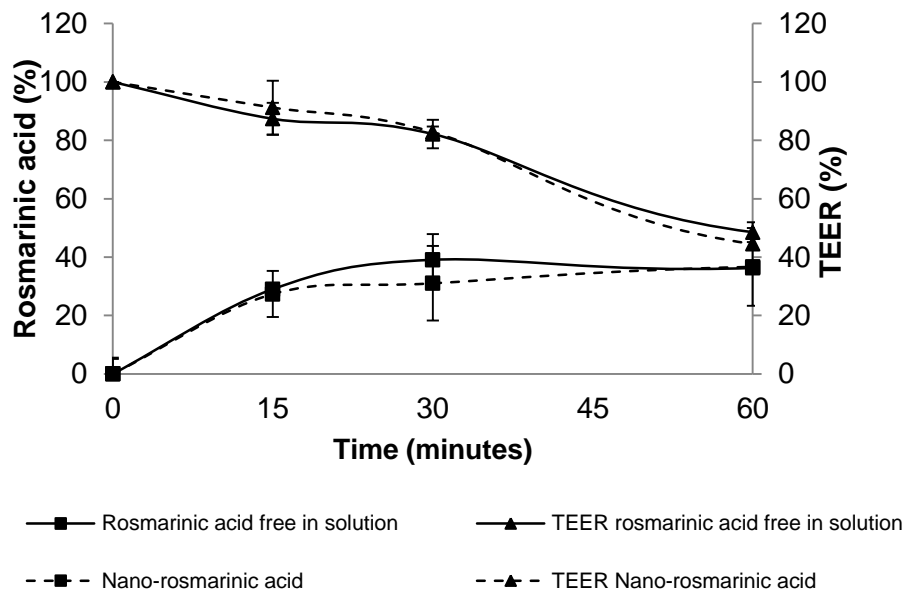


**Figure 6. 3.** Cumulative transport and TEER cell monolayer measurements of rosmarinic acid loaded chitosan-based nanoparticles and free in solution across HCE-T model cells (Values were means of 6 replicates, bars represent standard deviation).

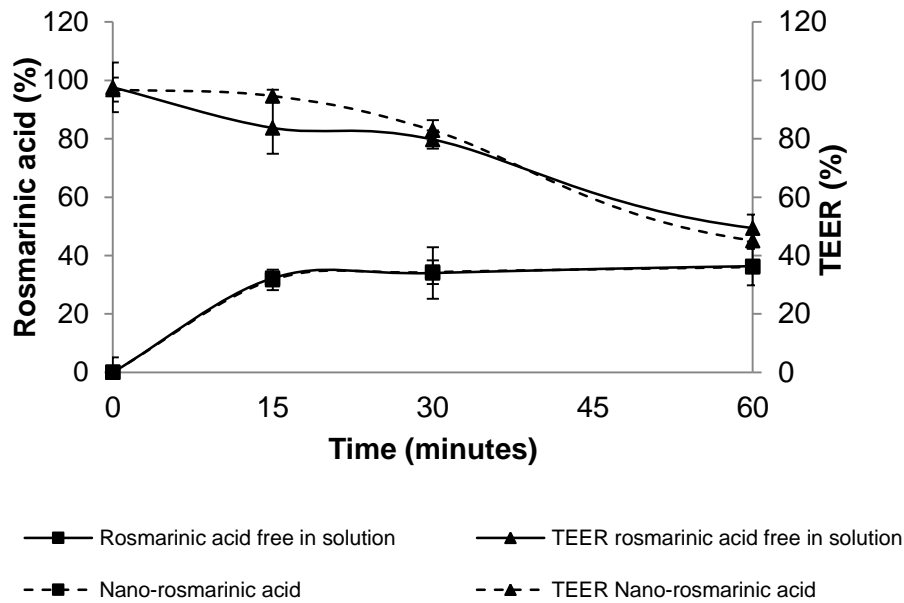


**Figure 6. 4.** Cumulative transport and TEER cell monolayer measurements of rosmarinic acid loaded chitosan-based nanoparticles and free in solution across ARPE-19 model cells (Values were means of 6 replicates, bars represent standard deviation).

### 6.3. Conclusion

In this study, was reported an extensive *in vitro* study for chitosan nanoparticles encapsulating rosmarinic acid, in a pure form, and also in two different natural extracts (e.g. sage and savory). Results demonstrated mucoadhesive nanoparticles ranging 200-300 nm with a surface charge between 20-30 mV and without relevant cytotoxicity against ocular cell lines (e.g. ARPE and HCE). Rosmarinic acid showed to be a compound highly permeable (loaded and unloaded chitosan nanoparticles), regarding both studied cell lines above ( $3.2 \times 10^{-5}$  cm/s) after 60 min. In this study it was proposed, for the first time, chitosan formulations as biodegradable mucoadhesive nanocarriers for delivery of rosmarinic acid, sage and savory natural antioxidants that in newer future may represent a suitable alternative to current invasive clinical methods. Nonetheless a better correlation with *in vivo* data should be deeply explored, in order to deeply understand the real potential of these systems in ocular diseases prevention and treatment.





*CHAPTER 7 - Therapeutical potential evaluation  
in ischemia-reperfusion animal model of chitosan  
based-nanoparticles*

---



## 7. Introduction

The ocular endogenous antioxidants act constantly like safeguard against oxidative ocular pathologies. Nonetheless, the constant eye insults of ROS such as UV light, visible light, ionizing radiation, chemotherapeutics, and environmental toxins contribute inevitable to some oxidative damage in ocular tissues (264). These long-term affronts lead to a considerable risk for pathological consequences of OS, such as glaucoma.

Glaucoma was deeply defined by an elevation of intraocular pressure (IOP), but nowadays it is considered as a neurodegenerative disease, characterized by degeneration of the optic nerve and loss of retinal ganglion cell (RGC) (265). The increased levels of proinflammatory cytokines in aqueous humor (266) and retina (267) of glaucoma patients also suggest disease intimate relationship with neuroinflammation. Rodent models are common chosen models for glaucoma study, namely I-R model. The I-R model simulates the retinal Ischemia, which may be defined as an inefficient blood supply to the tissue, resulting in hypoxia and failure of tissue nutrient demands (268). The ischemia clinical impairment in some ocular diseases like glaucoma is evident, being a common cause of visual impairment and blindness (269). The I-R model is characterized by an elevation of IOP above systolic pressure, which allows the control of the magnitude and duration of ischemia, as well as the duration of reperfusion, which are very important parameters concerning RGCs death (169). Even though it does not directly track the exact pathophysiology that occurs in human glaucoma, it induces a specific insult to RGCs, which is fundamental (169). Since it is very difficult to study the pathophysiology of glaucoma in human patients, animal models seem central in order to understand the underlying mechanism of disease and to develop new therapies. Therefore and considering the ethical concerns about *in vivo* tests, in this work it was aimed to investigate the rosmarinic acid effect on the retina inflammatory control in an I-R injury model. Rosmarinic acid is a powerful antioxidant, with anti-inflammatory, anti-proliferative, and anti-angiogenic activities associated (270). Rosmarinic acid is described to inhibited all angiogenic processes including proliferation, migration and tube formation of endothelial cells, which is mediated by suppression of induced VEGF (271). Its anti-proliferative effect suggests that proliferative vascular diseases including tumor, arthritis as well as retinopathy might be targets for the pharmacological application of rosmarinic acid.

## **7.1. Experimental**

### **7.1.1. Animals and drug administration**

All procedures involving animals were in accordance with the Association for Research in Vision and Ophthalmology (ARVO) statement for vision and ophthalmic research, and were approved by the Institutional Ethics Committee (Comissão de Ética da Faculdade de Medicina da Universidade de Coimbra) - Approval ID: FMUC/12/09. Male Wistar rats aged 8 weeks were housed under controlled environment ( $21.8 \pm 0.1$  °C of temperature and,  $67.6 \pm 1.6\%$  of relative humidity, 12 h-light/dark cycle) with free access to food and water. After intravitreal and I-R the 2 animals were maintained at  $22 \pm 1$  °C on a 12 h light/12 h dark cycle, with still access to water and food ad libitum for the best performance of ERG. One male Wistar rat was also used for saline intravitreal and ischemia control, the same conditions were maintained for the 3 animals. In the study rosmarinic acid was injected intravitreally in both left eyes, 2 h before I-R injury, at the reported therapeutic dosage (e.g. 50  $\mu$ M) (270), the right eyes in both animal were used as control with only the injection of rosmarinic acid at the same concentration.

### **7.1.2. Intravitreal administration of rosmarinic acid**

Animals were randomly selected for the treatment with rosmarinic acid. Intravitreal injection of 5  $\mu$ L was performed using a 10  $\mu$ L Hamilton syringe, in both left eyes 2 h before the induction of retinal I-R.

In each animal the eyes were considered for different proposes, in order to decrease the use of animals, in this sense:

- i) Right eyes: Intravitreal injection of 5  $\mu$ L of rosmarinic acid without I-R;
- ii) Left eyes: Intravitreal injection of 5  $\mu$ L of rosmarinic acid followed by retinal I-R;

### **7.1.3. Electroretinogram recordings**

ERG were performed as described previously (272). ERG recorded 24 h before treatment (intravitreal injection), which represents the Baseline ERG, and 24 h after treatment. The

animals were anesthetized by intramuscular injection of ketamine (50 mg/kg) and xylazine (10 mg/kg) and fully dilated pupil with topical tropicamide (1%) under red light, for weak illumination. Body temperature was maintained with a heating pad set to 37 °C during the procedure. Using a Ganzfeld stimulator, a series of flashes of white light ranging, 0095 to 9.49 cd-s/m<sup>2</sup> were applied under scotopic and photopic conditions. ERG was recorded with a corneal electrode gold wire, a reference at the head, and a ground electrode tail. A width of 1-300 Hz band and a sampling rate of 3.4 kHz (0.65 kHz to flicker test) were used to acquire (Roland Consult GmbH, Brandenburg, Germany). OFF-line digital filters were applied to the  $\beta$ -wave (high cut-off frequency of 50 Hz) and oscillatory potentials (lower cut-off frequency of 60 Hz ERG to scotopic and photopic ERG to 55 Hz) with the software RETIport (Roland Consult GmbH, Brandenburg, Germany).

#### **7.1.4. Retinal ischemia-reperfusion injury**

Retinal I-R was induced in left eyes by elevating the IOP to 80 mmHg for 60 min, after intravitreal injection of rosmarinic acid. Animals were anesthetized with 2.5% isoflurane (IsoFlo, Abbott Laboratories) in 1 L/min O<sub>2</sub> with a vaporizer throughout the procedure of ischemia, and were placed on a heating plate to maintain their body temperature. After topical anesthesia with application of oxybuprocaine (4 mg/mL, Anestocil, Edol) and pupillary dilation with topical application of tropicamide (10 mg/mL, Tropicil Top, Edol), the anterior chamber of the one eye, for I-R injury, was cannulated with a 30-gauge needle connected to reservoir infusing sterile saline solution. The IOP was raised by elevating the reservoir to a height of 1.8 m. Retinal ischemia was confirmed by whitening of the iris and loss of the red reflex. IOP was also measured with the Tonolab and it was increased to 80 ± 1 mmHg. In order to avoid corneal opacity, viscoelastic solution (2% Methocel, Dávi II – Farmacêutica S.A.) was applied to both eyes. After 60 min of ischemia the needle was withdrawn and reperfusion was established. Fusidic acid ointment (10 mg/g, Fucithalamic, Leo Pharmaceutical) was applied in the end of the experiment. Animals were sacrificed 24 h after ischemia.

#### **7.1.5. Preparation of frozen retinal sections**

Animals were anesthetized with an intraperitoneal injection of a solution of ketamine (90 mg/kg; Imalgene 1000) and xylazine (10 mg/kg; Ronpum 2%). The animals were then transcardially perfused with phosphate-buffered saline (PBS, in mM: 137 NaCl, 2.7 KCl,

Na<sub>2</sub>HPO<sub>4</sub>, 1.8 KH<sub>2</sub>PO<sub>4</sub>; pH 7.4) followed by 4% (w/v) paraformaldehyde (PFA). The eyes were further enucleated and post-fixed in 4% PFA for 1 h. The cornea and the lens were carefully dissected out and the eyecup was fixed for an additional 1 h in 4% PFA. After washing in PBS, the tissue was cryopreserved in 15% sucrose in PBS for 1 h followed by 30% sucrose in PBS for 1 h. The eyecups were embedded in tissue-freezing medium (Optimal Cutting Temperature, OCT; Shandon Cryomatrix, Thermo Scientific) with 30% of sucrose in PBS (1:1), and stored at -80 °C. The tissue was sectioned on a cryostat (Leica CM3050 S) into 10 µm thickness sections and mounted on Superfrost Plus glass slides (Menzel-Glaser, Thermo Scientific). Glass slides were dried overnight and then stored at -20 °C.

#### **7.1.6. Terminal deoxynucleotidyl transferase-mediated dUTP nick end labeling (TUNEL) assay**

Cell death was performed with a TUNEL assay kit with fluorescein detection following the instructions provided by the manufacture (Promega). Sections were washed twice in PBS and then permeabilized with proteinase K (20 µg/mL) for 10 min. After washing twice in PBS, the sections were incubated with equilibration buffer (200 mM potassium cacodylate, 25 mM Tris-HCl, 0.2 mM DTT, 0.25 mg/mL BSA and 2.5 mM cobalt chloride) for 10 min. Sections were further incubated with the recombinant TdT enzyme and with nucleotide mix containing dUTP conjugated to fluorescein at 37 °C for 1 h. The reaction was stopped by immersing the slides in saline-citrate (SSC) buffer (175 g/L NaCl, 88.1 g/L sodium citrate) for 15 min at room temperature. Samples were washed three times in PBS 5 min, followed by incubation with the nuclear dye DAPI (diluted 1:2000). Sections were washed in PBS and mounted with fluorescent mounting medium (Dako, USA).

#### **7.1.7. Immunohistochemistry**

The glass slides were defrosted at room temperature overnight. The sections were fixed with ice-cold acetone at -20 °C for 10 min, and then rehydrated in PBS twice until OCT. The tissue was surrounded with a hydrophobic pen and it was permeabilized with 0.25% Triton X-100 in PBS for 30 min. The sections were blocked in 10% Normal Goat Serum plus 1% bovine serum albumin (BSA) in PBS for 30 min at room temperature in a humidified environment. After washing with PBS, the sections were incubated overnight with primary antibody prepared in 1% BSA in PBS at 4 °C, in a humidified environment.

Then, the sections were rinsed in PBS followed by incubation with the corresponding secondary antibodies prepared in 1% BSA in PBS for 1 h at room temperature, in the dark. The sections were washed with PBS and then incubated with the nuclear dye 4',6-diamidino-2-phenylindole (DAPI), diluted 1:2000. The tissue was washed in PBS and mounted with fluorescent mounting medium (Dako, USA).

#### **7.1.8. Image analysis**

The samples were examined in a Zeiss LSM 710 confocal on an Axio Observer Z1 microscope using an EC Plan-Neofluar 40x/1.30 Oil DIC M27 objective. Images (1024x1024 formats) were collected using 405, 488 and 561 nm laser lines for excitation. Z-stacks images were acquired and merged using the maximum intensity projection mode of the Zeiss software (Zen 2009, Zeiss). For the analysis of microglial reactivity, 4 images per section were acquired (4 sections each eye). It was observed for microglial reactivity, the number of cells immunoreactive to both Iba1 (Ionized calcium binding adaptor molecule 1) and OX-6 (Iba1+ OX-6+). The survival of RGCs was assessed by immunoreactive to Brn3a (Brn3a+) cells in a Leica DM IRE2 fluorescence microscope using the 40x/0.70 HC PL APO objective. For each eye, 4 sections were analyzed and the observation of Brn3a+ cells taking into account in the entire retinal section. Representative images were acquired with a Zeiss LSM 710 confocal microscope, as described previously. The cell death was assessed by visualizing of TUNEL+ cells in a Leica DM IRE2 fluorescence microscope using the 40x/0.70 HC PL APO objective. For each eye, 4 sections were analyzed and the TUNEL+ cells were observed in the entire retinal section. Representative images were acquired with a Zeiss LSM 710 confocal microscope, as described previously.

### **7.2. Results and discussion**

#### **7.2.1. Differential effects of rosmarinic acid on electroretinograms**

It was assessed the potential changes in light responses of rats induced by a single intravitreal administration of rosmarinic acid. The ERG was chosen to measure responses of the global population retina, which tend to be dominated by specific group of retinal

layers technique, allowing pathophysiological interpretation (273). Rosmarinic acid potential effect on retinal physiology, scotopic and photopic was evaluated. ERG were recorded in animals administered with rosmarinic acid (50  $\mu\text{M}$ , single administration), 24 h before (Baseline ERG), and 24 h after rosmarinic acid intravitreal injection (Figure 7.1). Waveforms were elicited by flash light stimuli with intensities ranging from 0.0095 to 9.49  $\text{cd}\cdot\text{s}/\text{m}^2$ . The results showed an evident decrease in retina signaling. However it is difficult to evaluate the effect of application of rosmarinic acid, without distinguishing the nefarious effect of intravitreal injection itself and the insult of I-R injury. It may be complicated to study and distinguish individual and combined effects through a single injection of rosmarinic acid and in such small numbers of animals. In this sense, more studies should be considered.

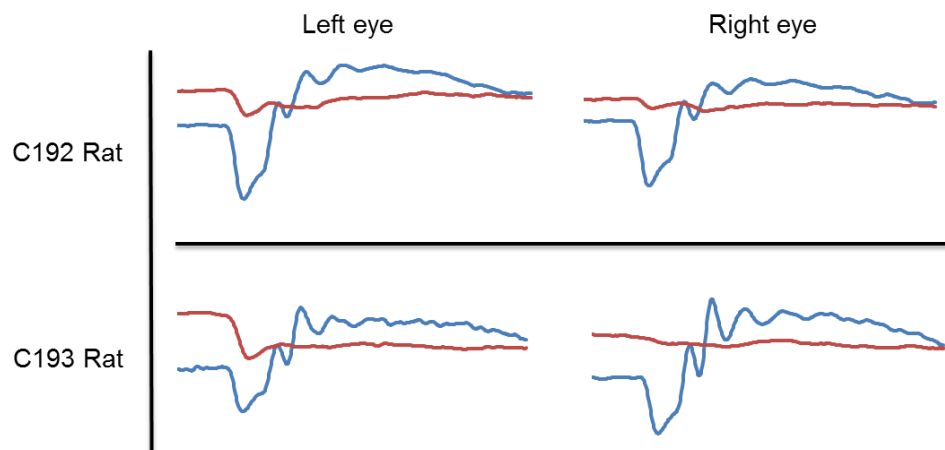


**Figure 7. 1.** Electroretinogram of mixture response of both rods and cones cell populations either in photopic or scotopic conditions ( $\alpha$  and  $\beta$  – waves) recordings of rosmarinic acid administration effect. Left eye: representative traces of individual ERG recorded 24 h before treatment injection (Baseline ERG – blue line) and 24 h after intravitreal injection in I-R model (red line); Right eye: representative traces of individual ERG recorded 24 h before treatment injection (Baseline ERG – blue line) and 24 h after intravitreal injection (red line).

In a mixture response of both rods and cones cell populations either in photopic or scotopic conditions the  $\alpha$ -wave (photoreceptors) undergoes in a very high decrease, being reduced to a small negative peak and there was an almost complete loss of  $\beta$ -wave (Muller/bipolar) (Figure 7.1). Since even without I-R injury the single intravitreal injection of



rosmarinic acid highly decreased the retina cell populations, when compared to baseline ERG, it can be assumed that by intravitreal injection, with or without I-R injury the effect of rosmarinic acid, at the tested concentration was not beneficial to retina. The results were different from that of antioxidant ergothioneine that seem to have a neuroprotective effect in the retina. (274). Evidences also support the fact that epigallocatechin gallate was a powerful antioxidant when injected into the eye, ERG data showed a significant protective effect of retinal photoreceptors (275). From the present results it is clear that future studies should evaluate multiple injections of rosmarinic acid in different concentrations, and other rosmarinic acid administration routes addressed to other animal models.

### **7.2.2. Effect of rosmarinic acid on retinal ischemia-reperfusion injury rat model - Microglial reactivity**

Microglia reactivity was assessed by immunohistochemistry using Iba 1 and OX-6 antibodies. Iba 1 can be used as a marker of microglia/macrophages and is recognized as microglia/macrophage-specific calcium-binding protein (276). OX-6 is an antibody knowing the major histocompatibility complex (MHC) class II antigen, which is only expressed by activated microglia/macrophage (277). Retinal sections reveal the positioning of cells Iba1+ at the level of internal layers of retina inner nuclear layer (INL), inner plexiform layer (IPL) and ganglion cell layer (GCL). In this work, the right eyes (from the two animals studied) were considered the control condition, since all eyes were injected with the drugs (except in saline-injected animals). In the animals' eyes it was not observed substantial microglia reactivity (cells immunoreactive to OX-6). Interestingly, there was no visualized difference in microglial cells with only intravitreal injection of rosmarinic acid or between intravitreal injection after treated I-R retinas (Figure 7.2). One possible explanation could be the fact that intravitreal injection, even if of saline, can somehow induce changes in the retinal environment and induce microglia reactivity. Recently, it was reported that ocular hypertension induces upregulation of OX-6 and microglia reactivity in the retinas (278).

## Iba1 + Ox6

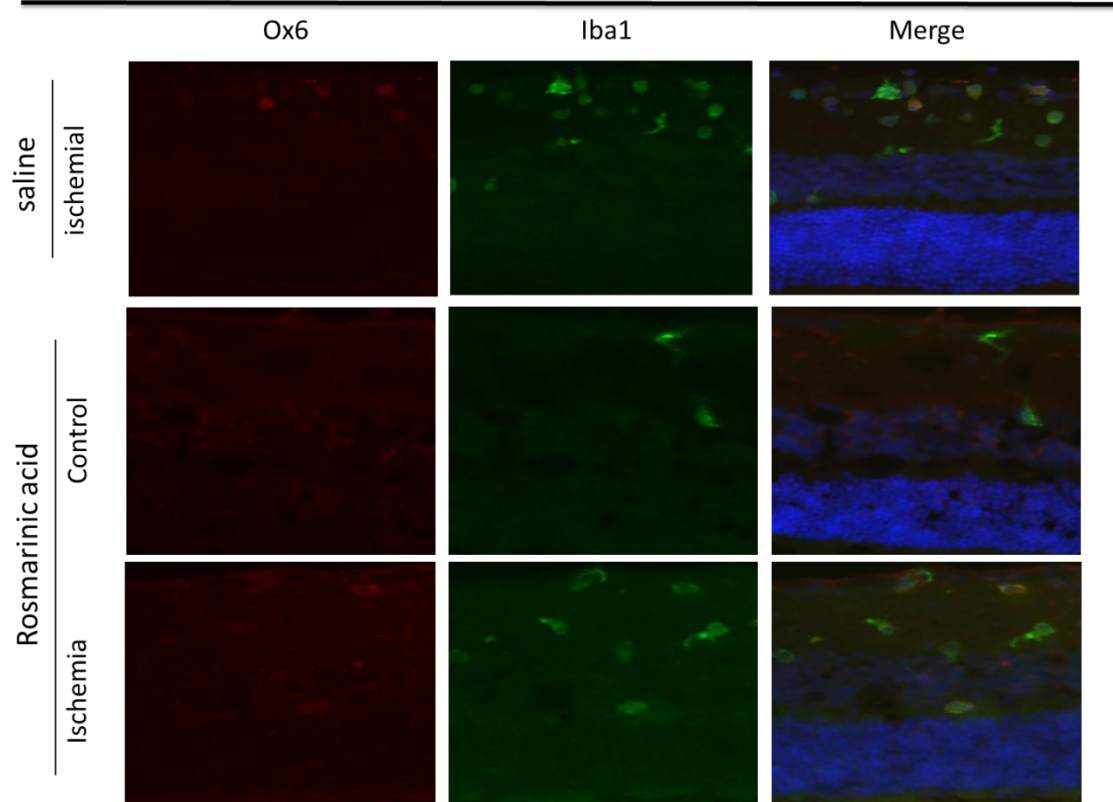


**Figure 7. 2.** Rosmarinic acid effect on activated microglia induced by I-R injury at 24 h of reperfusion retinal. Retinal sections were stained with antibodies against Iba1 (green) and OX-6 (red). Nuclei were stained with DAPI (blue). Representative images were depicted in: Activated microglia/macrophages (Iba 1 - OX-6 immunoreactive cells), comparing with saline ischemial.

Other important fact that may explain the inconclusive results upon rosmarinic acid administration is that OX-6 (MHC II antigen presenting cells) was reported not to be expressed 24 h after ischemia, but after 3 and 7 days (279). One important aspect to consider is that the markers used to identify microglia are also present in macrophages. Since there is no known cell-surface marker to distinguish central nervous system resident from blood-borne macrophages, it becomes difficult to discern the resident microglia from monocytes that enter the central nervous system from the bloodstream and subsequently adopt microglial-cell morphology (280). The neuroinflammatory response, either resident microglia or infiltrating monocytes, becomes a critical issue in determining, not only the nature of the response and characteristics of the injury, but also the effectiveness of modulating their response.

### **7.2.3. Effect of rosmarinic acid on cell death and retinal ganglion cell loss**

Cell death by apoptosis was assessed by TUNEL assay and the loss of RGCs was assessed by immunohistochemistry with an antibody that recognizes the transcription factor Brn3a that in the retina is expressed only in RGCs and can be used to identify these cells (Figure 7.3) (281). Regarding these results it was not observed any beneficial effect of rosmarinic acid administration after I-R injury in comparing with saline-treated retinas (Figure 7.3). This may indicate that rosmarinic acid after intravitreal injection at this value concentration, caused cell death. Rosmarinic acid per se also induced Brn3a+ cells loss after single intravitreal injection (Figure 7.3). Previously reports described that rosmarinic acid inhibited retinal neovascularization in an oxygen-induced retinopathy, a mouse model retinopathy of prematurity, as well as VEGF-induced tube formation of retinal endothelial cells (270). The authors also demonstrated that rosmarinic acid was not toxic to mice retina in concentrations five times higher the therapeutically effective concentration to retinal neovascularization (250  $\mu$ M). Nonetheless, it must be taking into account the animal model clinical differences that may compromise the success of the results, regarding even the same compound. Some studies also reported the effect of caffeine on microglia neuroinflammation and cell death controlling pro-inflammatory mediators (282). Nonetheless this beneficial effect may be difficult to achieve for the majority of compounds. It is well known that cell death can be the result of inflammatory process of the exaggerated microglial activation, which is a consequence difficult to revert, and it becomes difficult to distinguish the influence of the inflammation and nefarious intravitreal drugs administrations.

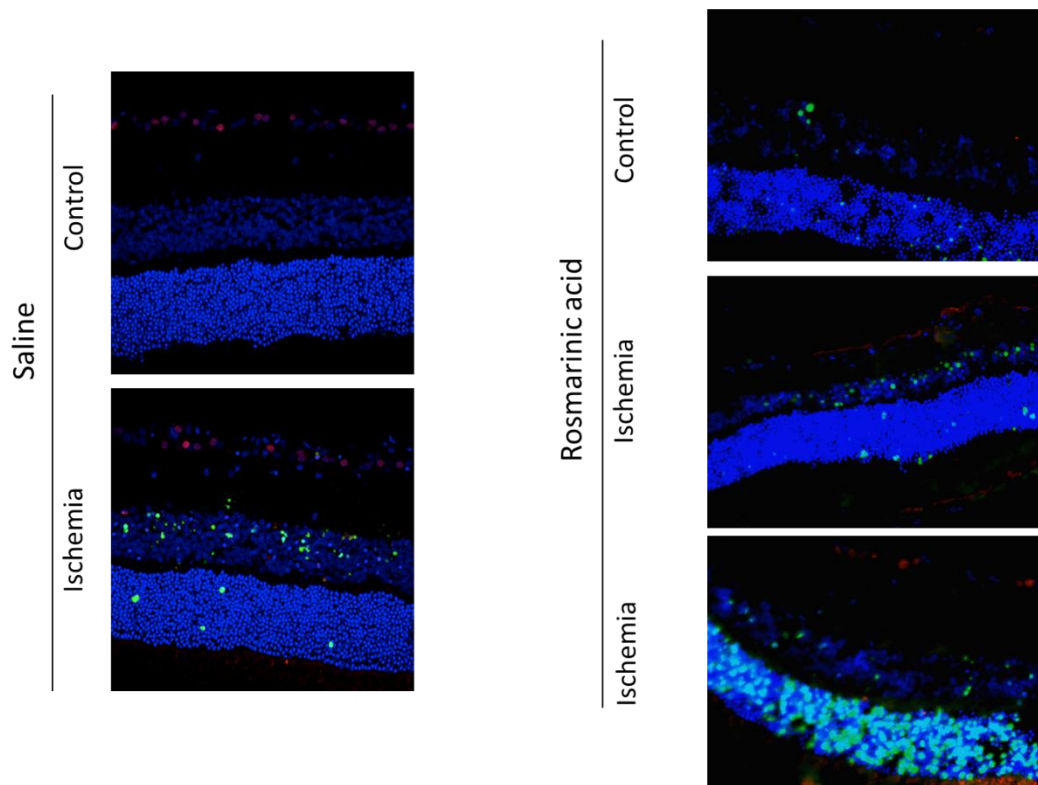


**Figure 7. 3.** Rosmarinic acid administration did not altered the cell death induced by I-R injury at 24 h of reperfusion. Cell death was assayed with TUNEL assay. Nuclei were stained with DAPI (blue). Representative images were depicted in: TUNEL+ cells (green) comparing with saline intravitreal and ischemial.

### 7.3. Conclusion

Intravitreal administration of rosmarinic acid did not show significant modulation of the pro-inflammatory response in the retina induced by I-R injury. Nevertheless, only one single injection of rosmarinic acid was studied, in a small number of animals which may not be sufficient for deep conclusions about this topic. The study respected the ethical concerns about *in vivo* tests and the 3 R's policy - reduce, reuse, recycle. Since the results were not promising no more animals were sacrificed. Moreover, other administration routes of rosmarinic acid, multiple injections, at different concentration, regarding long-term supervision, in different retinal neuroinflammatory animal models, at a more representative population of animal models should be considered in the future. Besides these and all the bioactive potential in different animal models, it must be underlined the potential effect of chitosan-based nanoparticles in the topical administration of rosmarinic

acid. Nanoparticles may increase the residence time in ocular surface, protecting rosmarinic acid from the surrounding physiological environment and improving rosmarinic acid bioavailability, being non-toxic and biodegradable drug delivery systems. More studies should be then developed in order to realize this chitosan-based nanoparticles effect in the rosmarinic acid enhancement performance on ocular pharmacological studies.



## PART VI

---

*“Everything seems impossible until it’s done”*

*Nelson Mandela*





## *CHAPTER 8 - General conclusions*

---



## 8. Conclusions

In this work, a bold attempt was made to achieve a new topical, mucoadhesive, natural, safe and non-invasive prophylaxis for degenerative eye diseases. For this purpose rosmarinic acid was encapsulated in chitosan based systems, using the commercial form and in natural extracts in which it is the major compound.

The studied nanoparticles aiming for a new rosmarinic acid-nanodelivery system, and remarkable results in terms of both their physical-chemical features as well as their behaviour in the conducted *in vitro* studies with ocular cell lines (e.g. HCE-T and ARPE-19) were demonstrated. Regarding particle size, nanoparticles presented sizes comprised within the range of 200-300 nm and with homogeneous distributions, demonstrating great potential for ocular administration. Through SEM and TEM it was possible to confirm these results and also to assess the nanoparticles morphology. The nanoparticles presented spherical and uniform shape, with a smooth surface.

Zeta potential values ranged from approximately 20 to 30 mV, justified by the presence of the positively-charged of chitosan amino groups, which help stabilizing nanoparticles in suspension during the storage time. Particle size and zeta potential were not significantly affected by neither the encapsulation of the commercial rosmarinic acid or by the natural extracts encapsulation.

Other successful proof of chitosan nanoparticles was the high association efficiency, (about 51.2%) for rosmarinic acid nanoparticles and even higher for sage and savory nanoparticles (e.g. 96.1 and 98.2%, respectively). Rosmarinic acid encapsulation in the different systems was further confirmed by FTIR spectroscopy studies, which identified the characteristic transmittance peak of the drug in rosmarinic acid and extracts-loaded chitosan nanoparticles. DSC demonstrated the carriers thermal stability and also that there were no significant covalent interactions between antioxidants and chitosan after encapsulation.

The antioxidant activity performance was confirmed by ABTS and ORAC methods. The antioxidant activity for the nanosystems was lower than that achieved for the unloaded compounds due to partial retention, which means that the compounds will take more time to build up their specific activity. Nevertheless the nanosystems with this entrapment effect still have good antioxidant activity, higher than 0.0348 eq [Asc. Ac.]/g/L/g extract and

0.4251  $\mu\text{mol/eq}$  Trolox/g extract. Even considering this decrease in the nanosystem antioxidant activity, it is well known that the systems protect the antioxidants from degradation by biological and enzymatic fluids, increasing their bioavailability and efficacy. Nonetheless regarding the encapsulation of the natural extracts, other antioxidant compounds in extract nanoparticles that have a close pKa of rosmarinic acid may be encapsulated adding a synergic antioxidant activity. This justifies that with lower rosmarinic acid concentrations, the extracts have the same antioxidant activity of rosmarinic acid nanoparticles. Associated to this synergic effect was the combination of other biological activities of those natural compounds that were incorporated at this pH value in the nanoparticles.

Additionally, *in vitro* release studies showed a fast release for all the formulations freshly and lyophilized within 60 min, which was adequate for ocular applications, since a rapid release was intentional on the effect. Regarding the mucin particle method the nanoparticles showed mucoadhesive proprieties. This is one of the most crucial advantages of these nanosystems, for ocular drug delivery. This propriety will help to overpass the topical drug loss issue, due to the ocular blinking mechanism. The developed chitosan-based nanocarriers were also not toxic to the HCE-T and ARPE-19 monolayer cell lines by MTT and LDH assays. The HET-CAM test also corroborates with the cytotoxicity tests and showed that the particles were not irritant to the eye. Permeability tests showed that in HCE monolayer cell line the rosmarinic acid  $P_{app}$  was  $3.41 \pm 0.99 \times 10^{-5}$  and  $3.24 \pm 0.79 \times 10^{-5}$  cm/s for rosmarinic acid loaded chitosan nanoparticles and free in solution, respectively. In ARPE-19 monolayer cell line the  $P_{app}$  was  $3.39 \pm 0.18 \times 10^{-5}$  and  $3.60 \pm 0.05 \times 10^{-5}$  cm/s for rosmarinic acid loaded chitosan nanoparticles and free in solution, respectively.

Besides pharmacokinetics and toxicological relevance of chitosan-based nanoparticles were guaranteed by *in vitro* model systems, the study of the effective biologic potential of rosmarinic acid required a minimum amount of *in vivo* experiments using an I-R animal model. The therapeutic efficacy and safety *in vivo* were performed in rats by intravitreal injection and the effects were monitored by immunohistochemistry and ERG assays. The purposed of the study was to evaluate if the intravitreal administration of rosmarinic acid modulate the pro-inflammatory response in the retina induced by I-R injury. In the study only one single injection of rosmarinic acid was considered, in a minimum number of animals which was clearly not sufficient to have conclusive results. Nonetheless it must be

underlined the topical purpose of these nanoparticles and the potential effect suggested and reported in this thesis of chitosan-based nanoparticles in the topical administration of rosmarinic acid.

Concluding, the attained results suggest that the devised formulations show a huge potential for rosmarinic acid ocular drug delivery, in chitosan nanoparticles and that sage and savory were good vehicles for rosmarinic acid. These natural extracts are a more natural and cheaper way to rosmarinic acid drug delivery, adding to the final formulation more biological compounds with a synergic effect. This study casts light on the improved therapeutic utilization of the rosmarinic acid loaded in chitosan-based nanoparticles for the novel development of pharmaceutically acceptable nanoparticles. The development of these antioxidant-nanoparticles provided a further insight on ocular application, benefiting from the advantages of the eye for drug delivery and, additionally, offering new potential applications of chitosan as drug carrier and of natural antioxidants for ocular diseases prevention.

At least, it should be underline that no subject was completely explored and there is always room for improvement. Further and more extensively studies should be conducted for nanotechnology approaches of this kind to become a reality in the clinical practice of rosmarinic acid drug delivery to degenerative eye diseases prophylaxis.



## *CHAPTER 9 - Future prospects*

---





## 9. Future prospects

For future work, regarding nanoparticles development, other mucoadhesive systems should be considered, optimized and characterized. Encapsulate antioxidant compounds into different chitosan-based nanoparticles, namely chitosan matrix, alginate/chitosan and chitosan-coated solid lipid nanoparticles and optimize nanoparticulate systems after deep physical-chemical characterization;

Additionally, a more comprehensive study should be directed to the targeting efficacy and internalisation of the devised nanoparticles. Taking into consideration cellular uptake, nanoparticles can be further functionalised with a hydrophilic polymer providing stealthness, aiming to both increase their blood circulation time and to promote cellular internalisation.

The cellular uptake and internalisation of antioxidants through the use of nanoparticles could also be assessed resorting to additional techniques such as fluorescence microscopy or flow cytometry.

Evaluate the mucoadhesion, permeability, absorption and stability of nanoparticles on the ocular surface by *in vitro* cell cultures using the HCE-T, ARPE and conjunctival cell line (IOBA-NHC), through confocal laser scanning microscopy (CLSM) and flux cytometry, and to measure time of action and bioavailability of antioxidant-containing chitosan nanoparticles (162, 165).

To study the actual effects of the antioxidant power in the elimination of free radicals and decreased vascularity in the retina, as well as, to evaluate the toxicity, bioavailability and effectiveness, by using the immortalized human ARPE-19 cells, with subsequent study of the monolayers (162, 166, 167).

Measure the therapeutic effects of antioxidant-containing chitosan nanoparticles after topical administration *in vivo* by monitoring retina morphology and biological parameters both before and during appearance of the symptomatology, in distinguish animal model.



## References

1. Prabakaran M, Mano JF. Chitosan-Based Particles as Controlled Drug Delivery Systems. *Drug Delivery* 2005;12:41-57.
2. Campos A, Diebold Y, Carvalho E, Sánchez A, Alonso MJ. Chitosan Nanoparticles as New Ocular Drug Delivery Systems: *In Vitro* Stability, *in Vivo* Fate, and Cellular Toxicity. *Pharmaceutical Research* 2004;21:803-10.
3. Sosnik A, das Neves J, Sarmento B. Mucoadhesive Polymers in the Design of Nano-Drug Delivery Systems for Administration by Non-Parenteral Routes: A Review. *Progress in Polymer Science* 2014;In press.
4. George M, Abraham E. Polyionic Hydrocolloids for the Intestinal Delivery of Protein Drugs: Alginate and Chitosan - a Review. *Journal of Controlled Release* 2006;114:1-14.
5. Rahman K. Studies on Free Radicals, Antioxidants, and Co-Factors. *Journal of Clinical Interventions in Aging* 2007;2:219–36.
6. Pietta P-G. Flavonoids as Antioxidants. *Journal of Natural Products* 2000;63:1035-42.
7. Petersen M, Simmonds MSJ. Molecules of Interest: Rosmarinic Acid. *Phytochemistry* 2003;62:121-5.
8. Swarup V, Ghosh J, Ghosh S, Saxena A, Basu A. Antiviral and Anti-Inflammatory Effects of Rosmarinic Acid in an Experimental Murine Model of Japanese Encephalitis. *Antimicrobial Agents and Chemotherapy* 2007;51:3367–70.
9. Shahidi F, Yanita PK, Nanosudra PD. Phenolic Antioxidants. *Critical Reviews in Food Science and Nutrition* 1992;32:67-103.
10. Lu Y, Foo LY. Polyphenolics of *Salvia*-a Review. *Phytochemistry* 2002;75:197–202.
11. Perry NSL, Houghton PJ, Sampson J, Theobald AE, Hart S, Lis-Balchin M. *In Vitro* Activity of *Salvia Lavandulaefolia* (Spanish Sage) Relevant to Treatment of Alzheimer's Disease. *Journal of Pharmacy and Pharmacology* 2001;53:1347–56.
12. Tepe B. Antioxidant Potentials and Rosmarinic Acid Levels of the Methanolic Extracts of *Salvia Virgata* (Jacq), *Salvia Staminea* (Montbret & Aucher Ex Benth) and *Salvia Verbenaca* (L.) from Turkey. *Bioresource Technology* 2008;99:1584–8.
13. Petersena M, Simmonds MSJ. Rosmarinic Acid. *Phytochemistry* 2003;62 121–5.
14. Gião MS, Pereira CI, Fonseca SC, Pintado ME, Malcata FX. Effect of Particle Size Upon the Extent of Extraction of Antioxidant Power from the Plants Agrimonia Eupatoria, *Salvia* Sp. And Satureja Montana. *Food Chemistry* 2009;117:412-6

15. Kowluru RA, Chan P-S. Oxidative Stress and Diabetic Retinopathy. *Experimental Diabetes Research* 2007;2007:1-12.
16. Frank RN. Potential New Medical Therapies for Diabetic Retinopathy: Protein Kinase C Inhibitors. *American Journal of Ophthalmology* 2002;133:693-8.
17. Kalishwaralal K, BarathManiKanth S, Ram S, Pandian K, Deepak V, Gurunathan S. Silver Nano—a Trove for Retinal Therapies. *Journal of Controlled Release* 2010;145:2.
18. Ratnam DV, Ankola DD, Bhardwaj V, Sahana DK, Ravi Kumar MNV. Role of Antioxidants in Prophylaxis and Therapy: A Pharmaceutical Perspective. *Journal of Controlled Release* 2006;113:189–207.
19. You X, Peng Q, Yuan Y, Cheung Y, Lei J. Segmentation of Retinal Blood Vessels Using the Radial Projection and Semi-Supervised Approach. *Pattern Recognition* 2011;44:2314–24.
20. Aruoma OI, Neergheen VS, Bahorun T, Jen L-S. Free Radicals, Antioxidants and Diabetes: Embryopathy, Retinopathy, Neuropathy, Nephropathy and Cardiovascular Complications. *Neuroembryology and Aging* 2007;4:117–37.
21. Chu J, Ali Y. Diabetic Retinopathy: A Review. *Drug Development Research* 2008;69:1–14
22. Glenn JV, Stitt AW. The Role of Advanced Glycation End Products in Retinal Ageing and Disease. *Biochimica et Biophysica Acta* 2009;1790:1109–16.
23. Wiwanitkit V. Endothelin-1 and Protein Kinase C Co-Expression in the Pathogenesis of Diabetic Retinopathy. *Journal of Diabetes and Its Complications* 2007;21:359– 62.
24. Terrasa AM, Guajardo MH, Marra CA, Zapata G. Alpha-Tocopherol Protects against Oxidative Damage to Lipids of the Rod Outer Segments of the Equine Retina. *The Veterinary Journal* 2009;182:463-8.
25. Kowluru RA, Koppolu P. Diabetes-Induced Activation of Caspase-3 in Retina: Effect of Antioxidant Therapy. *Free Radical Research* 2002;36:993–9.
26. Kowluru RA. Diabetic Retinopathy: Mitochondrial Dysfunction and Retinal Capillary Cell Death. *Antioxidants and Redox Signaling* 2005;7:1581-7.
27. da Silva SB, Costa JP, Pintado ME, Ferreira DC, Sarmento B. Antioxidants in the Prevention and Treatment of Diabetic Retinopathy – a Review. *Journal of Diabetes and Metabolism* 2010;1:2-10.
28. Tavaría FK, Fernandes JC, Santos-Silva A, Baptista da Silva S, Sarmento B, Pintado MM. Biological Activities of Chitin, Chitosan and Respective Oligomers. In: O'Neill ANFaAG, editor. *Focus on Chitosan Research*: Nova Publishers; 2011.

29. Prow TW, Bhutto I, Grebe R, Uno K, Merges C, Mcleod DS, et al. Nanoparticle-Delivered Biosensor for Reactive Oxygen Species in Diabetes. *Vision Research* 2008;48:478-85.
30. Rinaudo M. Chitin and Chitosan: Properties and Applications. *Progress in Polymer Science* 2006;31:603-32.
31. Vásconez MB, Flores SK, Campos CA, Alvarado J, Gerschenson LN. Antimicrobial Activity and Physical Properties of Chitosan–Tapiocastarch Based Edible Films and Coatings. *Food Research International* 2009;42:762-9.
32. Paulino AT, Simionato JI, Garcia JC, Nozaki J. Characterization of Chitosan and Chitin Produced from Silkworm Crysalides. *Carbohydrate Polymers* 2006;64:98-103.
33. Wu T, Zivanovic S, Draughon A, Sams CE. Chitin and Chitosansvalue-Added Products from Mushroom Waste. *Journal of Agriculture and Food Chemistry* 2004;52:7905-10.
34. Sinha VR, Singla AK, Wadhawan S, Kaushik R, Kumria R, Bansal K, et al. Chitosan Microspheres as a Potential Carrier for Drugs. *International Journal of Pharmaceutics* 2004;274:1-33.
35. Shih C-M, Shieh Y-T, Twu Y-K. Preparation and Characterization of Cellulose/Chitosan Blend Films. *Carbohydrate Polymers* 2009;78:169-74.
36. Alonso MJ, Sánchez A. The Potential of Chitosan in Ocular Drug Delivery. *Journal of Pharmacy and Pharmacology* 2003;55:1451-63.
37. Nunthanid J, Laungtana-anan M, Sriamornsak P, Limmatvapirat S, Puttipipatkachorn S, Lim LY, et al. Characterization of Chitosan Acetate as a Binder for Sustained Release Tablets. *Journal of Controlled Release* 2004;99:15-26.
38. Dyer AM, Hinchcliffe M, Watts P, Castile J, Jabbal-Gill I, Nankervis R, et al. Nasal Delivery of Insulin Using Novel Chitosan Based Formulations: A Comparative Study in Two Animal Models between Simple Chitosan Formulations and Chitosan Nanoparticles. *Pharmaceutical Research* 2002;19:998-1008.
39. Ishihara M, Fujita M, Kishimoto S, Hattori H, Kanatani Y. Biological, Chemical, and Physical Compatibility of Chitosan and Biopharmaceuticals. In: Sarmiento B, Neves Jd, editors. *Chitosan-Based Systems for Biopharmaceuticals: Delivery, Targeting and Polymer Therapeutics*: Elsevier; 2012. p. 93-106.
40. Andrade F, Antunes F, Nascimento AV, Silva SBd, Neves Jd, Ferreira D, et al. Chitosan Formulations as Carriers for Therapeutic Proteins. *Current Drug Discovery Technologies* 2011;8:157-72.

41. Shi Y, Huang G. Recent Developments of Biodegradable and Biocompatible Materials Based Micro/Nanoparticles for Delivering Macromolecular Therapeutics. *Critical Reviews in Therapeutic Drug Carrier Systems* 2009;26:29–84.
42. Aranaz I, Mengibar M, Harris R, Paños I, Miralles B, Acosta N, et al. Functional Characterization of Chitin and Chitosan. *Current Chemical Biology* 2009;3:203-30.
43. Sousa F, Guebitz GM, Kokol V. Antimicrobial and Antioxidant Properties of Chitosan Enzymatically Functionalized with Flavonoids. *Process Biochemistry* 2009;44:749-56.
44. Garcia MA, Pinotti A, Martino M, Zaritzky N. Electrically Treated Composite Films Based on Chitosan and Methylcellulose Blends. *Food Hydrocolloids* 2009;23 722-8.
45. Sashiwa H, Aiba S-i. Chemically Modified Chitin and Chitosan as Biomaterials. *Progress in Polymer Science* 2004;29:887-908.
46. Fernandez-Saiz P, Lagaron JM, Ocio MJ. Optimization of the Film-Forming and Storage Conditions of Chitosan as an Antimicrobial Agent. *Journal of Agriculture and Food Chemistry* 2009;57:3298–307.
47. Zhao QS, Ji QX, Xing K, Li XY, Liu CS, Chen XG. Preparation and Characteristics of Novel Porous Hydrogel Films Based on Chitosan and Glycerophosphate. *Carbohydrate Polymers* 2009;76:410-6.
48. Kumar MNVR. A Review of Chitin and Chitosan Applications. *Reactive & Functional Polymers* 2000;46:1-27.
49. Muzzarelli RAA. Genipin-Crosslinked Chitosan Hydrogels as Biomedical and Pharmaceutical Aids. *Carbohydrate Polymers* 2009;77:1-9.
50. Motwani SK, Chopra S, Talegaonkar S, Kohli K, Ahmad FJ, Khar RK. Chitosan–Sodium Alginate Nanoparticles as Submicroscopic Reservoirs for Ocular Delivery: Formulation, Optimisation and *in Vitro* Characterisation. *European Journal of Pharmaceutics and Biopharmaceutics* 2008;68:513–25.
51. Qun G, Ajun W. Effects of Molecular Weight, Degree of Acetylation and Ionic Strength on Surface Tension of Chitosan in Dilute Solution. *Carbohydrate Polymers* 2006;64:29-36.
52. Cano-Cebrián MJ, Zornoza T, Granero L, Polache A. Intestinal Absorption Enhancement Via the Paracellular Route by Fatty Acids, Chitosans and Others: A Target for Drug Delivery. *Current Drug Delivery* 2005;2:9-22.
53. Smith J, Wood E, Dornish M. Effect of Chitosan on Epithelial Cell Tight Junctions *Pharmaceutical Research* 2004;21:43-9.

54. Yu S, Zhao Y, Wu F, Zhang X, Lü W, Zhang H, et al. Nasal Insulin Delivery in the Chitosan Solution: *In Vitro* and *in Vivo* Studies. *International Journal of Pharmaceutics* 2004;281:11–23.
55. Zaharoff DA, Rogers CJ, Hance KW, Schlom J, Greiner JW. Chitosan Solution Enhances the Immunoadjuvant Properties of Gm-Csf. *Vaccine* 2007;25:8673-86.
56. Rodrigues LB, Leite HF, Yoshida MI, Saliba JB, Junior ASC, Faraco AAG. *In Vitro* Release and Characterization of Chitosan Films as Dexamethasone Carrier. *International Journal of Pharmaceutics* 2009;368:1-6.
57. Vargas M, Albors A, Chiralt A, Gonzalez-Martinez C. Characterization of Chitosan–Oleic Acid Composite Films. *Food Hydrocolloids* 2009;23:536-47.
58. Ferreira CO, Nunes CA, Delgadillo I, Lopes-da-Silva JA. Characterization of Chitosan–Whey Protein Films at Acid Ph. *Food Research International* 2009;42:807-13.
59. Shu XZ, Zhu KJ, Song W. Novel Ph-Sensitive Citrate Cross-Linked Chitosan Film for Drug Controlled Release. *International Journal of Pharmaceutics* 2001;212:19-28.
60. Noel SP, Courtney H, Bumgardner JD, Haggard WO. A Potential Local Drug Delivery System for Antibiotics. *Clinical Orthopaedics and Related Research* 2008;466:1377-82.
61. Silva CL, Pereira JC, Ramalho A, Pais AA, Sousa JJ. Films Based on Chitosan Polyelectrolyte Complexes for Skin Drug Delivery: Development and Characterization. *Journal of Membrane Science* 2008;320:268-79.
62. Abdul S, Poddar SS. A Flexible Technology for Modified Release of Drugs: Multi Layered Tablets. *Journal of Controlled Release* 2004;97:393- 405.
63. Schmid W, Picker-Freyer KM. Tableting and Tablet Properties of Alginates: Characterisation and Potential for Soft Tableting. *European Journal of Pharmaceutics and Biopharmaceutics* 2009;72:165-72.
64. Rege PR, Shukla DJ, Block LH. Chitinosans as Tableting Excipients for Modified Release Delivery Systems. *International Journal of Pharmaceutics* 1999;181 49-60.
65. Rege PR, Garmise RJ, Block LH. Spray-Dried Chitinosans Part Ii: *In Vitro* Drug Release from Tablets Made from Spray-Dried Chitinosans. *International Journal of Pharmaceutics* 2003;252:53-9.
66. Alsarra IA, El-Bagory I, Bayoni MA. Chitosan and Sodium Sulfate as Excipients in the Preparation of Prolonged Release Theophylline Tablets. *Drug development and industrial pharmacy* 2005;1:385-95.
67. Sinha VR, Kumria R. Binders for Colon Specific Drug Delivery: An *in Vitro* Evaluation. *International Journal of Pharmaceutics* 2002;249:23-31.

68. Roldo M, Hornof M, Caliceti P, Bernkop-Schnurch A. Mucoadhesive Thiolated Chitosan as Platforms for Oral Controlled Drug Delivery: Synthesis and *in Vitro* Evaluation. *European Journal of Pharmaceutics and Biopharmaceutics* 2004;57:115-21.
69. Mura P, Zerrouk N, Mennini N, Maestrelli F, Chemtob C. Development and Characterization of Naproxen-Chitosan Solid System with Improved Drug Dissolution Properties. *European Journal of Pharmaceutical Sciences* 2003;19:67-75.
70. Tapia C, Costa E, Terraza C, Munita AM, Azdani-Pedram M. Study of the Prolonged Release of Theophylline from Polymeric Matrices Based on Grafted Chitosan with Acrylamide. *Pharmazie* 2002;57:744-9.
71. Bernkop-Schnurch A, Schuhbauer H, Clausen AE, Hanel R. Development of a Sustained Release Dosage Form for Alpha-Lip Acid. I. Design and *in Vitro* Evaluation. *Drug Development and Industrial Pharmacy* 2004;30:27-34.
72. Tomida H, Yasufuku T, Fujii T, Kondo Y, Kai T, Anraku M. Polysaccharides as Potential Antioxidative Compounds for Extended-Release Matrix Tablets. *Carbohydrate Research* 2010;345 82-6.
73. Perioli L, Ambrogia V, Pagano C, Scuto S, Rossi C. Fg90 Chitosan as a New Polymer for Metronidazole Mucoadhesive Tablets for Vaginal Administration. *International Journal of Pharmaceutics* 2009;377:120-7.
74. Opdahl A, Kim SH, Koffas TS, Marmo C, Somorjai GA. Surface Mechanical Properties of Phema Contact Lenses: Viscoelastic and Adhesive Property Changes on Exposure to Controlled Humidity *Journal of Biomedical Materials Research Part A* 2003;67A:350-6.
75. Nowak AP, Breedveld V, Pakstis L, Ozbas B, Pine DJ, Pochan Dea. Rapidly Recovering Hydrogel Scaffolds from Selfassembling Diblock Copolyptide Amphiphiles. *Nature* 2002;417:424-8.
76. Qiu Y, Park K. Environment-Sensitive Hydrogels for Drug Delivery. *Advanced Drug Delivery Reviews* 2001;53:321-39.
77. Sen M, Avci EN. Radiation Synthesis of Poly(N-Vinyl-2-Pyrrolidone)- Kappa-Carrageenan Hydrogels and Their Use in Wound Dressing Applications. I. Preliminary Laboratory Tests. *Biomedical Materials Research Part A* 2005;74A:187-96.
78. Yang X, Liu Q, Chen X, Yu F, Zhu Z. Investigation of Pva/Ws-Chitosan Hydrogels Prepared by Combined C-Irradiation and Freeze-Thawing. *Carbohydrate Polymers* 2008;73:401-8.



79. Liu X, Xu W, Liu Q, Yu W, Fu Y, Xiong X, et al. Swelling Behaviour of Alginate-Chitosan Microcapsules Prepared by External Gelation or Internal Gelation Technology. *Carbohydrate Polymers* 2004;56:459-64.
80. Abreu FOMS, Bianchini C, Forte MMC, Kist TBL. Influence of the Composition and Preparation Method on the Morphology and Swelling Behavior of Alginate–Chitosan Hydrogels. *Carbohydrate Polymers* 2008;74:283-9.
81. Ta HT, Dass CR, Dunstan DE. Injectable Chitosan Hydrogels for Localised Cancer Therapy. *Journal of Controlled Release* 2008;126:205-16.
82. Kandile NG, Mohamed MI, Zaky HT, Nasr AS, Abdel-Bary EM. Synthesis and Properties of Chitosan Hydrogels Modified with Heterocycles. *Carbohydrate Polymers* 2009;75:580-5.
83. Gratieri T, Gelfuso GM, Rocha EM, Sarmiento VH, Freitas Od, Lopez RFV. A Poloxamer/Chitosan in Situ Forming Gel with Prolonged Retention Time for Ocular Delivery. *European Journal of Pharmaceutics and Biopharmaceutics* 2010;75:186-93.
84. Senel S, Ikinici G, Kas S, Yousefi-Rad A, Sargon MF, Hincal AA. Chitosan Films and Hydrogels of Chlorhexidine Gluconate for Oral Mucosal Delivery. *International Journal of Pharmaceutics* 2000;193 197-203.
85. Wu ZM, Zhangb XG, Zhengb C, Li CX, Zhanga SM, Donga RN, et al. Disulfide-Crosslinked Chitosan Hydrogel for Cell Viability and Controlled Protein Release. *European Journal of Pharmaceutical Sciences* 2009;37:198-206.
86. Varshosaz J, Sadrai H, Heidari A. Nasal Delivery of Insulin Using Bioadhesive Chitosan Gel. *Drug Delivery* 2006;13:31-8.
87. Bonferoni MC, Giunchedi P, Scalia S, Rossi S, Sandri G, Caramella C. Chitosan Gels for the Vaginal Delivery of Lactic Acid: Relevance of Formulation Parameters to Mucoadhesion and Release Mechanisms. *AAPS PharmSciTech* 2006;7:104.
88. Ta HT, Dass CR, Larson I, Choong PFM, Dunstan DE. A Chitosan Hydrogel Delivery System for Osteosarcoma Gene Therapy with Pigment Epithelium-Derived Factor Combined with Chemotherapy. *Biomaterials* 2009;30:4815-23.
89. Crcarevska MS, Dodov MG, Goracinova K. Chitosan Coated Ca–Alginate Microparticles Loaded with Budesonide for Delivery to the Inflamed Colonic Mucosa. *European Journal of Pharmaceutics and Biopharmaceutics* 2008;68:565-78.
90. Krauland AH, Guggi D, Bernkop-Schnürch A. Thiolated Chitosan Microparticles: A Vehicle for Nasal Peptide Drug Delivery. *International Journal of Pharmaceutics* 2006;307:270-7.

91. Coppi G, Iannuccelli V. Alginate/Chitosan Microparticles for Tamoxifen Delivery to the Lymphatic System. *International Journal of Pharmaceutics* 2009;367:127-32.
92. Uyguna DA, Uyguna M, Karagözlere A, Öztürka N, Akgöla S, Denizli A. A Novel Support for Antibody Purification: Fatty Acid Attached Chitosan Beads. *Colloids and Surfaces B: Biointerfaces* 2009;70:266-70.
93. Baudner BC, Verhoef JC, Giuliani MM, Peppoloni S, Rappuoli R, Giudice GD, et al. Protective Immune Responses to Meningococcal C Conjugate Vaccine after Intranasal Immunization of Mice with the Ltk63 Mutant Plus Chitosan or Trimethyl Chitosan Chloride as Novel Delivery Platform. *Journal of Drug Targeting* 2005;13:489-98.
94. Lubben IMVd, Kersten G, Fretz MM, Beuvery C, Verhoef C, Junginger HE. Chitosan Microparticles for Mucosal Vaccination against Diphtheria: Oral and Nasal Efficacy Studies in Mice. *Vaccine* 2003;21:1400-8.
95. Van Der Lubben IM, Verhoef JC, Borchard G, Junginger HE. Chitosan for Mucosal Vaccination. *Advanced Drug Delivery Reviews* 2001;52:139-44.
96. Wu Y, Yang W, Wang C, Hu J, Fu S. Chitosan Nanoparticles as a Novel Delivery System for Ammonium Glycyrrhizinate. *International Journal of Pharmaceutics* 2005;295:235-45.
97. Wang Q, Zhang L, Hu W, Hu Z-H, Bei Y-Y, Xu J-Y, et al. Norcantharidin-Associated Galactosylated Chitosan Nanoparticles for Hepatocyte-Targeted Delivery. *Nanomedicine: Nanotechnology, Biology, and Medicine* 2010;6:371-81.
98. Amidi M, Romeijn SG, Borchard G, Junginger HE, Hennink WE, Jiskoot W. Preparation and Characterization of Protein-Loaded N-Trimethyl Chitosan Nanoparticles as Nasal Delivery System. *Journal of Controlled Release* 2006;111:107-16.
99. Amidi M, Romeijn SG, Verhoef JC, Junginger HE, Bungener L, Huckriede A, et al. N-Trimethyl Chitosan (Tmc) Nanoparticles Loaded with Influenza Subunit Antigen for Intranasal Vaccination: Biological Properties and Immunogenicity in a Mouse Model. *Vaccine* 2007;25:144-53.
100. Sayin B, Somavarapu S, Li XW, Thanou M, Sesardic D, Alpar HO, et al. Mono-N-Carboxymethyl Chitosan (Mcc) and N-Trimethyl Chitosan (Tmc) Nanoparticles for Non-Invasive Vaccine Delivery. *International Journal of Pharmaceutics* 2008;363:139-48.
101. Prow TW, Bhutto I, Kim SY, Grebe R, Merges C, McLeod DS, et al. Ocular Nanoparticle Toxicity and Transfection of the Retina and Retinal Pigment Epithelium. *Nanomedicine: Nanotechnology, Biology, and Medicine* 2008;4:340-9.

102. Borges O, Silva M, Sousa Ad, Borchard G, Junginger HE, Cordeiro-da-Silva A. Alginate Coated Chitosan Nanoparticles Are an Effective Subcutaneous Adjuvant for Hepatitis B Surface Antigen. *International Immunopharmacology* 2008;8:1773-80.
103. Amidi M, Romeijn SG, Verhoef C, Junginger HE, Bungener L, Huckriede A, et al. N-Trimethyl Chitosan (Tmc) Nanoparticles Loaded with Influenza Subunit Antigen for Intranasal Vaccination: Biological Properties and Immunogenicity in a Mouse Model. *Vaccine* 2007;25:144-53.
104. Bivas-Benita M, Meijgaarden KEV, Franken KLMC, Junginger HE, Borchard G, Ottenhoff THM, et al. Pulmonary Delivery of Chitosan-DNA Nanoparticles Enhances the Immunogenicity of a DNA Vaccine Encoding Hla-a\*0201-Restricted T-Cell Epitopes of Mycobacterium Tuberculosis. *Vaccine* 2004;22:1609-15.
105. Bayat A, Larijani B, Ahmadian S, Junginger HE, Rafiee-Tehrani M. Preparation and Characterization of Insulin Nanoparticles Using Chitosan and Its Quaternized Derivatives. *Nanomedicine: Nanotechnology, Biology, and Medicine* 2008;4:115-20.
106. Sarmento B, Martins S, Ribeiro A, Veiga F, Neufeld R, Ferreira D. Development and Comparison of Different Nanoparticulate Polyelectrolyte Complexes as Insulin Carriers. *International Journal of Peptide Research and Therapeutics* 2006;12(2).
107. Sarmento B, Ribeiro A, Veiga F, Sampaio P, Neufeld R, Ferreira D. Alginate/Chitosan Nanoparticles Are Effective for Oral Insulin Delivery. *Pharmaceutical Research* 2007;24(12).
108. Sarmento B, Ribeiro A, Veiga F, Ferreira D, Neufeld R. Oral Bioavailability of Insulin Contained in Polysaccharide Nanoparticles. *Biomacromolecules* 2007 Oct;8:3054-60.
109. Trials C. Clinical Trials: A Service of the U.S. National Institutes of Health. [cited 2010 21 of January]; <http://clinicaltrials.gov/ct2/results?term=chitosan>].
110. Scott NW, McPherson GC, Ramsay CR, Campbell MK. The Method of Minimization for Allocation to Clinical Trials: A Review. *Controlled Clinical Trials* 2002;23:662-74.
111. Trials C. Safety and Tolerability of Chitosan-N-Acetylcysteine Eye Drops in Healthy Young Volunteers. [cited 2010 21 of January]; <http://clinicaltrials.gov/ct2/show/NCT01015209?term=chitosan&rank=4>].
112. Al-Guborya KH, Fowler PA, Garrelc C. The Roles of Cellular Reactive Oxygen Species, Oxidative Stress and Antioxidants in Pregnancy Outcomes. *The International Journal of Biochemistry & Cell Biology* 2010;42:1634–50.

113. Al-Jaber NA, Awaad AS, Moses JE. Review on Some Antioxidant Plants Growing in Arab World. *Journal of Saudi Chemical Society* 2011;15:293–307.
114. Sergent T, Piront N, Meurice J, Toussaint O, Schneider Y-J. Anti-Inflammatory Effects of Dietary Phenolic Compounds in an *in Vitro* Model of Inflamed Human Intestinal Epithelium. *Chemico-Biological Interactions* 2010;188:659–67.
115. Gião MS, Gonzalez-Sanjose ML, Rivero-Perez MD, Pereira CI, Pintado ME, Malcata FX. Infusions of Portuguese Medicinal Plants: Dependence of Final Antioxidant Capacity and Phenol Content on Extraction Features. *Journal of the Science of Food and Agriculture* 2007;87:2638-47.
116. Liu JR, Chen GF, Shih HN, Kuo PC. Enhanced Antioxidant Bioactivity of *Salvia Miltiorrhiza* (Danshen) Products Prepared Using Nanotechnology. *Phytomedicine* 2008;15:23-30.
117. Azzi A, Davies KJA, Kelly F. Free Radical Biology—Terminology and Critical Thinking. *Federation of European Biochemical Societies Letters* 2004;558:3–6.
118. Silva SBd, Costa JP, Pintado ME, Ferreira DdC, Sarmento B. Antioxidants in the Prevention and Treatment of Diabetic Retinopathy – a Review. *Journal of Diabetes & Metabolism* 2010;1(111).
119. Yoshihara D, Fujiwara N, Suzuki K. Antioxidants: Benefits and Risks for Long-Term Health. *Maturitas* 2010;67:103–7.
120. Matteucci E, Giampietro O. Oxidative Stress in Families of Type 1 Diabetic Patients. *Diabetes Care* 2000;23:1182-6.
121. Liu RH. Potential Synergy of Phytochemicals in Cancer Prevention: Mechanism of Action. *Journal of Nutrition* 2004;134:3479S–85S.
122. Scalbert A, Johnson IT, Saltmarsh M. Polyphenols: Antioxidants and Beyond. *American Journal of Clinical Nutrition* 2005;81:215S–7S.
123. Herrera E, Barbas C. Vitamin E: Action, Metabolism and Perspectives. *Journal of Physiology and Biochemistry* 2001;57:43–56.
124. Mohamed MSA, Fatma MA, Mona MA, Amira GM, Elsayed AA. Anticancer and Antioxidant Tannins from *Pimenta Dioica* Leaves. *Zeitschrift für Naturforschung* 2006;62:526–36.
125. Fadel O, Kirat KE, Morandat S. The Natural Antioxidant Rosmarinic Acid Spontaneously Penetrates Membranes to Inhibit Lipid Peroxidation *in Situ*. *Biochimica et Biophysica Acta* 2011;1808:2973-80.

126. Fujimoto A, Masuda T. Antioxidation Mechanism of Rosmarinic Acid, Identification of an Unstable Quinone Derivative by the Addition of Odourless Thiol. *Food Chemistry* 2012;132:901-6.
127. Huang H, Hauk C, Yum M-Y, Rizshsky L, Widrechner MP, McCoy J-A, et al. Rosmarinic Acid in *Prunella Vulgaris* Ethanol Extract Inhibits Lipopolysaccharide-Induced Prostaglandin E2 and Nitric Oxide in Raw 267.7 Mouse Macrophages. *Journal of Agricultural and Food Chemistry* 2009;57:10579-89.
128. Furtado MA, de Almeida LC, Furtado RA, Cunha WR, Tavares DC. Antimutagenicity of Rosmarinic Acid in Swiss Mice Evaluated by the Micronucleus Assay. *Mutation Research* 2008;657:150-4.
129. Lee J, Jung E, Kog J, Kim YS, Park D. Effect of Rosmarinic Acid on Atopic Dermatitis. *Journal of Dermatology* 2008;35:768-71.
130. Hamaguchi T, Ono K, Murase A, Yamada M. Phenolic Compounds Prevent Alzheimer's Pathology through Different Effects on the Amyloid-Beta Aggregation Pathway. *American Journal of Pathology* 2009;175:2557-65.
131. Xavier CP, Lima CF, Fernandes-Ferreira M, Pereira-Wilson C. *Salvia Fruticosa*, *Salvia Officinalis*, and Rosmarinic Acid Induce Apoptosis and Inhibit Proliferation of Human Colorectal Cell Lines: The Role in Maok/Erk Pathway. *Nutrition and Cancer* 2009;61:564-71.
132. Gunda S, Hariharan S, Mandava N, Mitra AK. Barriers in Ocular Drug Delivery. In: Barnstable JT-TaCJ, editor. *Ophthalmology Research: Ocular Transporters in Ophthalmic Diseases and Drug Delivery*: Human Press; 2008. p. 399-413.
133. Duvvuri S, Majumdar S, Mitra AK. Role of Metabolism in Ocular Drug Delivery. *Current Drug Metabolism* 2004;5:507-15.
134. Barar J, Javadzadeh AR, Omid Y. Ocular Novel Drug Delivery: Impacts of Membranes and Barriers. *Expert Opinion on Drug Delivery* 2008;5:567-81.
135. Urtti A. Challenges and Obstacles of Ocular Pharmacokinetics and Drug Delivery. *Advanced Drug Delivery Reviews* 2006;58:1131-5.
136. Jakus V. The Role of Free Radicals, Oxidative Stress and Antioxidant Systems in Diabetic Vascular Disease. *Bratisl Lek Listy* 2000;101:541-51.
137. Kowluru RA, Tang J, Kern TS. Abnormalities of Retinal Metabolism in Diabetes and Experimental Galactosemia. VII. Effect of Long-Term Administration of Antioxidants on the Development of Retinopathy. *Diabetes* 2001;50:1938-42.
138. Kowluru RA, Kanwar M. Effects of Curcumin on Retinal Oxidative Stress and Inflammation in Diabetes. *Nutrition and Metabolism* 2007;4:1-8.

139. Bursell S, Clermont A, Aiello L, Aiello L, Schlossman D, Feener E, et al. High-Dose Vitamin E Supplementation Normalizes Retinal Blood Flow and Creatinine Clearance in Patients with Type 1 Diabetes. *Diabetes Care* 1999;22:1245–51.
140. Ellis EA, Guberski DL, Somogyi-Mann M, Grant MB. Increased H<sub>2</sub>O<sub>2</sub>, Vascular Endothelial Growth Factor and Receptors in the Retina of the Bbz/Wor Diabetic Rat. *Free Radical Biology and Medicine* 2000;28:91–101.
141. Kern TS, Tang J, Mizutani M, Kowluru RA, Nagaraj RH, Romeo G, et al. Response of Capillary Cell Death to Aminoguanidine Predicts the Development of Retinopathy: Comparison of Diabetes and Galactosemia. *Investigative Ophthalmology and Visual Science* 2000;41:3972–8.
142. Gan Q, Wang T. Chitosan Nanoparticle as Protein Delivery Carrier—Systematic Examination of Fabrication Conditions for Efficient Loading and Release. *Colloids and Surfaces B: Biointerfaces* 2007;59:24–34.
143. Jo DH, Kim JH, Yu YS, Lee TG, Kim JH. Antiangiogenic Effect of Silicate Nanoparticle on Retinal Neovascularization Induced by Vascular Endothelial Growth Factor. *Nanomedicine: Nanotechnology, Biology, and Medicine* 2012;8:784-91.
144. Kim JH, Kim MH, Jo DH, Yu YS, Lee TG, Kim JH. The Inhibition of Retinal Neovascularization by Gold Nanoparticles Via Suppression of Vegfr-2 Activation. *Biomaterials* 2011;32:1865-71.
145. Chew EY, Clemons T, SanGiovanni JP, Danis R, Domalpally A, McBee W, et al. The Age-Related Eye Disease Study 2 (Areds2) - Study Design and Baseline Characteristics (Areds2 Report Number 1). *Ophthalmology* 2012;119:2282-9.
146. Gao X, Meng X, Wang H, Wen B, Ding Y, Zhang S, et al. Antioxidant Behaviour of a Nanosilica-Immobilized Antioxidant in Polypropylene. *Polymer Degradation and Stability* 2008;93:1467–71.
147. Chorny M, Hood E, Levy RJ, Muzykantov VR. Endothelial Delivery of Antioxidant Enzymes Loaded into Non-Polymeric Magnetic Nanoparticles. *Journal of Controlled Release* 2010;146:144–51.
148. Amorim CdM, Couto AG, Netz DJA, Freitas RAd, Bresolin TMB. Antioxidant Idebenone-Loaded Nanoparticles Based on Chitosan and N-Carboxymethylchitosan. *Nanomedicine: Nanotechnology, Biology, and Medicine* 2010;6:745–52.
149. Harris R, Lecumberri E, Mateos-Aparicio I, Mengibar M, Heras A. Chitosan Nanoparticles and Microspheres for the Encapsulation of Natural Antioxidants Extracted from *Ilex Paraguariensis*. *Carbohydrate Polymers* 2011;84:803–6.

150. Kim S, Park H, Song Y, Hong D, Kim O, Jo E, et al. Reduction of Oxidative Stress by P-Hydroxybenzyl Alcohol-Containing Biodegradable Polyoxalate Nanoparticulate Antioxidant. *Biomaterials* 2011;32:3021-9.
151. Wu T, Yen F, Lin L, Tsai T, Lin C, Cham T. Preparation, Physicochemical Characterization, and Antioxidant Effects of Quercetin Nanoparticles. *International Journal of Pharmaceutics* 2008;346:160–8.
152. Kumari A, SudeshYadav, Pakade Y, Kumar V, Singh B, Chaudhary A, et al. Nanoencapsulation and Characterization of *Albizia Chinensis* Isolated Antioxidant Quercitrin on Pla Nanoparticles. *Colloids and Surfaces B: Biointerfaces* 2011;82:224-32.
153. Nie Z, Liu K, Zhong C, Wang L, Yang Y, Tian Q, et al. Enhanced Radical Scavenging Activity by Antioxidant-Functionalized Gold Nanoparticles: A Novel Inspiration for Development of New Artificial Antioxidants. *Free Radical Biology & Medicine* 2007;43:1243–54
154. Orosz KE, Gupta S, Hassink M, Abdel-Rahman M, Moldovan L, Davidorf FH, et al. Delivery of Antiangiogenic and Antioxidant Drugs of Ophthalmic Interest through a Nanoporous Inorganic Filter. *Molecular Vision* 2004;10:555–65.
155. Mitri K, Shegokar R, Gohla S, Anselmi C, Müller RH. Lutein Nanocrystals as Antioxidant Formulation for Oral and Dermal Delivery. *International Journal of Pharmaceutics* 2011;420:141-6.
156. Torchillin V. Recent Advances with Liposomes as Pharmaceutical Carriers. *Nature Reviews Drug Discovery* 2005;4:145–60.
157. Stone WL, Smith M. Therapeutic Uses of Antioxidant Liposomes. *Molecular Biotechnology* 2004;27:217–30.
158. Bhardwaj V, Hariharan S, Bala I, Lamprecht A, Kumar N, Panchagnula R, et al. Pharmaceutical Aspects of Polymeric Nanoparticles for Oral Delivery. *Journal of Biomedical Nanotechnology* 2005;1:235–58.
159. Alonso MJ. Nanomedicines for Overcoming Biological Barriers. *Biomedical Pharmacotherapy* 2004;58:168–72.
160. Sherris D. Ocular Drug Development - Future Directions. *Angiogenesis* 2007;10:71–6.
161. Penn JS, Madan A, Caldwell RB, Bartoli M, Caldwell RW, Hartnett ME. Vascular Endothelial Growth Factor in Eye Disease. *Progress in Retinal and Eye Research* 2008;27:331– 71.
162. Hornof M, Toropainen E, Urtti A. Cell Culture Models of the Ocular Barriers. *European Journal of Pharmaceutics and Biopharmaceutics* 2005;60:207-25.

163. Reichl S. Cell Culture Models of the Human Cornea - a Comparative Evaluation of Their Usefulness to Determine Ocular Drug Absorption *in-Vitro*. *Journal of Pharmacy and Pharmacology* 2008;60:299-307.
164. Diebold Y, Calonge M, Salamanca A, Callejo S, Corrales RM, Sáez V, et al. Characterization of a Spontaneously Immortalized Cell Line (Ioba-Nhc) from Normal Human Conjunctiva. *Investigative Ophthalmology & Visual Science* 2003;44:4263-74.
165. Barar J, Asadi M, Abdolreza S, Mortazavi-Tabatabaei, Omid Y. Ocular Drug Delivery; Impact of *in Vitro* Cell Culture Models. *Journal of Ophthalmologic Vision Research* 2009;4:238-52.
166. Aukunuru JV, Sunkara G, Ayalasomayajula SP, DeRuiter J, Clark RC, Kompella UB. A Biodegradable Injectable Implant Sustains Systemic and Ocular Delivery of an Aldose Reductase Inhibitor and Ameliorates Biochemical Changes in a Galactose-Fed Rat Model for Diabetic Complications. *Pharmaceutical Research* 2002;19:278-85.
167. Luthra S, Narayanan R, Marques LEA, Chwa M, KIM DW, Dong J, et al. Evaluation of *in Vitro* Effects of Bevacizumab (Avastin) on Retinal Pigment Epithelial, Neurosensory Retinal and Microvascular Endothelial Cells. *The Journal of Retinal and Vitreous Diseases* 2006;26.
168. Leithner K, Bernkop-Schnürch A. Chitosan and Derivatives for Biopharmaceutical Use: Mucoadhesive Properties In: Sarmiento B, Neves Jd, editors. *Chitosan-Based Systems for Biopharmaceuticals: Delivery, Targeting and Polymer*. John Wiley & Sons, Ltd; 2012. p. 159-80.
169. Johnson TV, Tomarev SI. Rodent Models of Glaucoma. *Brain Research Bulletin* 2010;81:349-58.
170. Li H, Zhao X, Ma Y, Zhai G, Li L, Lou H. Enhancement of Gastrointestinal Absorption of Quercetin by Solid Lipid Nanoparticles. *Journal of Controlled Release* 2009;133:238-44.
171. Jakubowicz-Gil J, Paduch R, Piersiak T, Głowniak K, Gawron A, Kandefer-Szerszeń M. The Effect of Quercetin on Pro-Apoptotic Activity of Cisplatin in Hela Cells. *Biochemical Pharmacology* 2005;69:1343-50.
172. Vijayababu MR, Kanagaraj P, Arunkumar A, Ilangovan R, Aruldas MM, Arunakaran J. Quercetin-Induced Growth Inhibition and Cell Death in Prostatic Carcinoma Cells (Pc-3) Are Associated with Increase in P21 and Hypophosphorylated Retinoblastoma Proteins Expression. *Journal of Cancer Research and Clinical Oncology* 2005;131:765-71.



173. Yang JH, Hsia TC, Kuo HM, Chao PD, Chou CC, Wei YH, et al. Inhibition of Lung Cancer Cell Growth by Quercetin Glucuronides Via G2/M Arrest and Induction of Apoptosis. *Drug Metabolism and Disposition* 2006;34:296–304.
174. ICH. *Validation of Analytical Procedures Text and Methodology Q2(R1)*. International Conference on Harmonisation of Technical Requirements for Registration of Pharmaceuticals for Human Use; Geneva, Switzerland. 2005.
175. Neves Jd, Sarmento B, Amiji MM, Bahia MF. Development and Validation of a Rapid Reversed-Phase Hplc Method for the Determination of the Non-Nucleoside Reverse Transcriptase Inhibitor Dapivirine from Polymeric Nanoparticles. *Journal of Pharmaceutical and Biomedical Analysis* 2010;52:167–72.
176. Liang Y-Z, Xie P, Chan K. Quality Control of Herbal Medicines. *Journal of Chromatography B* 2004;812:53–70.
177. Épshtein N. Validation of Hplc Techniques for Pharmaceutical Analysis. *Pharmaceutical Chemistry Journal* 2004;38.
178. Shabir GA, Lough JW, Arain SA, Bradshaw TK. Evaluation and Application of Best Practice in Analytical Method Validation. *Journal of Liquid Chromatography & Related Technologies* 2007;30:311-33.
179. Gião M, Pereira C, Fonseca S, Pintado M, Malcata X. Effect of Particle Size Upon the Extent of Extraction of Antioxidant Power from the Plants Agrimonia Eupatoria, *Salvia* Sp. And *Satureja Montana*. *Food Chemistry* 2009;117:412-6.
180. Djenane D, Yangüela J, Montañés L, Djerbal M, Roncalés P. Antimicrobial Activity of *Pistacia Lentiscus* and *Satureja Montana* Essential Oils against *Listeria Monocytogenes* Cect 935 Using Laboratory Media: Efficacy and Synergistic Potential in Minced Beef. *Food Control* 2011;22:1046-53.
181. Zavatti M, Zanolì P, Benelli A, Rivasi M, Baraldi C, Baraldi M. Experimental Study on *Satureja Montana* as a Treatment for Premature Ejaculation. *Journal of Ethnopharmacology* 2011;133:629-33.
182. Abada ANA, Nourib MHK, Tavakkolia F. Effect of *Salvia Officinalis* Hydroalcoholic Extract of Vincristine-Induced Neuropathy in Mice. *Chinese Journal of Natural Medicines* 2011;9:0354-8.
183. Cardilea V, Russob A, Formisanoc C, Riganoc D, Senatorec F, Arnold NA, et al. Essential Oils of *Salvia Bracteata* and *Salvia Rubifolia* from Lebanon: Chemical Composition, Antimicrobial Activity and Inhibitory Effect on Human Melanoma Cells. *Journal of Ethnopharmacology* 2009;126:265-72.

184. Zhoua Y, Lib W, Xua L, Chenc L. In *Salvia Miltiorrhiza*, Phenolic Acids Possess Protective Properties against Amyloid Beta-Induced Cytotoxicity, and Tanshinones Act as Acetylcholinesterase Inhibitors. *Environmental toxicology and pharmacology* 2011;31:443-52.
185. Skoula M, Abbes JE, Johnson CB. Genetic Variation of Volatiles and Rosmarinic Acid in Populations of *Salvia Fruticosa* Mill Growing in Crete. *Biochemical Systematics and Ecology* 2000;28:551-61.
186. Hou Y, Wang J, Jin W, Zhang H, Zhang Q. Degradation of *Laminaria Japonica Fucoïdan* by Hydrogen Peroxide and Antioxidant Activities of the Degradation Products of Different Molecular Weights. *Carbohydrate Polymers* 2012;87:153-9.
187. Silva SBd, Fernandes J, Tavira F, Pintado M, Sarmiento B. The Potential of Chitosan in Drug Delivery Systems. In: O'Neill ANFaAG, editor. *Focus on Chitosan Research*: Nova Publishers; 2011.
188. Calvo P, Remunan-Lopez C, Vila-Jato JL, Alonso MJ. Novel Hydrophilic Chitosan–Polyethylene Oxide Nanoparticles as Protein Carriers. *Journal of Applied Polymer Science* 1997;63:125-32.
189. Orthner MP, Lin G, Avula M, Buetefisch S, Magda J, Rieth LW, et al. Hydrogel Based Sensor Arrays (2 × 2) with Perforated Piezoresistive Diaphragms for Metabolic Monitoring (*in Vitro*). *Sensors and Actuators B: Chemical* 2010;145:807–16.
190. Silva SBd, Oliveira A, Ferreira D, Sarmiento B, Pintado M. Development and Validation Method for Simultaneous Quantification of Phenolic Compounds in Natural Extracts and Nanosystems. *Phytochemical Analysis* 2013;24:638-44.
191. Kumari A, Yadav S, Pakade Y, Singh B, Yadav S. Development of Biodegradable Nanoparticles for Delivery of Quercetin. *Colloids and Surfaces B: Biointerfaces* 2010;80:184-92.
192. Mohanraj VJ, Chen Y. Nanoparticles: A Review. *Tropical Journal of Pharmaceutical Research* 2006;5:561-73.
193. Harris R, Lecumberri E, Mateos-Aparicio I, Mengibar M, Heras A. Chitosan Nanoparticles and Microspheres for the Encapsulation of Natural Antioxidants Extracted from *Ilex Paraguariensis*. *Carbohydrate Polymers* 2011;84:803-6.
194. Liu Y, Sun Y, Li Y, Xu S, Tang J, Ding J, et al. Preparation and Characterization of Alpha-Galactosidase-Loaded Chitosan Nanoparticles for Use in Foods. *Carbohydrate Polymers* 2011;83:1162-8.

195. Chatrabhuti S, Chirachanchai S. Chitosan Core-Corona Nanospheres: A Convenient Material to Tailor Ph and Solvent Responsive Magnetic Nanoparticles. *Polymer* 2013;54:4318-24.
196. Silva SBd, Amorim M, Fonte P, Madureira R, Ferreira D, Pintado M, et al. Natural Extracts into Chitosan Nanocarriers for Rosmarinic Acid Drug Delivery. *Pharmaceutical Biology* 2014;In press.
197. Wu Y, Luo Y, Wang Q. Antioxidant and Antimicrobial Properties of Essential Oils Encapsulated in Zein Nanoparticles Prepared by Liquidliquid Dispersion Method. *LWT - Food Science and Technology* 2012;48:283-90.
198. Dudhania AR, Kosarajua SL. Bioadhesive Chitosan Nanoparticles: Preparation and Characterization. *Carbohydrate Polymers* 2010;81:243-51.
199. Peres I, Rocha S, Gomes J, Morais S, Pereira C, Coelho M. Preservation of Catechin Antioxidant Properties Loaded in Carbohydrate Nanoparticles. *Carbohydrate Polymers* 2011;86:147-53.
200. Deladino L, Anbinder PS, Navarro AS, Martino MN. Encapsulation of Natural Antioxidants Extracted from *Ilex Paraguariensis*. *Carbohydrate Polymers* 2008;71:126-34.
201. Amorim C, Couto A, Netz D, Freitas R, Bresolin T. Antioxidant Idebenone-Loaded Nanoparticles Based on Chitosan and N-Carboxymethylchitosan. *Nanomedicine: Nanotechnology, Biology, and Medicine* 2010;6:745-52.
202. Foster B, Lee B. Tear Film Anatomy, Structure and Function. In: Holland E, Mannis M, Lee B, editors. *Ocular Surface Disease, Cornea, Conjunctiva and Tear Film*: Elsevier; 2013. p. 17-21.
203. Guinesi L, Cavalheiro E. The Use of Dsc Curves to Determine the Acetylation Degree of Chitin/Chitosan Samples. *Thermochimica Acta* 2006;444:128-33.
204. Vikas R, Kumar B, Dinesh G, Rakesh G, Ashok T. Optimization of Chitosan Films as a Substitute of Animal and Human Epidermal Sheets for in Vitro Permeation of Polar and Non Polar Drugs. *Acta Pharmaceutica* 2004;54:287-99.
205. Sarmiento B, Ferreira D, Veiga F, Ribeiro A. Characterization of Insulin-Loaded Alginate Nanoparticles Produced by Iontropic Pre-Gelation through Dsc and Ftir Studies. *Carbohydrate Polymers* 2006 Oct 5;66:1-7.
206. Stehfest K, Boese M, Kerns G, Piry A, Wilhelm C. Fourier Transform Infrared Spectroscopy as a New Tool to Determine Rosmarinic Acid in Situ. *Journal of Plant Physiology* 2004;161:151-6.
207. Roeges N. *A Guide to the Complete Interpretation of Infrared Spectra of Organic Structures*. Wiley and Sons, Chichester 1995.

208. Ajun W, Yan S, li G, Huili L. Preparation Os Aspirin and Probucol in Combination Loaded Chitosan Nanoparticles and *in Vitro* Release Study. *Carbohydrate Polymers* 2009;75:566-74.
209. Contreras MM, Hernández-Ledesma B, Amigo L, Martín-Alvarez PJ, Recio I. Production of Antioxidant Hydrolysates from a Whey Protein Concentrate with Thermolysin: Optimization by Response Surface Methodology. *LWT - Food Science and Technology* 2011;44:9-15.
210. Hernández-Ledesma B, Dávalos A, Bartolomé B, Amigo L. Preparation of Antioxidant Enzymatic Hydrolysates from  $\alpha$ -Lactalbumin and B-Lactoglobulin, Identification of Active Peptides by Hplcems. *Journal of Agricultural and Food Chemistry* 2005;53:588-93.
211. Han L, Du L-B, Kumar A, Jia H-Y, Liang X-J, Tian Q, et al. Inhibitory Effects of Trolox-Encapsulated Chitosan Nanoparticles on Tertbutylhydroperoxide Induced Raw264.7 Apoptosis. *Biomaterials* 2012;33:8517-28.
212. Coneaca G, Gafițanub E, Hădărugăc N, Hădărugăd D, Rivișc A, Pârvuc D. Quercetin and Rutin/2-Hydroxypropyl-B-Cyclodextrin Nanoparticles: Obtaining, Characterization and Antioxidant Activity. *Journal of Agroalimentary Processes and Technologies* 2009;15:441-8.
213. de la Fuente M, Raviña M, Paolicelli P, Sanchez A, Seijo B, Alonso MJ. Chitosan-Based Nanostructures: A Delivery Platform for Ocular Therapeutics. *Advanced Drug Delivery Reviews* 2010;62:100-17.
214. Sahoo SK, Dilnawaz F, Krishnakumar S. Nanotechnology in Ocular Drug Delivery. *Drug Discovery Today* 2008;13:144-51.
215. Kim YC, Chiang B, Wu X, Prausnitz MR. Ocular Delivery of Macromolecules. *Journal of Controlled Release* 2014;190:172-81.
216. Silva SBd, Borges S, Ramos Ó, Pintado M, Ferreira D, Sarmento B. Treating Retinopathies: Nanotechnology as a Tool in Protecting Antioxidants Agents. *Systems Biology of Free Radicals and Antioxidants*. Germany: Springer-Verlag; 2014.
217. Hammond BR, Johnson B, George ER. Oxidative Photodegradation of Ocular Tissues: Beneficial Effects of Filtering and Exogenous Antioxidants. *Experimental Eye Research* 2014;In press.
218. Lee H, Arnouk H, Sripathi S, Chen P, Zhang R, Bartoli M, et al. Prohibitin as an Oxidative Stress Biomarker in the Eye. *International Journal of Biological Macromolecules* 2010;47:685-90.

219. Andrade AS, Salomon TB, Behling CS, Mahl CD, Hackenhaar FS, Putti J, et al. Alpha-Lipoic Acid Restores Tear Production in an Animal Model of Dry Eye. *Experimental Eye Research* 2014;120:1-9.
220. Saijyothi AV, Fowjana J, Madhumathi S, Rajeshwari M, Thennarasu M, Prema P, et al. Tear Fluid Small Molecular Antioxidants Profiling Shows Lowered Glutathione in Keratoconus. *Experimental Eye Research* 2012;103:41-6.
221. Guinedi AS, Mortada ND, Mansour S, Hathout RM. Preparation and Evaluation of Reverse-Phase Evaporation and Multilamellar Niosomes as Ophthalmic Carriers of Acetazolamide. *International Journal of Pharmaceutics* 2005;306:71-82.
222. Bhatta RS, Chandasana H, Chhonker YS, Rathi C, Kumar D, Mitra K, et al. Mucoadhesive Nanoparticles for Prolonged Ocular Delivery of Natamycin: In Vitro and Pharmacokinetics Studies. *International Journal of Pharmaceutics* 2012;432:105-12.
223. Mannermaa E, Reinisalo M, Ranta V-P, Vellonen K-S, Kokki H, Saarikko A, et al. Filter-Cultured Arpe-19 Cells as Outer Blood–Retinal Barrier Model. *European Journal of Pharmaceutical Sciences* 2010;40:289–96.
224. Toropainen E, Ranta V-P, Vellonen K-S, Palmgrén J, Talvitie A, Laavola M, et al. Paracellular and Passive Transcellular Permeability in Immortalized Human Corneal Epithelial Cell Culture Model. *European Journal of Pharmaceutical Sciences* 2003;20:99-106.
225. Garcia-Ramírez M, Hernández C, Ruiz-Meana M, Villarroel M, Corraliza L, García-Dorado D, et al. Erythropoietin Protects Retinal Pigment Epithelial Cells against the Increase of Permeability Induced by Diabetic Conditions: Essential Role of Jak2/ Pi3k Signaling. *Cellular Signalling* 2011;23:1596-602.
226. Mazzarino L, Travelet C, Ortega-Murillo S, Otsuka I, Pignot-Paintrand I, Lemos-Senna E, et al. Elaboration of Chitosan-Coated Nanoparticles Loaded with Curcumin for Mucoadhesive Applications. *Journal of Colloid and Interface Science* 2012;370:58–66.
227. Berger L, Stamford T, Stamford-Arnaud T, Franco L, Nascimento A, Cavalcante H, et al. Effect of Corn Steep Liquor (Csl) and Cassava Wastewater (Cw) on Chitin and Chitosan Production by *Cunninghamella Elegans* and Their Physicochemical Characteristics and Cytotoxicity. *Molecules* 2014;19:2771-92.
228. Kalweit S, Besoke R, Gerner I, Spielmann H. A National Validation Project of Alternative Methods to the Draize Rabbit Eye Test. *Toxicology In Vitro* 1990;4:702–6.
229. Xia T, Kovichich M, Brant J, Hotze M, Sempf J, Oberley T, et al. Comparison of the Abilities of Ambient and Manufactured Nanoparticles to Induce Cellular Toxicity According to an Oxidative Stress Paradigm. *Nano Letters* 2006;6:1794-807.

230. Campos DA, Madureira AR, Gomes AM, Sarmento B, Pintado MM. Optimization of the Production of Solid Witepsol Nanoparticles Loaded with Rosmarinic Acid. *Colloids and Surfaces B: Biointerfaces* 2014;115:109-17.
231. Sakurai E, Ozeki H, Kunou N, Ogura Y. Effect of Particle Size of Polymeric Nanospheres on Intravitreal Kinetics. *Ophthalmic Research* 2001;33:31-6.
232. Kompella UB, Amrite AC, Ravi RP, Durazo SA. Nanomedicines for Back of the Eye Drug Delivery, Gene Delivery, and Imaging. *Progress in Retinal and Eye Research* 2013;36:172-98.
233. Sarmento B, Martins S, Ribeiro A, Veiga F, Neufeld R, Ferreira D. Development and Comparison of Different Nanoparticulate Polyelectrolyte Complexes as Insulin Carriers. *International Journal of Peptide Research and Therapeutics* 2006 Jun;12:131-8.
234. Hosseini SF, Zandi M, Rezaei M, Farahmandghavi F. Two-Step Method for Encapsulation of Oregano Essential Oil in Chitosan Nanoparticles: Preparation, Characterization and in Vitro Release Study. *Carbohydrate Polymers* 2013;95:50-6.
235. Azevedo MA, Bourbon AI, Vicente AA, Cerqueira MA. Alginate/Chitosan Nanoparticles for Encapsulation and Controlled Release of Vitamin B2. *International Journal of Biological Macromolecules* 2014;In press.
236. Olmsted SS, Padgett JL, Yudin AI, Whaley KJ, Moench TR, Cone RA. Diffusion of Macromolecules and Virus-Like Particles in Human Cervical Mucus. *Biophysical Journal* 2001;81:1930-7.
237. Neves Jd, Bahia MF, Amiji MM, Sarmento B. Mucoadhesive Nanomedicines: Characterization and Modulation of Mucoadhesion at the Nanoscale. *Expert Opinion Drug Delivery* 2011;8:1085-104.
238. Mazzarino L, Coche-Guérente L, Labbé P, Lemos-Senna E, Borsali R. On the Mucoadhesive Properties of Chitosan-Coated polycaprolactone Nanoparticles Loaded With curcumin Using Quartz Crystal Microbalance with Dissipation Monitoring. *Journal of Biomedical Nanotechnology* 2013;9:1-8.
239. Takeuchi H, Thongborisute J, Matsui Y, Sugihara H, Yamamoto H, Kawashima Y. Novel Mucoadhesion Tests for Polymers and Polymer-Coated Particles to Design Optimal Mucoadhesive Drug Delivery Systems. *Advanced Drug Delivery Reviews* 2005;57:1583-94.
240. Mugabe C, Hadaschik BA, Kainthan RK, Brooks DE, So AI, Gleave ME, et al. Paclitaxel Incorporated in Hydrophobically Derivatized Hyperbranched Polyglycerols for Intravesical Bladder Cancer Therapy. *British Journal of Urology International* 2009;103:978-86.

241. Jintapattanakit A, Junyaprasert VB, Kissel T. The Role of Mucoadhesion of Trimethyl Chitosan and Pegylated Trimethyl Chitosan Nanocomplexes in Insulin Uptake. *Journal of Pharmaceutical Sciences* 2009;98:4818-30.
242. Svensson O, Thuresson K, Arnebrant T. Interactions between Drug Delivery Particles and Mucin in Solution and at Interfaces. *Langmuir* 2008;24:2573-9.
243. Lai S, O'Hanlon E, Hanes J. Rapid Transport of Large Polymeric Nanoparticles in Fresh Undiluted Human Mucus. *Proceedings of the National Academy of Sciences of the United States of America* 2007;104:1482-7.
244. Zambito Y, Felice F, Fabiano A, Stefano RD, Colo GD. Mucoadhesive Nanoparticles Made of Thiolated Quaternary Chitosan Crosslinked with Hyaluronan. *Carbohydrate Polymers* 2013;92:33–9.
245. Wen Z-S, Liu L-J, Qu Y-L, OuYang X-K, Yang L-Y, Xu Z-R. Chitosan Nanoparticles Attenuate Hydrogen Peroxide-Induced Stress Injury in Mouse Macrophage Raw264.7 Cells *Marine Drugs* 2013;11:3582-600.
246. Narayanan D, Anitha A, Jayakumar R, Nair SV, Chennazhi KP. Synthesis, Characterization and Preliminary *in Vitro* Evaluation of Pth 1-34 Loaded Chitosan Nanoparticles for Osteoporosis. *Journal of Biomedical Nanotechnology* 2012;8:98-106.
247. Ragelle H, Riva R, G. V, Naeye B, Pourcelle V, Le Duff CS, et al. Chitosan Nanoparticles for Sirna Delivery: Optimizing Formulation to Increase Stability and Efficiency. *Journal of Controlled Release* 2014;176:54–63.
248. Vargas A, Zeisser-Labouèbe M, Lange N, Gurny R, Delie F. The Chick Embryo and Its Chorioallantoic Membrane (Cam) for the *in Vivo* Evaluation of Drug Delivery Systems. *Advanced Drug Delivery Reviews* 2007;59:1162–76.
249. Rahul L, Verma A, Jain S. Development and Characterization of Nanoparticulate Carrier System for Ophthalmic Delivery of Gatifloxacin. *International Journal of Pharmaceutical Science* 2012;1:732 -7.
250. Shinde U, Ahmed MH, Singh K. Development of Dorzolamide Loaded 6-O-Carboxymethyl Chitosan Nanoparticles for Open Angle Glaucoma. *Journal of Drug Delivery* 2013;2013:562-727.
251. Himanshu G, Aqil M, Khar RK, Ali A, Bhatnagar A, Mittal G. Biodegradable Levo-Oxacin Nanoparticles for Sustained Ocular Drug Delivery. *Journal of Drug Targeting* 2011;19:409–17.
252. Gukasyan HJ, Kim K-J, Lee VHL. The Conjunctival Barrier in Ocular Drug Delivery. In: Ehrhardt C, Kim KJ, editors. *Drug Absorption Studies: In Situ, in Vitro and in Silico*. New York: Springer; 2008. p. 307-20.

253. Hernández-Covarrubias C, Vilchis-Reyes MA, Yépez-Mulia L, Sánchez-Díaz R, Navarrete-Vázquez G, Hernández-Campos A, et al. Exploring the Interplay of Physicochemical Properties, Membrane Permeability and Giardicidal Activity of Some Benzimidazole Derivatives. *European Journal of Medicinal Chemistry* 2012;52:193-204.
254. Gbate D, Edelhauser HF. Ocular Drug Delivery. *Expert Opinion on Drug Delivery* 2006;3:275-87.
255. Nagai N, Ito Y, Okamoto N, Shimomur Y. A Nanoparticle Formulation Reduces the Corneal Toxicity Ofindomethacin Eye Drops and Enhances Its Corneal Permeability. *Toxicology* 2014;319:53–62.
256. Behrens I, Kamm W, Dantzig AH, Kissel T. Variation of Peptide Transporter (Pept1 and Hpt1) Expression in Caco-2 Cells as a Function of Cell Origin. *Journal of Pharmaceutical Science* 2004;93:1743-54.
257. Kaldas MI, Walle UK, Walle T. Resveratrol Transport and Metabolism by Human Intestinal Caco-2 Cells. *Journal of Pharmacy and Pharmacology* 2003;55:307-12.
258. Fichert T, Yazdanian M, Proudfoot JR. A Structure-Permeability Study of Small Drug-Like Molecules. *Bioorganic & Medicinal Chemistry Letters* 2003;13:719-22.
259. Camenisch G, Alsenz J, van de Waterbeemd H, Folkers G. Estimation of Permeability by Passive Diffusion through Caco-2 Cell Monolayers Using the Drugs' Lipophilicity and Molecular Weight. *European Journal of Pharmaceutical Sciences* 1998;6:317-24.
260. Yildirim Z, Irem Ucgun N, Kilic N, E. G, Sepici-Dinçel A. Antioxidant Enzymes and Diabetic Retinopathy. *Annals New York Academy of Sciences* 2007;1100:199–206.
261. Patel A, Cholkar K, Agrahari V, Mitra AK. Ocular Drug Delivery Systems: An Overview. *World Journal Pharmacology* 2013;9:47-64.
262. Qiang Z, Ye Z, Hauck C, Murphy P, McCoy J-A, Widrlechner M, et al. Permeability of Rosmarinic Acid in *Prunella Vulgaris* and Ursolic Acid in *Salvia Officinalis* Extracts across Caco-2 Cell Monolayers. *Journal of Ethnopharmacology* 2011;137:1107– 12.
263. Konishi Y, Kobayashi S. Transepithelial Transport of Rosmarinic Acid in Intestinal Caco-2 Cell Monolayers. *Bioscience, Biotechnology, and Biochemistry* 2005;69:583-91.
264. Saccà SC, Roszkowskab AM, Izzottic A. Environmental Light and Endogenous Antioxidants as the Main Determinants of Non-Cancer Ocular Diseases. *Mutation Research/Reviews in Mutation Research* 2013;752:153–71.
265. Vohra R, Tsai JC, Kolko M. The Role of Inflammation in the Pathogenesis of Glaucoma. *Survey of Ophthalmology* 2013;58:311-20.



266. Chua J, Vania M, Cheung CM, Ang M, Chee SP, Yang H, et al. Expression Profile of Inflammatory Cytokines in Aqueous from Glaucomatous Eyes. *Molecular Vision* 2012;18:431-8.
267. Tezel G, Li LY, Patil RV, Wax MB. Tnf-Alpha and Tnf-Alpha Receptor-1 in the Retina of Normal and Glaucomatous Eyes. *Investigative Ophthalmology & Visual Science* 2001;42:1787-94.
268. Osborne NN, Casson RJ, Wood JPM, Chidlow G, Graham M, Melena J. Retinal Ischemia: Mechanisms of Damage and Potential Therapeutic Strategies. *Progress in Retinal and Eye Research* 2004;23:91-147.
269. Chen FT, Yang CM, Yang CH. The Protective Effects of the Proteasome Inhibitor Bortezomib (Velcade) on Ischemia-Reperfusion Injury in the Rat Retina. *Plos one* 2013;8:e64262.
270. Kim JH, Lee BJ, Kim JH, Yu YS, Kim MY, Kim K-W. Rosmarinic Acid Suppresses Retinal Neovascularization Via Cell Cycle Arrest with Increase of P21waf1 Expression. *European Journal of Pharmacology* 2009;615:150-4.
271. Huang SS, Zheng RL. Rosmarinic Acid Inhibits Angiogenesis and Its Mechanism of Action *in Vitro*. *Cancer Letters* 2006;239:271-80.
272. Martins J, Castelo-Branco M, Batista A, Oliveiros B, Santiago AR, Galvao J, et al. Effects of 3,4-Methylenedioxymethamphetamine Administration on Retinal Physiology in the Rat. *Plos one* 2011;6:e29583.
273. Velten IM, Horn FK, Korth M, Velten K. The B-Wave of the Dark Adapted Flash Electroretinogram in Patients with Advanced Asymmetrical Glaucoma and Normal Subjects. *British Journal of Ophthalmology* 2001;85:403-9.
274. Moncaster JA, Walsh DT, Gentleman SM, Jen L-S, Aruoma OI. Ergothioneine Treatment Protects Neurons against N-Methyl-D-Aspartate Excitotoxicity in an *in Vivo* Rat Retinal Model. *Neuroscience Letters* 2002;328:55-9.
275. Zhang B, Osborne NN. Oxidative-Induced Retinal Degeneration Is Attenuated by Epigallocatechin Gallate. *Brain Research* 2006;1124:176-87.
276. Ito D, Tanaka K, Suzuki S, Dembo T, Fukuuchi Y. Enhanced Expression of Iba1, Ionized Calcium-Binding Adapter Molecule 1, after Transient Focal Cerebral Ischemia in Rat Brain. *Stroke* 2001;32:1208-15.
277. Kettenmann H, Hanisch UK, Noda M, Verkhratsky A. Physiology of Microglia. *Physiological Reviews* 2011;91:461-553.

278. Gallego BI, Salazar JJ, de Hoz R, Rojas B, Ramirez AI, Salinas-Navarro M, et al. Iop Induces Upregulation of Gfap and Mhc-li and Microglia Reactivity in Mice Retina Contralateral to Experimental Glaucoma. *Journal of Neuroinflammation* 2012;9:2-18.
279. Zhang C, Lam TT, Tso MO. Heterogeneous Populations of Microglia/Macrophages in the Retina and Their Activation after Retinal Ischemia and Reperfusion Injury. *Experimental Eye Research* 2005;81:700-9.
280. Flugel A, Bradl M, Kreutzberg GW, Graeber MB. Transformation of Donorderived Bone Marrow Precursors into Host Microglia During Autoimmune Cns Inflammation and During the Retrograde Response to Axotomy. *Journal of neuroscience research* 2001;66:74-82.
281. Nadal-Nicolas FM, Jimenez-Lopez M, Sobrado-Calvo P, Nieto-Lopez L, Canovas-Martinez I, Salinas-Navarro M, et al. Brn3a as a Marker of Retinal Ganglion Cells: Qualitative and Quantitative Time Course Studies in Naive and Optic Nerveinjured Retinas. *Investigative Ophthalmology & Visual Science* 2009;50:3860-8.
282. Kang CH, Jayasooriya RG, Dilshara MG, Choi YH, Jeong YK, Kim ND, et al. Caffeine Suppresses Lipopolysaccharide-Stimulated Bv2 Microglial Cells by Suppressing Akt-Mediated Nf-Kappab Activation and Erk Phosphorylation. *Food Chemistry Toxicology* 2012;50:4270-6.